

AN INTRODUCTION TO
THE ANALYSIS OF
FIBRE REINFORCED COMPOSITE STRUCTURES

AN INTRODUCTION TO
THE ANALYSIS OF
FIBRE REINFORCED COMPOSITE STRUCTURES

BY

BRIAN E. RISEBOROUGH, B.Eng.

A Thesis

Submitted to the Faculty of Graduate
Studies in Partial Fulfilment of the
Requirements for the Degree

Master of Engineering

McMaster University

December 1972

MASTER OF ENGINEERING (1973)
(Mechanical Design)

McMASTER UNIVERSITY
Hamilton, Ontario

TITLE: AN INTRODUCTION TO THE ANALYSIS OF FIBRE
REINFORCED COMPOSITE STRUCTURES

AUTHOR: Brian Edward Riseborough, B. Eng.

SUPERVISOR: Dr. G. Kardos

NUMBER OF PAGES: xvii, 213

SCOPE AND CONTENTS: Prevailing approaches to the analysis of laminated composite structures are reviewed and serious shortcomings are noted in each. A promising new, more rational method, founded upon the recently developed theory of laminated composites, is described and equations of laminate behaviour are established in accordance with the theory.

The new method is employed in the analysis of a fibre-reinforced cylindrical storage tank and a new equation of deflection, applicable for both laminated orthotropic and isotropic materials of construction, is derived. A computer program, based upon this analysis, and capable of performing a complete stress analysis at any point in the tank, is included.

Results of a series of parametric studies, relative to the construction of filament wound storage tanks, are reported and new design guidelines are suggested.

PREFACE

During the brief life of the High Altitude Research Project (H.A.R.P.) at McGill University, considerable effort was directed towards the development of filament wound fibreglass rocket motor cases capable of withstanding gun launch. Initial motor case designs in this program were based upon traditional strength of materials design formulas but it soon became apparent that a completely new approach was required in order to derive maximum benefits from this anisotropic composite material.

Fibreglass motor case development work, however, was only a part of the overall H.A.R.P. program; there were not sufficient funds available for an in depth study of composite materials analysis techniques. Following a rather sterile literature search for information on this subject, it was decided that a more empirical approach would have to be taken towards the development of operational hardware until better analytical methods became available. The search for these methods continued thereafter but only on a spare time basis.

At the time of project cancellation in 1967, considerable progress had been made theoretically as well as practically, however. By then it had been learned that

a layer of filament wound fibreglass could generally be treated as a planar orthotropic material and that the elastic properties of such a layer were predictable. Thus it became possible, through application of the strain compatibility condition, to determine theoretically the effective elastic constants of any filament wound laminate. The structural analysis reported by O'Connell (1) indicates the manner in which these new concepts were applied in conjunction with conventional plate and shell theory to study the behaviour of the rocket motor case during launch. On the practical side, rocket motor cases loaded with solid rocket propellants in both end and centre burning configurations were being successfully launched from 155 and 175 millimetre smooth bore guns at accelerations of up to 10,000 g.

Unfortunately, the analytical approach outlined above could still not be considered entirely satisfactory. O'Connell's assumption that conventional shell deformation equations (which were developed for isotropic structures) could be applied to the analysis of non-isotropic structures was questionable, to say the least. Further, although hoop and axial layer stresses were predicted by the analysis, no serious attempt was made to identify a condition of structural failure.

A similar concern over the adequacy of available

design methods was apparent in the FRP (Fibre Reinforced Plastic) industry at that time. The consensus of opinion among knowledgeable FRP designers and manufacturers contacted seemed to be that the growth of the industry was being severely constrained by a lack of knowledge in the area of FRP design. Numerous structural failures of FRP products, caused primarily by improper design, were being attributed to the material itself; as a result, the reputation of FRP as a structural material was being severely damaged.

Accordingly, when Fiberglas Canada Limited was approached in 1967, with a suggestion that they sponsor a study of this problem, their response was immediately favourable. The objective of this study was quite simple: to carry out a thorough study of the available methods for analyzing structures composed of fibre reinforced materials and to determine which of these afforded the best opportunity for circumventing the limitations of those methods generally employed. It was particularly hoped that an analytical technique would be found which would enable a more rational analysis of H.A.R.P. rocket motor cases.

This thesis describes the results of this study.

ACKNOWLEDGEMENTS

The author wishes to express his appreciation to the many people who have assisted in the preparation of this thesis. Particular thanks are extended to Dr. G. Kardos who encouraged this study from the outset and offered advice and guidance as it progressed. Thanks are also due to Dr. S. Tsai of the United States Air Force Materials Laboratory and to Mr. D.P. Hanley of Bell Aerosystems for their most helpful suggestions. Finally, I would like to sincerely thank my wife, Barbara, for both her patience and her many hours spent typing, and my mother, who also assisted in the typing.

The study was supported by a Ford Foundation Scholarship, awarded by the Department of Mechanical Engineering, McMaster University, and by Fiberglas Canada Limited. This support is gratefully acknowledged.

TABLE OF CONTENTS

	Page No.
Preface	iii
Acknowledgements	vi
List of Illustrations	xi
List of Tables	xiii
List of Principal Symbols	xiv
INTRODUCTION	1
SECTION 1: AN INTRODUCTION TO FIBRE REINFORCED COMPOSITE MATERIALS	5
1.1 Composite Materials	5
1.2 Theory of Fibre reinforcement	7
1.2.1 Fibres	7
1.2.2 Matrices	10
1.2.3 Effects of Fibre Length and Volume Fraction	12
1.2.3.1 Continuous Fibre Reinforced Materials	13
1.2.3.2 Discontinuous Fibre Reinforced Materials	17
1.2.4 Fibre Orientation Effects	20
1.2.4.1 Unidirectional Reinforcement	21
1.2.4.2 Bidimensional Reinforcement	22
1.2.4.3 Tridimensional Reinforcement	24
1.3 Closing	25
SECTION 2: STRESS ANALYSIS OF FIBRE REINFORCED COMPOSITE MATERIALS	26
2.1 Prevailing Methods	27

	Page No.	
2.1.1	The Strength of Materials Approach	28
2.1.2	Netting Analysis	30
2.1.3	Orthotropic Lamina Approach	34
2.2	The Theory of Laminated Composites	41
SECTION 3: LAMINA STRESS-STRAIN RELATIONSHIPS		44
3.1	Hooke's Law	44
3.2	Transformation of Properties	50
3.2.1	Transformation of Stress Components	50
3.2.2	Transformation of Strain Components	52
3.2.3	Transformation of Stiffness and Compliances	53
3.3	Effects of Material Symmetry	54
3.3.1	Materials Possessing One Plane of Elastic Symmetry	54
3.3.2	Two planes of Elastic Symmetry	56
3.3.3	Three Planes of Elastic Symmetry - Orthotropic Materials	58
3.4	The Plane Stress Assumption	59
3.4.1	The Stress-Strain Relationships for a Specially Orthotropic Layer	59
3.4.2	The Reduced Stress and Strain Transformation Matrices	63
3.4.3	The Generalized Hooke's Law for an Orthotropic Layer	65
3.4.4	Simplifications in Stress-Strain Relationships Resulting from Material Isotropy	67
3.5	Failure Criteria	69
3.6	Determination of Lamina Properties	72
3.7	Closing	75
SECTION 4: LAMINATE CONSTITUTIVE EQUATIONS		76
4.1	Laminate Displacement Relationships	76

	Page No.	
4.2	Strain-Displacement Relationships	78
4.3	Force and Moment Resultants	81
4.4	Constitutive Equations	84
	4.4.1 Force Resultant Considerations	84
	4.4.2 Moment Resultant Considerations	88
4.5	Coupling between Bending and Stretching	92
4.6	Laminate Failure Analysis	95
4.7	Plate and Shell Problems	96
SECTION 5: CYLINDRICAL TANK ANALYSIS		97
5.1	Strain-Displacement Relationships	98
5.2	The Equations of Equilibrium	101
5.3	Laminate Constitutive Relationships	102
5.4	Compatibility Condition	104
5.5	The Governing Differential Equation of Displacement	104
5.6	General Solution of the Governing Differential Equation	107
5.7	Application of Boundary Conditions	108
5.8	Failure Analysis	110
5.9	Computer Program	111
5.10	Gun-Launched Rocket Motor Case Analysis	111
	5.10.1 Background Information	111
	5.10.2 Computational Procedure	113
	5.10.3 Results of Initial Study	114
	5.10.4 Additional Parametric Studies	115
	5.10.5 Closing Remarks	126
SECTION 6: CONCLUSION		128

	Page No.
APPENDIX A: COMPUTER PROGRAM FOR DETERMINING LAMINA STIFFNESS COEFFICIENTS	134
A.1 Description of Program	134
A.2 Input Parameter Definition	134
A.3 Typical Input	135
A.4 Typical Output	136
A.5 Program Listing	139
 APPENDIX B: DETERMINATION OF LAMINATE STIFFNESS COEFFICIENTS	 142
B.1 Description of Program	142
B.2 Input Parameter Definition	142
B.3 Typical Input	144
B.4 Typical Output	145
B.5 Program Listing	149
 APPENDIX C: SOLUTION OF THE GOVERNING DIFFERENTIAL EQUATION OF DISPLACEMENT	 163
 APPENDIX D: PROGRAM FOR ANALYZING CYLINDRICAL STORAGE TANKS	 166
D.1 Description of Program	166
D.2 Input Parameter Definitions	166
D.3 Typical Input	167
D.4 Typical Output	169
D.5 Program Listing	173
References	178
Illustrations	183

LIST OF ILLUSTRATIONS

Page No.

SECTION 1:

1.1.	Model of Continuous Fibre Composite	183
1.2	Theoretical Variation of Composite Modulus with Volume Fraction of Fibres	184
1.3	Typical Composite Stress-Strain Behaviour	185
1.4	Model of Discontinuous Fibre Composites	186
1.5	Fibre Orientation	187
1.6	Fabric, Reinforcing Mat and Woven Rovings	188

SECTION 2:

2.1	Typical Laminate in Bending	189
2.2	Netting Analysis Load Diagram	190
2.3	Common Forms of Reinforcement	191
2.4	Off-Axis Loading of an Orthotropic Layer	192

SECTION 3:

3.1	Stresses Acting on a Cubic Element	193
3.2	Transformation of Stress Components	194
3.3	Transformation of Stresses in the Case of Plane Stress	195
3.4	Filament Wound Cylinder	196
3.5	Failure Surface	197

SECTION 4:

4.1	Element of a Deformed Laminate	198
4.2	Deformation in the X-Z Plane	199
4.3	Stress Distribution in a Deformed Laminate	200
4.4	Stress and Moment Resultants Acting at the Geometric Midplane	201

SECTION 5:

5.1	Cylindrical Storage Tank	202
5.2	Loads Acting on an Element of a Shell	203
5.3	Rocket at Gun Muzzle	204
5.4	Tank Deflection Curve	205
5.5	Tank Deformation in the Vicinity of the Base	206
5.6	Maximum Deflection versus A_{22}^*	207
5.7	Axial Curvature at Base versus $(A_{22}^*/D_{11}^*)^{1/2}$	208
5.8	The Effect of the Hoop Wound Layer Thickness on Laminate Elastic Properties	209
5.9	The Effect of the Hoop Wound Layer Thickness on Laminate Structural Performance	210
5.10	The Effect of the Helical Wind Angle on Laminate Elastic Properties	211
5.11-a	The Effect of the Helical Wind Angle on Structural Performance at the Base	212
5.11-b	The Effect of the Helical Wind Angle on Structural Performance at the Point of Maximum Deflection	213

LIST OF TABLES

	Page No.
<u>SECTION 1:</u>	
1.1 Fibre Reinforcements	9
1.2 Common Plastic Matrix Materials	11
<u>SECTION 5:</u>	
5.1 Comparison of Stresses at Maximum Deflection	116
5.2 Summary of Laminates Analyzed	118
5.3-a Summary of Results - The Point of Maximum Deflection	119
5.3-b Summary of Results - The Base of the Structure	120

LIST OF PRINCIPAL SYMBOLS

A_{ij} ($= \bar{b}_{ij} = A$)	Laminate in-plane stiffness matrix
A_{ij}^* ($= A^*$)	Intermediate in-plane matrix
A'_{ij} ($= A'$)	In-plane compliance matrix
A	Area
B_{ij} ($= B$)	Laminate stiffness coupling matrix
B_{ij}^* ($= B^*$)	Intermediate coupling matrix
B'_{ij} ($= B'$)	Compliance coupling matrix
C_{ijkl}	Stiffness matrix for a completely anisotropic material
C_{ij} ($= b_{ij} = C$)	Lamina in-plane stiffness matrix
C'_{ij} ($= C'$)	Transformed lamina stiffness matrix
c	Distance from neutral axis to the most remote point in a beam
D_{ij} ($= D$)	Laminate flexural stiffness matrix
D_{ij}^* ($= D^*$)	Intermediate flexural modulus
D'_{ij} ($= D'$)	Flexural compliance matrix
d_f	Fibre diameter
d	Depth of tank
E	Modulus of Elasticity
E_{11} ($= E_1$)	Composite lamina axial stiffness
E_{22} ($= E_2$)	Composite lamina transverse stiffness
F ($= f$)	Force
G	Shear modulus
G_{12}	Composite lamina in-plane shear modulus

H_{ij}^* ($= H^*$)	Laminate intermediate coupling matrix
h	Plate, shell or laminate thickness
I	Moment of inertia of cross-section
L	Fibre length
L_c	Critical fibre length
l_i, m_i, n_i	Coordinate transformation cosines
M	Bending moment
M_i ($= M$)	Distributed bending (and twisting) moments
m	$\cos\theta$
N_i ($= N$)	Stress resultant
n	$\sin\theta$ or number of layers
P	Material property
r	Radius
S_{ij} ($= S$)	Lamina compliance matrix
S'_{ij} ($= S'$)	Transformed lamina compliance matrix
S	Lamina in-plane shear strength
T_{ij} ($= T$)	Stress transformation matrix
T'_{ij} ($= T'$)	Strain transformation matrix
t	Thickness
u_i ($= u, v, w$)	Displacement components
u_0, v_0, w	Midplane displacement components
V	Volume fraction
X	Lamina axial strength
x_i ($= x, y, z$)	Cartesian coordinates
Y	Lamina transverse strength

Z	Lateral load
z	Distance as measured from the laminate midplane
γ_{ij}	Shear strain components
ϵ	Strain
ϵ_{ij}	Tensorial strain components
ϵ_i	Engineering strain components
ϵ_i^0	Midplane strain components
θ	Fibre orientation or lamination angle
χ_i ($= -\chi_i = \chi$)	Curvatures
ν	Poisson's ratio
ν_{12}	Major Poisson's ratio
ν_{21}	Minor Poisson's ratio
ρ	Fluid density
σ	Stress
σ_{ij}	Tensorial stress components
σ_i	Engineering stress components
$\bar{\sigma}_x, \bar{\sigma}_y, \bar{\tau}_{xy}$	Average laminate stresses
τ_{ij}	Shear stress components

SUBSCRIPTS

c	Composite
f	Fibre
m	Matrix
i, j, k	1, 2...6 or x, y (or θ), z in 3-dimensional space, or 1, 2, 6(12) or x, y (or θ), xy (or x0) in 2-dimensional space

y Yield point

SUBSCRIPTS

k kth layer of a laminated composite
-l Inverse matrix
c Compressive property
t Tensile property

INTRODUCTION

The primary objective of this thesis is to demonstrate to structural designers that a recently developed theory - the theory of laminated composites - has at last made it possible to approach the design of fibre-reinforced composite structures on an entirely rational basis.

In Section 1, the fundamentals of reinforcement are briefly reviewed in order to establish a reference point for subsequent analytical discussions. Though other forms of reinforcement are considered herein, the emphasis is on fibre reinforcement. The effects of key variables, e.g. constituent material properties, fibre length, volume fraction and orientation, on the performance of the composite are analyzed and rough guidelines are presented for estimating the strength and stiffness properties of unidirectionally reinforced materials.

The design methods which prevailed prior to the development of the aforementioned theory are reviewed in Section 2. Relative strengths and weaknesses of each method are discussed and specific design limitations indicated. Towards the end of the section, the theory of laminated composites is itself introduced.

One of the basic premises of this theory is that a laminate is comprised of a number of thin isotropic and / or orthotropic layers. Section 3 comprises a detailed development of layer or lamina stress-strain relationships. The development starts with the generalized Hooke's Law (which describes the behaviour of a completely anisotropic material) and proceeds through the introduction of transformation relationships, material symmetry considerations and the plane stress assumption, to the lamina constitutive equations. In addition, commonly used lamina failure criteria are reviewed and methods of determining principal lamina properties are discussed.

The objective of Section 4 is to demonstrate the interrelationship between gross laminate behaviour and the response characteristics of the individual layers. It is shown that laminate constitutive equations are derived by following exactly the same procedure as is employed in the establishment of the force and moment resultant equations in conventional plate and shell theory. The only significant difference is that in this instance, the constituent material, i.e., lamina, stress-strain relationships vary from layer to layer. It is further revealed that these laminate constitutive equations are, in effect, a more general form of the force and moment resultant equations and that they can in fact be used in

place of them in the analysis of laminated plate or shell structures.

Another important topic dealt with in Section 4 is laminate failure analysis. This simply involves working backwards from gross laminate deformations to individual layer strains and stresses to determine whether or not failure has occurred, according to the selected failure criterion.

To demonstrate the application of the theory, a particular shell problem is studied in Section 5. A vertical cylindrical storage tank is analyzed and equations are developed for predicting wall deflections, mid-plane strains and shell curvatures at any point in the structure. These equations, it is pointed out, can be used to provide the necessary input for a complete stress (failure) analysis of the tank.

A secondary objective of this investigation is also realized in this section. It is clearly shown, through a series of design studies of one of the H.A.R.P. gun-launched rockets, that the tank analysis developed according to the theory of laminated composites is a considerable improvement over the one originally used in the H.A.R.P. program.

Section 6 concludes the main body of the thesis. It contains general comments concerning the study as a

whole, a number of specific conclusions relative to the design of FRP cylindrical storage tanks (or gun-launched rocket motor cases) and several suggestions for future work.

There are, in addition, four appendices. Appendix A contains a listing of a computer program for calculating the lamina stiffness coefficients of a generally orthotropic layer. It is one of two programs developed during the course of this study. The second, which is listed in Appendix D, performs a stress analysis at any point of interest in a laminated cylindrical tank in accordance with the theoretical analysis presented in Section 5. Yet another computer program listing is included in Appendix B. This program, which is capable of computing laminate stiffnesses and performing a laminate strength analysis is not original, however; it is included herein for the sake of completeness. In Appendix C, the mathematical details of solving the governing differential equation of displacement are provided.

SECTION 1
AN INTRODUCTION TO
FIBRE-REINFORCED COMPOSITE MATERIALS

Fibre-reinforced composites are, without doubt, the most attractive of the many new materials that have become available to structural designers in recent years. Many are stiffer, stronger and lighter than any of the structural materials previously known to man.

A particularly interesting feature of these new materials is that the fibres can be oriented within the composite, thus enabling their optimum positioning relative to anticipated load conditions. This means that a new dimension - design of the material itself - has been introduced to the traditional problem of structural design. It will be advantageous, therefore, to review some of the fundamentals of reinforcement before proceeding to discussions relating to structural design with these new materials.

1.1 COMPOSITE MATERIALS

Composite materials are not new; reinforced materials have been with us since man first constructed crude huts from mixtures of mud and straw. They also

abound in nature, wood being a prime example.

The modern science of composite materials, however, did not evolve until this century. It is therefore worthwhile to differentiate between these traditional materials and the modern composites that have been developed through scientific understanding.

A reasonable definition for a modern composite material has been suggested by Broutman and Krock (2):

- 1) the composite material must be man-made
- 2) the composite must be a combination of at least two chemically distinct materials with a distinct interface separating the components
- 3) the separate materials forming the composite must be combined three-dimensionally (clad metals and honeycomb sandwiches are not considered to be basic composite materials)
- 4) the composite material should be created to obtain properties which would not be achieved by any of the components acting alone.

Composites can generally be classified according to the basic forms of reinforcement:

- a) particle - the orthogonal dimensions of the reinforcement are approximately equal
- b) flake - two orthogonal dimensions of the reinforcement are much greater than the third
- c) fibre - one dimension of the reinforcement is much

greater than the other two orthogonal dimensions.

The highest performance composite materials developed to date, i.e., those with the greatest strength and stiffness-to-weight ratios, fall into the fibre-reinforced category, and it is to this general class of materials that subsequent discussion will be limited.

1.2 THEORY OF FIBRE REINFORCEMENT

Fibre-reinforced composite materials usually consist of fibres, which are the primary load bearing constituent, and a matrix, whose principal role, apart from holding the fibres together, is to distribute the applied loads evenly among the fibres. Their properties are dependent upon a number of factors including:

- 1) the physical properties of the fibres
- 2) the physical properties of the matrix
- 3) fibre length
- 4) the volume fraction of the fibre material relative to the total volume
- 5) fibre orientation

Each of these will be considered in the following subsections.

1.2.1 Fibres

The principal role of the fibres is to carry load. Accordingly, their mechanical properties such as strength

and modulus are of primary importance. Table 1.1 lists some of the fibre reinforcements that are currently available and their most significant mechanical properties. Since in many structural applications the weight of the structure itself must be considered, the specific strengths and moduli of these materials are also provided for reference.

Disregarding asbestos fibres and whiskers which are available only in a discontinuous form, it is apparent from the table that the most interesting reinforcing materials are the boron and carbon fibres. Unfortunately, at this time their costs are prohibitive and they are generally limited to aerospace applications where weight saving is of the utmost importance. Of the remaining more economical materials, glass fibres offer very high strengths but relatively low modulus values in comparison to steel. On a specific basis, however, they appear to be the superior reinforcing material. Nylon fibres are not often considered for structural applications due to their extremely low modulus.

Additional fibre properties to be considered are thermal stability, i.e., effect of temperature on strength and stiffness, and chemical reactivity. The latter property determines the effectiveness of the bond between the fibres and the matrix and is of extreme importance.

TABLE 1.1FIBRE REINFORCEMENTS

Material	Specific Gravity ρ	Tensile Strength σ (10^3 psi)	Specific Strength σ/ρ (10^3 psi)	Modulus E (10^6 psi)	Specific Modulus E/ρ (10^6 psi)
Drawn nylon 6/6	1.1	120	110	0.7	0.6
High tensile steel wire	7.87	190	24	30	3.8
E glass fibre	2.54	250	98	10.5	3.9
S glass fibre	2.54	380	150	12	4.7
Asbestos fibre	2.5	440	180	23	9.3
Boron fibre	2.65	500	188	50	18.8
Carbon fibre, Type 2	1.74	430	250	33	19
Carbon fibre, Type 1	2.0	300	150	60	30
SiC whiskers	3.21	3000	935	70-125	23-38
Al ₂ O ₃ whiskers	3.96	6200	1565	70-330	18-83

1.2.2 Matrices

The role of the matrix is an extremely demanding one. It must have mechanical properties compatible with the requirements stated earlier (Section 1.2), ductility to deter crack propagation, corrosion resistance (in many applications) and, occasionally, the ability to withstand high temperatures.

Metals are ideally suited for this role, principally because alloy compositions which are able to resist corrosive environments and high temperatures have already been developed. However, economical processes are not yet available to produce large volumes of metal matrix composite material for general structural application.

Commonly used plastic matrices and their principal mechanical properties are listed in Table 1.2. The so-called advanced composites, i.e., the high performance composite materials, are almost exclusively based upon thermosetting plastic matrices and continuous fibres of boron, carbon or glass. Thermoplastic matrices are mainly used in conjunction with discontinuous fibre reinforcements. The resulting composites readily lend themselves to mass production processes such as injection moulding or extrusion.

The primary consideration in the selection of a matrix material for a particular application is environment.

TABLE 1.2
COMMON PLASTIC MATRIX MATERIALS

	Specific Gravity ρ	Tensile Strength σ (10^3 psi)	Specific Strength σ/ρ (10^3 psi)	Modulus E (10^6 psi)	Specific Modulus E/ρ (10^6 psi)
<u>Thermosets</u>					
Polyesters	1.10-1.46	6-13	4.1-11.8	0.3-0.64	0.2-0.56
Epoxies	1.11-1.40	4-13	2.9-11.8	0.35	0.25-0.32
<u>Thermoplastics</u>					
ABS	1.04	6.0	5.8	0.32	0.31
SAN	1.08	9.6	8.9	0.50	0.46
Polystyrene	1.06	7.5	7.1	0.49	0.46
Polypropylene	0.91	5.0	5.5	0.18	0.20
Polyethylene	0.96	4.3	4.5	0.24	0.25
Nylon 6/6	1.14	11.8	10.4	0.41	0.36

Temperature and chemical resistance requirements will usually quickly narrow down the field of applicable materials. Final decisions are then usually based upon mechanical property requirements.

A wealth of additional information on plastic matrix materials is available from publications such as the Modern Plastics Encyclopedia (4) and manufacturers' literature.

1.2.3 Effects of Fibre Length and Volume Fraction

Fibre-reinforced composites are normally classified as either continuous or discontinuous-fibre reinforced. Broutman (5) has defined discontinuous-fibre reinforced plastics as plastics whose reinforcing fibres have length to diameter (L/d_f) ratios varying between 100 and 5000. Accordingly, continuous-fibre reinforced plastics refer to plastics reinforced by fibres which have length to diameter ratios of greater than 5000. The effect of the fibre length on composite properties is perhaps best understood by studying the fundamental mechanics of reinforcement of both continuous and discontinuous-fibre reinforced materials. Such a study, however, is not possible without also considering the effects of the volume fraction, as will soon be apparent.

1.2.3.1 Continuous-Fibre Reinforced Materials

Most common continuous-fibre reinforced materials are reinforced either unidirectionally, bi-axially or randomly. For the purposes of this discussion, however, only unidirectional reinforcement will be considered. The remaining forms will be discussed later in the section on the effects of orientation.

Consider the small element of unidirectionally reinforced material indicated in Figure 1.1 and assume the following conditions:

- 1) the fibres all have the same strength, uniform size and shape and are fully bonded to the matrix, i.e., no slippage can occur at the interface
- 2) they are aligned parallel to the tension axis and are completely surrounded by matrix
- 3) they are dispersed throughout the composite
- 4) both the fibres and the matrix are Hookean substances.

It is apparent from the figure that the total load or composite load, F_c , is shared between the fibres which carry a load F_f , and the matrix which carries a load F_m . Therefore,

$$F_c = F_f + F_m \quad (1-1)$$

or, in terms of stresses,

$$\sigma_c A_c = \sigma_f A_f + \sigma_m A_m \quad (1-2)$$

thus

$$\sigma_c = \sigma_f (A_f/A_c) + \sigma_m (A_m/A_c) \quad (1-3)$$

where σ and A represent stress and area respectively.

However, the area ratios, (A_f/A_c) and (A_m/A_c) , are in fact the volume fractions of the fibre, V_f , and of the matrix, V_m , in the composite. Therefore,

$$\sigma_c = \sigma_f V_f + \sigma_m V_m \quad (1-4)$$

Since both the fibres and the matrix are assumed to behave elastically,

$$\sigma_c = E_f \epsilon_f V_f + E_m \epsilon_m V_m \quad (1-5)$$

where E denotes elastic modulus and ϵ strain.

Also from condition (1),

$$\epsilon_c = \epsilon_f = \epsilon_m \quad (1-6)$$

hence,

$$\sigma_c = E_f \epsilon_c V_f + E_m \epsilon_c V_m \quad (1-7)$$

or

$$(\sigma_c/\epsilon_c) = E_f V_f + E_m V_m \quad (1-8)$$

Equation (1-8) indicates that the stress-strain behaviour of the composite is also linear. Consequently, the equation can assume the form

$$E_c = E_f V_f + E_m V_m \quad (1-9)$$

where E_c is the elastic modulus of the composite.

Equations (1-4) and (1-9) both follow the so-called "rule of mixtures". According to this rule, a particular

composite property is dependent upon that same property of the fibre and of the matrix and upon their respective volume fractions. The general form of equations following this rule is

$$P_c = P_f V_f + P_m V_m \quad (1-10)$$

or, since

$$V_m = 1 - V_f \quad (1-11)$$

$$P_c = P_f V_f + P_m (1 - V_f) \quad (1-12)$$

where P represents the particular property of interest e.g., E.

The effect of fibre volume fraction on the initial modulus of a theoretical glass fibre/polyester resin composite is illustrated graphically in Figure 1.2. According to equation (1-9), which is the basis for the graph, composite modulus is a linear function of the fibre volume fraction throughout the range of possible values. This obviously cannot be true since the maximum volume fraction of cylindrical fibres which can be packed into a composite is only approximately 93 percent. Furthermore, according to Broutman (6), when fibre volume fractions exceed 0.8, properties are usually found to drop off because of the inability of the matrix to wet and infiltrate the bundles of fibres.

In Figure 1.3, the general deformation process for a unidirectionally reinforced material is shown. It is

commonly accepted (7,8) that the deformation proceeds in four stages:

Stage I - both the fibres and matrix deform elastically

Stage II - the fibres continue to deform elastically,
but the matrix now deforms plastically

Stage III - the fibres and matrix deform plastically

Stage IV - the fibres fracture followed by composite fracture.

The stress-strain behaviour of idealized composites, such as those assumed earlier in this section, is described entirely by Stage I of the graph. More typical brittle fibre/plastic matrix composites go through Stages I and II before their ultimate failure. It is only with ductile fibre/ductile matrix composites that all four stages of deformation are encountered. Glass fibre/polyester materials are typical of brittle fibre/plastic matrix composites and steel wire/epoxy of the latter type.

Clearly, unidirectional fibre reinforcement significantly improves the composite properties in the direction of the fibres. It must be pointed out, however, that the fibres have a far less beneficial effect on the transverse properties, i.e., in the x and z directions (refer to Figure 1.1). Generally, they tend to increase the stiffness in these directions without significantly improving the related strengths. Thus, composites of this

type are frequently relatively brittle transverse to the primary direction of reinforcement.

1.2.3.2 Discontinuous-Fibre Reinforced Materials

In discontinuous-fibre reinforced materials, the relatively short reinforcing fibres are generally dispersed randomly throughout the composite. However, to facilitate understanding, discussions herein will be limited, as in the previous section, to the case of reinforcing fibres aligned parallel to each other and to the tensile load axis.

From Figure 1.4, it is apparent that an applied tensile load is shared by the fibres and the matrix in much the same way that it was in the continuously reinforced sample. In this case, however, the maximum load carrying capability of a given fibre may not be dependent upon its breaking strength; it may instead pull out of the matrix before it is fully stressed.

Consider the load on an individual fibre, such as the one indicated in the figure. This load, f_f , can be related to both the fibre stress,

$$f_f = \sigma_f (\pi d_f^2 / 4) \quad (1-13)$$

and to the shear stress at the fibre/matrix interface,

$$f_f = \tau_m \pi d_f l \quad (1-14)$$

where σ_f is the tensile stress in the fibre

τ_m is the shear stress at the fibre/resin interface

d_f is the fibre diameter

l is the length of the fibre embedded in the matrix.

Thus, the fibre will pull out of the matrix when the load is less than that which causes tensile failure, but greater than that which induces a shear failure, i.e., when τ_m becomes higher than the allowable shear stress, τ'_m , of the matrix or of the interfacial bonding agent (whichever is smaller). The load carrying capability of the fibre is therefore dependent entirely upon the length, l , of fibre embedded in the matrix, or

$$f_f = \tau'_m \pi d_f l \quad (1-15)$$

This length, l , is limited however to the range of values

$$0 < l \leq l' \quad (1-16)$$

where l' represents the value of l at which the fibre tensile strength, σ'_f , is reached.

At this point where both fibre tensile and matrix shear failures are possible,

$$f'_f = \sigma'_f (\pi d_f^2 / 4) \quad (1-17)$$

and

$$f'_f = \tau'_m \pi d_f l' \quad (1-18)$$

hence,

$$\sigma'_f (\pi d_f^2 / 4) = \tau'_m \pi d_f l' \quad (1-19)$$

or

$$l' = (1/4) (\sigma'_f / \tau'_m) d_f \quad (1-20)$$

To attain this condition, the fibre has to be

twice this length, i.e., $2l'$ (since it must be embedded to the same depth in the matrix on both sides of the cross section). The fibre length in this special case is termed the critical fibre length, L_c , and, since $L_c = 2l'$, is defined by

$$L_c = (1/2)(\sigma'_f/\tau'_m)d_f \quad (1-21)$$

where L_c is the critical fibre length

σ'_f is the fibre tensile strength

τ'_m is the allowable shear stress of the matrix or of the interconstituent binding agent, whichever is smaller

d_f is the fibre diameter.

Kelly and Tyson (9) have derived an equation which shows the relationship between the strength of discontinuous fibre composites and fibre length:

$$\sigma_c = \sigma_f V_f \left(1 - \left(\frac{1}{2\alpha}\right)\right) + \sigma_m (1 - V_f) \quad (1-22)$$

where α is the ratio of the actual fibre length to the critical fibre length (L/L_c). Due to its obvious similarity to the "rule of mixtures" equations developed earlier for continuous-fibre reinforced composites, it is frequently referred to as the "modified rule of mixtures".

Equation (1-22) indicates that discontinuous fibres will not contribute 100 percent of their strength to the composite. Nevertheless, they should contribute

almost as much strength as continuous fibre reinforcements if they are sufficiently long. For example, theoretically when $L/L_c = 10$, 95 percent of the fibre strength is contributed; with $L/L_c = 100$, 99.5 percent. This is an extremely important point as the strongest materials known at this time are the short single crystals commonly referred to as whiskers (see Table 1.1). Whiskers typically have aspect ratios ranging between 150 and 2500.

An additional point of interest arising from this brief study concerns the breaking of a fibre in a continuous fibre composite. It is clear from the foregoing that even when a fibre breaks, it does not stop being useful as a load carrying member. After breaking, the remaining portions will take up and carry load in much the same way as discontinuous fibre reinforcements. Only in the region of the fracture will the composite strength decrease slightly.

1.2.4 Fibre Orientation Effects

Fibre orientation has a very pronounced effect on the properties of both continuous and discontinuous-fibre reinforced materials. In particular, it will determine whether a fibre provides unidirectional, bidimensional (planar) or tridimensional reinforcement. Various conditions of fibre orientation are illustrated in Figure 1.5.

1.2.4.1 Unidirectional Reinforcement

The maximum possible composite strength and modulus are obtained when all of the reinforcing fibres are aligned parallel to one another. These maximum properties, however, are attained only in the fibre axis direction; the composite strength in the two orthogonal directions is in general no better than that of the matrix. Unfortunately, there are relatively few applications for purely unidirectionally reinforced materials; seldom are uniaxial loads encountered in practice.

One way of getting around this problem, at least in the case of continuous reinforcement, is to combine layers of unidirectionally reinforced materials to form composite laminates with biaxial load carrying capabilities. The advantage of this method is that laminate properties can be closely tailored to meet the anticipated loading conditions. For example, in a pressure vessel application, the ratio of hoop to longitudinal layers would be 2 to 1. In this way, extremely efficient structures can be achieved. Filament wound pipes and tanks are two examples of the application of this principle.

Discontinuous reinforcements, as was pointed out earlier, are generally oriented randomly in their composites. Unidirectional reinforcement is occasionally encountered in practice, however. For example, an extruded reinforced thermoplastic rod of limited cross section will

likely have at least the majority, if not all, of its fibres oriented in the axial direction because the fibres tend to align themselves in the direction of the melt flow at the die orifice and are subsequently frozen in that position. A similar condition is encountered in the injection-moulding of parts such as bars, rods or channels of limited cross section.

1.2.4.2 Bidimensional Reinforcement

Bidimensional reinforcement is achieved by constraining the orientation of the reinforcing fibres to a plane rather than to a direction. This results in composites with improved strength and modulus properties in two dimensions compared to one in the unidirectional case. The out-of-plane dimension remains effectively unreinforced.

The improvement in planar properties in this case can never equal that realized in the direction of the fibres with unidirectional reinforcement. The composite strength and modulus properties of planar reinforced materials will seldom be higher than 50 percent of those attainable through complete fibre alignment.

Bidimensional, or planar, reinforcement can be accomplished by using either continuous or discontinuous fibres. In the case of continuous fibres, there are two ways of obtaining planar reinforcement. The first method

is to weave the fibres into a fabric and subsequently to combine it with the matrix material. The second is to orient the fibres randomly in-plane, either during the manufacture of the composite or in a preforming operation such as that used in the production of continuous strand mat. Woven fabric, chopped and continuous strand mat materials are pictured in Figure 1.6, along with another form of woven reinforcement commonly known as woven roving. It is clear from Figure 1.6 that the woven materials actually provide bidirectional rather than bidimensional reinforcement.

Discontinuous fibres are generally oriented randomly in composite materials. In the bidimensional case, the fibres are oriented randomly in-plane, which yields a material with planar properties which are not directionally dependent, i.e., they are quasi-isotropic. Composites of this kind are commonly produced by:

- a) spraying up a combination of chopped strand glass and a thermosetting plastic resin onto a mould surface
- b) laying-up (by hand) a preformed chopped strand mat material in combination with a thermosetting resin
- c) sheet extrusion of discontinuous-fibre reinforced thermoplastic film, and
- d) injection-moulding of reinforced thermoplastic parts having thin, planar sections.

The most widely used fibre-reinforced composites

today are those which are bidimensionally reinforced. Storage tanks, boats, cars and a myriad of other products are produced by laminating together assorted combinations of woven fabric (or roving), chopped strand mat and chopped fibre (through the spray-up process).

1.2.4.3 Tridimensional Reinforcement

The most common way of achieving tridimensional reinforcement is through the use of randomly oriented discontinuous fibres. It is also possible by using three-dimensionally woven fabrics (10) or continuous fibres oriented randomly throughout the matrix, but these methods are seldom employed in practice.

Material properties in this case depend substantially on the shape of the part being produced and the manufacturing process involved. For example, in the extrusion of a thick cross section, the properties may tend to be a little higher in the direction of extrusion than in the transverse directions. A complex injection-moulded RTP part might even have unidirectional, planar and quasi-isotropic tridimensional reinforcement, all within the same part.

Processes for the production of parts reinforced three-dimensionally include (1) the extrusion of RTP shapes, (2) the injection-moulding of RTP products, and (3) the press moulding of bulk moulding compounds

(premixed thermosetting plastic resin and chopped strand fibres).

1.3 CLOSING

The foregoing brief review of the fundamentals of reinforcement provides little more than a basis for discussing the various methods of analyzing composite structures. It is left to the individual to pursue the subject further in the references noted.

SECTION 2
STRESS ANALYSIS OF
FIBRE-REINFORCED COMPOSITE STRUCTURES

As Tsai and Adams (11) have stated, many engineers involved in the design of fibre-reinforced composite structures "talk about composites but think in terms of isotropic homogeneous materials". This quotation aptly describes the foremost problem of the FRP industry today. Until more engineers learn to think in terms of the highly directional effects of fibre reinforcement, the use of fibrous composites in structural applications will be severely constrained.

In the past, very few undergraduate courses in design or strength of materials did more than acknowledge the existence of anisotropic materials, let alone teach the student how to work with them. Further, constituent material suppliers appear to play down the potential anisotropy of fibre-reinforced composites in their design literature for the commercial FRP industry (12, 13, 14). Instead of pursuing the potential advantages of directional reinforcement, they create the impression (perhaps for marketing purposes) that fibre-reinforced plastics are generally isotropic and that "in most cases, the standard

engineering formulas apply" (13, 14).

Only in the aerospace field have the problems of designing with composite materials been taken seriously. There, the need for lighter, more efficient structures has induced numerous government and industry sponsored research and development programs to study these problems. As a result, a new method of analysis has evolved in recent years which makes it relatively easy for an engineer to "think composites" and hence to design much more efficient fibrous structures.

2.1 PREVAILING METHODS

The stress analysis of fibre-reinforced composite structures is generally accomplished by making one of three fundamental assumptions relative to the composite material behaviour:

- 1) that fibre-reinforced composites are not substantially different from other common engineering materials, i.e., they are isotropic
- 2) that only the fibres have load carrying capabilities
- 3) that fibre-reinforced composites generally consist of a series of homogeneous orthotropic layers.

These assumptions provide the basis for three entirely different methods of analyzing composite material structures.

2.1.1 The Strength of Materials Approach

The strength of materials approach, based upon the use of generally available strength of materials design formulas, is without doubt the most widely used in the design of reinforced structures in the FRP industry at the present time.

Unfortunately, it is also the most imprecise. In order to make use of these conventional design formulas, originally developed for homogeneous isotropic materials, one must accept the first of the assumptions noted above. This, it will soon be seen, can lead to very serious problems.

Consider the case of an FRP laminate subjected to a bending load as is shown in Figure 2.1. Using the strength of materials approach, the maximum flexural stresses would be predicted by the flexural formula (15)

$$\sigma_{\text{MAX}} = \frac{Mc}{I} \quad (2-1)$$

where σ_{MAX} is the maximum resultant stress

M is the applied bending moment

c is the distance from the neutral axis to the most remote point in the beam at the section of interest

I is the moment of inertia of the cross section.

The resulting predictions may in fact be

substantially in error, however, depending upon the construction of the laminate. For example, if layer 1 of the laminate shown in Figure 2.1 is somewhat stiffer than layers 2 or 3, e.g., $E^{(1)}$ is twice $E^{(2)}$ or $E^{(3)}$, the stress at the outer surface will be considerably higher than the value predicted by equation (2-1). Alternatively, layer 2 might be considerably stiffer than either layers 1 or 3 in which case it is quite possible that the maximum stresses would be at the layer interfaces and not at the outer surfaces at all.

Similar arguments can be employed to show that serious errors are possible with many of the commonly used strength of materials design formulas. The magnitude of the error generally depends upon the variation in the constituent layer strength and modulus properties. In quasi-isotropic laminates, e.g., a chopped strand mat laminate, stresses predicted by the conventional formulas are probably fairly accurate. However, if the same formulas were used to compute the equivalent stresses in similarly loaded laminates comprising layers with substantially different properties, e.g., mat and unidirectional reinforcement, errors of 100 percent or more are possible.

Clearly, the effectiveness of the strength of materials approach to laminate analysis is substantially dependent upon the degree of material anisotropy involved,

i.e., the approach works best for nearly isotropic laminates. Further, since relatively few commercial laminates, apart from those produced by the filament winding process, are significantly anisotropic, this may perhaps explain in part the continued predominance of this approach.

Use of the method of equivalent sections (16) in conjunction with the conventional formulas, as suggested by the engineers of Gibbs and Cox, Inc. (17) enables a much more accurate laminate analysis. Unfortunately, this involves a large number of computations and appears to have discouraged most designers from using it.

It can thus be concluded that the strength of materials approach to the analysis of composite structures should be employed only if sufficient consideration is given to the properties of the individual layers and to the limitations of the particular formulas involved.

2.1.2 Netting Analysis

The development of the filament winding process in 1947 (18) firmly established the need for improved analytical techniques. It became immediately apparent that filament wound composites were not isotropic and that traditional design formulas could no longer be applied. As a result, a new method known as netting analysis came into wide use soon after the introduction of the process.

Netting analysis is based upon the assumption that only the reinforcing fibres have load carrying capability; it is used principally in the analysis of pressure vessels where all fibres are in tension. The only functions of the resin, it assumes, are to hold the fibres in position and to distribute the stress throughout the structure. It cannot, therefore, be used to determine bending, shear or discontinuity stresses or resistance to buckling (19) since in these cases resin properties are of prime importance.

The underlying principles of netting analysis can be readily demonstrated. Consider the system of forces acting on the fibres in Figure 2.2. The resultant force or load carrying capability in the direction of the fibres is given by

$$F_{hel} = F_s S_{hel} L_{hel} \quad (2-2)$$

where F_{hel} is the force per inch in the direction of the fibres

F_s is the force per strand

S_{hel} is the number of strands per inch per layer

L_{hel} is the number of helically wound layers

and its components in the hoop and longitudinal directions are

$$F_{ho} = F_s S_{hel} L_{hel} \sin^2 \theta \quad (2-3)$$

and

$$F_L = F_s S_{hel} L_{hel} \cos^2 \theta \quad (2-4)$$

respectively.

In a thin walled pressure vessel, the hoop stress

$$\sigma_{ho} = \frac{Pd}{2t} \quad (2-5)$$

is twice the longitudinal stress

$$\sigma_L = \frac{Pd}{4t} \quad (2-6)$$

Also,

$$F_{ho} = \sigma_{ho} t \quad (2-7)$$

and

$$F_L = \sigma_L t = \frac{\sigma_{ho} t}{2} \quad (2-8)$$

therefore,

$$\frac{F_{ho}}{F_L} = 2 \quad (2-9)$$

Substitution of Expressions (2-3) and (2-4) for F_{ho} and F_L respectively yields

$$\frac{F_s S_{hel} L_{hel} \sin^2 \theta}{F_s S_{hel} L_{hel} \cos^2 \theta} = 2 \quad (2-10)$$

which immediately reduces to

$$\tan^2 \theta = 2 \quad (2-11)$$

thus

$$\theta = 54.75^\circ \quad (2-12)$$

This indicates that, in order to obtain maximum structural efficiency in a filament wound pressure vessel, a wind (helix) angle of 54.75° should be employed. Hydrostatic tests conducted on pressure vessels so wound have demonstrated the practical validity of this value (20).

It is, however, generally easier to manufacture filament wound pressure vessels by using a combination of a low helix angle wind pattern and straight hoop winding. In this instance, the analysis proceeds in much the same way as was demonstrated in the foregoing.

The load carrying capability of the helically wound layers is once again resolved into hoop and longitudinal components. Thus

$$F_{ho} = F_s S_{hel} L_{hel} \sin^2 \theta \quad (2-13)$$

and

$$F_L = F_s S_{hel} L_{hel} \cos^2 \theta \quad (2-14)$$

However, the extra hoop layers now provide an additional load carrying capability in the hoop direction

$$F'_{ho} = F_s S_{ho} L_{ho} \quad (2-15)$$

Therefore, the total resultant force or load carrying ability of the laminate in the hoop direction is

$$F_{Ho} = F_{ho} + F'_{ho} \quad (2-16)$$

$$= F_s S_{hel} L_{hel} \sin^2 \theta + F_s S_{ho} L_{ho} \quad (2-17)$$

and in the longitudinal direction

$$F_L = F_s S_{hel} L_{hel} \cos^2 \theta \quad (2-18)$$

Clearly, though limited in application, netting analysis is a relatively easy method with which to work.

2.1.3 Orthotropic Lamina Approach

This approach (21, 22, 23) is based upon the previously noted hypothesis that the individual layers of a laminate are homogeneous and orthotropic. It was used for many years in the study of plywood structures prior to being adopted for the analysis of FRP laminates. A prime reference (23) on this subject issued by the United States Department of Defense "as an aid in the design of reinforced plastic elements for aircraft missiles and other flight vehicles" was in fact prepared largely by the Forest Products Laboratory of the Department of Agriculture.

Fischer (21) outlined the principal assumptions of the method in his paper on the analysis of fibreglass laminates:

- 1) a layer of fibreglass is elastic and homogeneous
- 2) a layer of fibreglass is orthotropic (has different strength properties parallel to two orthogonal axes which are the natural axes of the material)
- 3) layers in a fibreglass laminate are connected by a material that has infinite shear rigidity
- 4) dimensions of the fibreglass laminate are such that buckling will not occur.

Although all of these assumptions refer specifically to fibreglass, they are equally valid for other forms of fibre reinforcement, e.g., carbon fibres. Furthermore, the second of these assumptions does not preclude the analysis of

laminates consisting of isotropic as well as orthotropic layers; the response characteristics of an isotropic layer are entirely described by orthotropic stress-strain relationships.

Orthotropic layers within a laminate, comprising either of the first two forms of reinforcement shown in Figure 2.3, have a natural system of orthogonal axes corresponding to the warp and fill directions of the reinforcing material. The other common forms of reinforcement shown in the figure do not have a natural system of axes and, since their in-plane properties are not directionally dependent, co-ordinate axes can be arbitrarily selected. The relationship between strains and stresses in the natural (or arbitrarily selected) co-ordinate system of such materials is

$$\left. \begin{aligned} \epsilon_1 &= \frac{\sigma_1}{E_1} - \nu_{21} \frac{\sigma_2}{E_2} \\ \epsilon_2 &= \frac{\sigma_2}{E_2} - \nu_{12} \frac{\sigma_1}{E_1} \\ \gamma_{12} &= \frac{\tau_{12}}{G_{12}} \end{aligned} \right\} (2-19)$$

Also, by solving these equations for the stresses,

$$\left. \begin{aligned} \sigma_1 &= \frac{E_1}{1 - \nu_{12}\nu_{21}} \epsilon_1 + \frac{\nu_{21}E_1}{1 - \nu_{12}\nu_{21}} \epsilon_2 \\ \sigma_2 &= \frac{\nu_{12}E_2}{1 - \nu_{12}\nu_{21}} \epsilon_1 + \frac{E_2}{1 - \nu_{12}\nu_{21}} \epsilon_2 \\ \tau_{12} &= G_{12}\gamma_{12} \end{aligned} \right\} (2-20)$$

In many cases, however, the natural co-ordinate system (1,2) of an individual layer does not coincide with the co-ordinate system (x,y) of the laminated structure of which it is a part. This situation is illustrated in Figure 2.4 where the natural axes (1,2) of the layer material are separated from the laminate axes (x,y) by an angle θ . The material stress-strain relationship in this case, i.e., in the (x,y) co-ordinate system is:

$$\left. \begin{aligned} \sigma_x &= b_{11}\epsilon_x + b_{12}\epsilon_y + b_{13}\gamma_{xy} \\ \sigma_y &= b_{21}\epsilon_x + b_{22}\epsilon_y + b_{23}\gamma_{xy} \\ \tau_{xy} &= b_{31}\epsilon_x + b_{32}\epsilon_y + b_{33}\gamma_{xy} \end{aligned} \right\} \quad (2-21)$$

where

$$\begin{aligned} b_{11} &= \phi(E_1 \cos^4 \theta + E_2 \sin^4 \theta + (2\nu_{21}E_1 + 4\lambda G_{12}) \sin^2 \theta \cos^2 \theta) \\ b_{12} &= \phi((E_1 + E_2 - 4\lambda G_{12}) \sin^2 \theta \cos^2 \theta + \nu_{21}E_1 (\cos^4 \theta + \sin^4 \theta)) \\ b_{13} &= \phi((E_2 - \nu_{21}E_1 - 2\lambda G_{12}) \sin^3 \theta \cos \theta - \\ &\quad (E_1 - \nu_{21}E_1 - 2\lambda G_{12}) \sin \theta \cos^3 \theta) \\ b_{21} &= b_{12} \\ b_{22} &= \phi(E_2 \cos^4 \theta + E_1 \sin^4 \theta + (2\nu_{21}E_1 + 4\lambda G_{12}) \sin^2 \theta \cos^2 \theta) \\ b_{23} &= \phi((E_2 - \nu_{21}E_1 - 2\lambda G_{12}) \sin \theta \cos^3 \theta - \\ &\quad (E_1 - \nu_{21}E_1 - 2\lambda G_{12}) \sin^3 \theta \cos \theta) \\ b_{31} &= b_{13} \\ b_{32} &= b_{23} \\ b_{33} &= \phi((E_1 + E_2 - 2\nu_{21}E_1) \sin^2 \theta \cos^2 \theta + \lambda G_{12} (\cos^2 \theta - \sin^2 \theta)^2) \end{aligned}$$

....(2-22)

and

$$\lambda = (1/\phi) = 1 - \nu_{12}\nu_{21} \quad (2-23)$$

It must therefore be generally assumed, for analytical purposes, that the non-alignment condition exists in all layers. Consider a laminate comprising n orthotropic layers oriented at angles of $\theta^{(1)}, \theta^{(2)}, \theta^{(3)}, \theta^{(k)} \dots \theta^{(n)}$, respectively, relative to the laminate axes, x and y . The relationships between stresses and strains can be written

$$\left. \begin{aligned} \sigma_x^{(1)} &= b_{11}^{(1)} \epsilon_x^{(1)} + b_{12}^{(1)} \epsilon_y^{(1)} + b_{13}^{(1)} \gamma_{xy}^{(1)} \\ \sigma_y^{(1)} &= b_{21}^{(1)} \epsilon_x^{(1)} + b_{22}^{(1)} \epsilon_y^{(1)} + b_{23}^{(1)} \gamma_{xy}^{(1)} \\ \tau_{xy}^{(1)} &= b_{31}^{(1)} \epsilon_x^{(1)} + b_{32}^{(1)} \epsilon_y^{(1)} + b_{33}^{(1)} \gamma_{xy}^{(1)} \end{aligned} \right\} \quad (2-24)$$

for the first layer, or more generally,

$$\left. \begin{aligned} \sigma_x^{(k)} &= b_{11}^{(k)} \epsilon_x^{(k)} + b_{12}^{(k)} \epsilon_y^{(k)} + b_{13}^{(k)} \gamma_{xy}^{(k)} \\ \sigma_y^{(k)} &= b_{21}^{(k)} \epsilon_x^{(k)} + b_{22}^{(k)} \epsilon_y^{(k)} + b_{23}^{(k)} \gamma_{xy}^{(k)} \\ \tau_{xy}^{(k)} &= b_{31}^{(k)} \epsilon_x^{(k)} + b_{32}^{(k)} \epsilon_y^{(k)} + b_{33}^{(k)} \gamma_{xy}^{(k)} \end{aligned} \right\} \quad (2-25)$$

for the k th layer.

When such a laminate is subjected to normal and shear stresses (with respect to the x and y axes), the layers within it must deform together. Thus, in order to satisfy the strain compatibility condition,

$$\left. \begin{aligned} \epsilon_x^{(1)} &= \epsilon_x^{(2)} = \dots = \epsilon_x^{(k)} = \dots = \epsilon_x^{(n)} = \epsilon_x \\ \epsilon_y^{(1)} &= \epsilon_y^{(2)} = \dots = \epsilon_y^{(k)} = \dots = \epsilon_y^{(n)} = \epsilon_y \\ \gamma_{xy}^{(1)} &= \gamma_{xy}^{(2)} = \dots = \gamma_{xy}^{(k)} = \dots = \gamma_{xy}^{(n)} = \gamma_{xy} \end{aligned} \right\} \quad (2-26)$$

and hence equations (2-25) simplify to

$$\left. \begin{aligned} \sigma_x^{(k)} &= b_{11}^{(k)} \epsilon_x + b_{12}^{(k)} \epsilon_y + b_{13}^{(k)} \gamma_{xy} \\ \sigma_y^{(k)} &= b_{21}^{(k)} \epsilon_x + b_{22}^{(k)} \epsilon_y + b_{23}^{(k)} \gamma_{xy} \\ \tau_{xy}^{(k)} &= b_{31}^{(k)} \epsilon_x + b_{32}^{(k)} \epsilon_y + b_{33}^{(k)} \gamma_{xy} \end{aligned} \right\} (2-27)$$

In addition, from force equilibrium considerations, it is apparent that

$$\left. \begin{aligned} \bar{\sigma}_x t &= \sigma_x^{(1)} t^{(1)} + \sigma_x^{(2)} t^{(2)} + \dots + \sigma_x^{(k)} t^{(k)} + \dots + \sigma_x^{(n)} t^{(n)} \\ \bar{\sigma}_y t &= \sigma_y^{(1)} t^{(1)} + \sigma_y^{(2)} t^{(2)} + \dots + \sigma_y^{(k)} t^{(k)} + \dots + \sigma_y^{(n)} t^{(n)} \\ \bar{\tau}_{xy} t &= \tau_{xy}^{(1)} t^{(1)} + \tau_{xy}^{(2)} t^{(2)} + \dots + \tau_{xy}^{(k)} t^{(k)} + \dots + \tau_{xy}^{(n)} t^{(n)} \end{aligned} \right\} (2-28)$$

or, more concisely,

$$\left. \begin{aligned} \bar{\sigma}_x &= \frac{1}{t} \sum_{k=1}^n \sigma_x^{(k)} t^{(k)} \\ \bar{\sigma}_y &= \frac{1}{t} \sum_{k=1}^n \sigma_y^{(k)} t^{(k)} \\ \bar{\tau}_{xy} &= \frac{1}{t} \sum_{k=1}^n \tau_{xy}^{(k)} t^{(k)} \end{aligned} \right\} (2-29)$$

where t is the total laminate thickness and $t^{(k)}$ is the thickness of the k th layer.

Substitution of the expressions for the layer stresses given in equations (2-25) then yields

$$\left. \begin{aligned} \bar{\sigma}_x &= \frac{1}{t} \sum_{k=1}^n (b_{11}^{(k)} \epsilon_x + b_{12}^{(k)} \epsilon_y + b_{13}^{(k)} \gamma_{xy}) t^{(k)} \\ \bar{\sigma}_y &= \frac{1}{t} \sum_{k=1}^n (b_{21}^{(k)} \epsilon_x + b_{22}^{(k)} \epsilon_y + b_{23}^{(k)} \gamma_{xy}) t^{(k)} \\ \bar{\tau}_{xy} &= \frac{1}{t} \sum_{k=1}^n (b_{31}^{(k)} \epsilon_x + b_{32}^{(k)} \epsilon_y + b_{33}^{(k)} \gamma_{xy}) t^{(k)} \end{aligned} \right\} (2-30)$$

and hence

$$\left. \begin{aligned} \bar{\sigma}_x &= \left[\frac{1}{t} \sum_{k=1}^n b_{11}^{(k)} t^{(k)} \right] \epsilon_x + \left[\frac{1}{t} \sum_{k=1}^n b_{12}^{(k)} t^{(k)} \right] \epsilon_y + \left[\frac{1}{t} \sum_{k=1}^n b_{13}^{(k)} t^{(k)} \right] \gamma_{xy} \\ \bar{\sigma}_y &= \left[\frac{1}{t} \sum_{k=1}^n b_{21}^{(k)} t^{(k)} \right] \epsilon_x + \left[\frac{1}{t} \sum_{k=1}^n b_{22}^{(k)} t^{(k)} \right] \epsilon_y + \left[\frac{1}{t} \sum_{k=1}^n b_{23}^{(k)} t^{(k)} \right] \gamma_{xy} \\ \bar{\tau}_{xy} &= \left[\frac{1}{t} \sum_{k=1}^n b_{31}^{(k)} t^{(k)} \right] \epsilon_x + \left[\frac{1}{t} \sum_{k=1}^n b_{32}^{(k)} t^{(k)} \right] \epsilon_y + \left[\frac{1}{t} \sum_{k=1}^n b_{33}^{(k)} t^{(k)} \right] \gamma_{xy} \end{aligned} \right\} (2-31)$$

This can also be written

$$\left. \begin{aligned} \bar{\sigma}_x &= \bar{b}_{11} \epsilon_x + \bar{b}_{12} \epsilon_y + \bar{b}_{13} \gamma_{xy} \\ \bar{\sigma}_y &= \bar{b}_{21} \epsilon_x + \bar{b}_{22} \epsilon_y + \bar{b}_{23} \gamma_{xy} \\ \bar{\tau}_{xy} &= \bar{b}_{31} \epsilon_x + \bar{b}_{32} \epsilon_y + \bar{b}_{33} \gamma_{xy} \end{aligned} \right\} (2-32)$$

where

$$\left. \begin{aligned} \bar{b}_{11} &= \frac{1}{t} \sum_{k=1}^n b_{11}^{(k)} t^{(k)} \\ \bar{b}_{12} &= \frac{1}{t} \sum_{k=1}^n b_{12}^{(k)} t^{(k)} \end{aligned} \right\} (2-33)$$

etc.

It is evident from the foregoing that laminate elastic properties are quite predictable when the properties of the constituent layers and their geometry are known. Further, it is possible to obtain a reasonably good estimate of the strength properties of a laminate in its principal directions.

In order to determine the load carrying capability of a laminate in, for example, the x direction, equations (2-32) are first solved for the laminate/layer strains

ϵ_x , ϵ_y and γ_{xy} by assuming the loads in the other two directions, $\bar{\sigma}_y$ and $\bar{\tau}_{xy}$, to be zero. As a result, expressions for the layer strains are obtained in terms of the load $\bar{\sigma}_x$, i.e.,

$$\begin{aligned}\epsilon_x &= \left[(\bar{b}_{22}\bar{b}_{33} - \bar{b}_{23}^2) / D \right] \bar{\sigma}_x \\ \epsilon_y &= \left[(\bar{b}_{13}\bar{b}_{23} - \bar{b}_{12}\bar{b}_{33}) / D \right] \bar{\sigma}_x \\ \gamma_{xy} &= \left[(\bar{b}_{12}\bar{b}_{23} - \bar{b}_{13}\bar{b}_{22}) / D \right] \bar{\sigma}_x\end{aligned}\quad (2-34)$$

where

$$D = \bar{b}_{11}\bar{b}_{22}\bar{b}_{33} - \bar{b}_{12}^2\bar{b}_{33} - \bar{b}_{13}^2\bar{b}_{22} - \bar{b}_{11}\bar{b}_{23}^2 + 2\bar{b}_{12}\bar{b}_{13}\bar{b}_{23}$$

Then, through the use of the strain transformation equations,

$$\left. \begin{aligned}\epsilon_1^{(k)} &= \epsilon_x \cos^2 \theta^{(k)} + \epsilon_y \sin^2 \theta^{(k)} - \gamma_{xy} \sin \theta^{(k)} \cos \theta^{(k)} \\ \epsilon_2^{(k)} &= \epsilon_x \sin^2 \theta^{(k)} + \epsilon_y \cos^2 \theta^{(k)} + \gamma_{xy} \sin \theta^{(k)} \cos \theta^{(k)} \\ \gamma_{12}^{(k)} &= 2(\epsilon_x - \epsilon_y) \sin \theta^{(k)} \cos \theta^{(k)} + \gamma_{xy} (\cos^2 \theta^{(k)} - \sin^2 \theta^{(k)})\end{aligned}\right\} (2-35)$$

and the layer constitutive equations (2-20), the principal strains and stresses in each layer, i.e., those in the directions of the natural axes of the material, can be defined in terms of $\bar{\sigma}_x$. Subsequent failure analysis of each layer reveals the minimum value of $\bar{\sigma}_x$ at which one of the layers will fail. This minimum value is the maximum load carrying capability of the laminate in the x direction. Similar analyses can be used to determine equivalent values for $\bar{\sigma}_y$ and $\bar{\tau}_{xy}$.

Although failure analysis will not be pursued at this time, full details are provided later in Section 4.6.

Clearly, this method of analysis is considerably

better than those described previously. It recognizes not only that the matrix plays an important structural role, but also that the individual layer materials may be orthotropic rather than isotropic and quite different from one another.

Nevertheless, there is one major limitation: the inherent assumption of equations (2-26) (that component strains are constant through a laminate) precludes the analysis of laminates subjected to flexure. As a result, the method is substantially limited in its scope. Available literature (24, 25, 26) indicates that it is used mainly in the prediction of laminate tensile properties.

2.2 THE THEORY OF LAMINATED COMPOSITES

The concept of a laminate consisting of a number of orthotropic layers is quite reasonable. Unfortunately, the method of analysis generally associated with it until now, i.e., that described in the previous section, is too limited to be of general use, simply because no consideration is given to the problem of bending.

A powerful new method of analysis which obviates this problem has evolved in recent years. It is an extended form of conventional small deflection thin plate (and shell) theory which takes into account not only lamina orthotropy but also variations in material properties through the thickness of the laminate.

This extended form of plate and shell theory, sometimes referred to as the theory of laminated composites, differs from the conventional theory in two ways. First, during the development of the force and moment resultant equations, orthotropic layer stress-strain relationships, similar in form to equations (2-21), are used in place of the single set of constitutive equations which usually describe the behaviour of any arbitrarily selected element in the cross section of an isotropic plate or shell.

The second difference relates to the stress and failure analysis which ensues once deformations and strains have been determined. The points of maximum stress are generally assumed to be located at the outer surfaces of a deformed plate or shell. In the case of a composite laminate, however, the maximum stress and hence the initial point of failure may be located at almost any location in the cross section. Thus, strains and stresses must be determined in each layer in order to carry out a complete failure analysis.

Since this new method is, without doubt, the best currently available, it will be advantageous to study the underlying theory in some detail. In the next section, lamina stress-strain relationships previously assumed valid, i.e., equations (2-20) and (2-21), are developed and relevant lamina failure criteria discussed. In Section 4, laminate constitutive equations (force and moment resultant

equations) are developed by introducing the lamina stress-strain relationships into the conventional theory of plates and shells.

SECTION 3

LAMINA STRESS-STRAIN RELATIONSHIPS

The response characteristics of any FRP laminate can be predicted as long as the stress-strain relationships of the constituent layers, or lamina, are known. Regardless of the type of reinforcement, these constitutive equations are all variations of the generalized Hooke's Law.

3.1 HOOKE'S LAW

In the seventeenth century, Robert Hooke proposed the law now named after him in the words "Ut tensio sic vis" - the force varies as the stretch (27). This conclusion was drawn by Hooke as a result of his load-deformation studies with springs. Today, Hooke's Law is more commonly associated with the linear stress-strain relationship for elastic materials.

The modern definition of Hooke's Law states that, within the elastic limits of the material, the stress is directly proportional to the strain (28). Symbolically, this may be expressed by the equation

$$\sigma = E \epsilon \quad (3-1)$$

where the constant of proportionality, E, is called the elastic modulus, modulus of elasticity or Young's Modulus.

This equation describes the stress-strain relationship of a homogeneous isotropic material in a one-dimensional state of stress. The so-called generalized Hooke's Law relates stress and strain in an anisotropic material subjected to a three-dimensional stress state and can be expressed: each stress component is directly proportional to each strain component (27).

The stresses acting on the surface of a body can be resolved into three components parallel to the axes of an arbitrary co-ordinate system. Accordingly, the state of stress on a small cubic element at a point in the body, such as that shown in Figure 3.1, is completely described by nine stress components: three normal components - σ_{11} , σ_{22} , σ_{33} , and six shear components - σ_{12} , σ_{13} , σ_{23} , σ_{21} , σ_{31} , σ_{32} .

Strains are associated with the displacement of a point in the body. If the co-ordinates of a point in the body change from x_1, x_2, x_3 to $x_1 + u_1, x_2 + u_2, x_3 + u_3$ as a result of deformation, the u_i are the components of displacement and the strains are defined in terms of the u_i by the equations

$$\epsilon_{ij} = \frac{1}{2} \left[\frac{\partial u_i}{\partial x_j} + \frac{\partial u_j}{\partial x_i} \right] \quad (3-2)$$

where $i, j = 1, 2$ or 3 .

It can then readily be seen that there are the same number

of strain components as there are of stress, i.e., three normal components - ϵ_{11} , ϵ_{22} , ϵ_{33} , and six shear components - ϵ_{12} , ϵ_{13} , ϵ_{23} , ϵ_{21} , ϵ_{31} , ϵ_{32} .

The generalized Hooke's Law, in symbolic terms, is therefore:

$$\sigma_{11} = C_{1111}\epsilon_{11} + C_{1112}\epsilon_{12} + C_{1113}\epsilon_{13} + C_{1121}\epsilon_{21} + C_{1122}\epsilon_{22} + C_{1123}\epsilon_{23} + C_{1131}\epsilon_{31} + C_{1132}\epsilon_{32} + C_{1133}\epsilon_{33}$$

$$\sigma_{12} = C_{1211}\epsilon_{11} + C_{1212}\epsilon_{12} + C_{1213}\epsilon_{13} + C_{1221}\epsilon_{21} + C_{1222}\epsilon_{22} + C_{1223}\epsilon_{23} + C_{1231}\epsilon_{31} + C_{1232}\epsilon_{32} + C_{1233}\epsilon_{33}$$

$$\sigma_{13} = C_{1311}\epsilon_{11} + C_{1312}\epsilon_{12} + C_{1313}\epsilon_{13} + C_{1321}\epsilon_{21} + C_{1322}\epsilon_{22} + C_{1323}\epsilon_{23} + C_{1331}\epsilon_{31} + C_{1332}\epsilon_{32} + C_{1333}\epsilon_{33}$$

$$\sigma_{21} = C_{2111}\epsilon_{11} + C_{2112}\epsilon_{12} + C_{2113}\epsilon_{13} + C_{2121}\epsilon_{21} + C_{2122}\epsilon_{22} + C_{2123}\epsilon_{23} + C_{2131}\epsilon_{31} + C_{2132}\epsilon_{32} + C_{2133}\epsilon_{33}$$

$$\sigma_{22} = C_{2211}\epsilon_{11} + C_{2212}\epsilon_{12} + C_{2213}\epsilon_{13} + C_{2221}\epsilon_{21} + C_{2222}\epsilon_{22} + C_{2223}\epsilon_{23} + C_{2231}\epsilon_{31} + C_{2232}\epsilon_{32} + C_{2233}\epsilon_{33}$$

$$\sigma_{23} = C_{2311}\epsilon_{11} + C_{2312}\epsilon_{12} + C_{2313}\epsilon_{13} + C_{2321}\epsilon_{21} + C_{2322}\epsilon_{22} + C_{2323}\epsilon_{23} + C_{2331}\epsilon_{31} + C_{2332}\epsilon_{32} + C_{2333}\epsilon_{33}$$

$$\sigma_{31} = C_{3111}\epsilon_{11} + C_{3112}\epsilon_{12} + C_{3113}\epsilon_{13} + C_{3121}\epsilon_{21} + C_{3122}\epsilon_{22} + C_{3123}\epsilon_{23} + C_{3131}\epsilon_{31} + C_{3132}\epsilon_{32} + C_{3133}\epsilon_{33}$$

$$\sigma_{32} = C_{3211}\epsilon_{11} + C_{3212}\epsilon_{12} + C_{3213}\epsilon_{13} + C_{3221}\epsilon_{21} + C_{3222}\epsilon_{22} + C_{3223}\epsilon_{23} + C_{3231}\epsilon_{31} + C_{3232}\epsilon_{32} + C_{3233}\epsilon_{33}$$

$$\sigma_{33} = C_{3311}\epsilon_{11} + C_{3312}\epsilon_{12} + C_{3313}\epsilon_{13} + C_{3321}\epsilon_{21} + C_{3322}\epsilon_{22} + C_{3323}\epsilon_{23} + C_{3331}\epsilon_{31} + C_{3332}\epsilon_{32} + C_{3333}\epsilon_{33}$$

.... (3-3)

In these equations, there are eighty-one strain coefficients which are termed the elastic stiffnesses.

It can be shown by a thermodynamic argument (27)

that

$$C_{2211} = C_{1122}$$

$$C_{1211} = C_{1112}$$

$$C_{2312} = C_{1223}$$

or, in general,

$$C_{ijkl} = C_{klij} \quad (3-4)$$

Further, the condition for zero rotation of the element in Figure 3.1 is

$$\sigma_{ij} = \sigma_{ji} \quad (i \neq j) \quad (3-5)$$

since the sum of the moments about axes through the centre of the cube and parallel to the co-ordinate axes must equal zero.

From the definition of strain, equation (3-2), it can also be seen that

$$\epsilon_{12} = \epsilon_{21} = \frac{1}{2} \left[\frac{\partial u_1}{\partial x_2} + \frac{\partial u_2}{\partial x_1} \right]$$

or, in general,

$$\epsilon_{ij} = \epsilon_{ji} \quad (i \neq j) \quad (3-6)$$

Incorporation of relationships (3-4), (3-5) and (3-6) into expression (3-3) results in a simplification of the generalized Hooke's Law to

$$\begin{aligned} \sigma_{11} &= C_{1111} \epsilon_{11} + C_{1112} \epsilon_{12} + C_{1113} \epsilon_{13} + C_{1122} \epsilon_{22} + C_{1123} \epsilon_{23} + C_{1133} \epsilon_{33} \\ \sigma_{12} &= C_{1211} \epsilon_{11} + C_{1212} \epsilon_{12} + C_{1213} \epsilon_{13} + C_{1222} \epsilon_{22} + C_{1223} \epsilon_{23} + C_{1233} \epsilon_{33} \\ \sigma_{13} &= C_{1311} \epsilon_{11} + C_{1312} \epsilon_{12} + C_{1313} \epsilon_{13} + C_{1322} \epsilon_{22} + C_{1323} \epsilon_{23} + C_{1333} \epsilon_{33} \\ \sigma_{22} &= C_{2211} \epsilon_{11} + C_{2212} \epsilon_{12} + C_{2213} \epsilon_{13} + C_{2222} \epsilon_{22} + C_{2223} \epsilon_{23} + C_{2233} \epsilon_{33} \\ \sigma_{23} &= C_{2311} \epsilon_{11} + C_{2312} \epsilon_{12} + C_{2313} \epsilon_{13} + C_{2322} \epsilon_{22} + C_{2323} \epsilon_{23} + C_{2333} \epsilon_{33} \\ \sigma_{33} &= C_{3311} \epsilon_{11} + C_{3312} \epsilon_{12} + C_{3313} \epsilon_{13} + C_{3322} \epsilon_{22} + C_{3323} \epsilon_{23} + C_{3333} \epsilon_{33} \end{aligned}$$

.... (3-7)

A contracted notation is generally adopted for purposes of engineering analysis, i.e.,

$$\begin{array}{lll}
 \sigma_{11} = \sigma_1 & C_{1111} = C_{11} & C_{3333} = C_{33} \\
 \sigma_{22} = \sigma_2 & C_{1122} = C_{12} & C_{3323} = C_{34} \\
 \sigma_{33} = \sigma_3 & C_{1133} = C_{13} & C_{3313} = C_{35} \\
 \sigma_{23} = \tau_{23} & C_{1123} = C_{14} & C_{3312} = C_{36} \\
 \sigma_{13} = \tau_{13} & C_{1113} = C_{15} & C_{2323} = C_{44} \\
 \sigma_{12} = \tau_{12} & C_{1112} = C_{16} & C_{2313} = C_{45} \\
 \epsilon_{11} = \epsilon_1 & C_{2222} = C_{22} & C_{2312} = C_{46} \\
 \epsilon_{22} = \epsilon_2 & C_{2233} = C_{23} & C_{1313} = C_{55} \\
 \epsilon_{33} = \epsilon_3 & C_{2223} = C_{24} & C_{1312} = C_{56} \\
 2\epsilon_{23} = \gamma_{23} & C_{2213} = C_{25} & C_{1212} = C_{66} \\
 2\epsilon_{13} = \gamma_{13} & C_{2212} = C_{26} & \\
 2\epsilon_{12} = \gamma_{12} & &
 \end{array} \quad \left. \vphantom{\begin{array}{lll}} \right\} (3-8)$$

Thus, the generalized material constitutive relationships can also be expressed:

$$\begin{aligned}
 \sigma_1 &= C_{11}\epsilon_1 + C_{12}\epsilon_2 + C_{13}\epsilon_3 + C_{14}\gamma_{23} + C_{15}\gamma_{13} + C_{16}\gamma_{12} \\
 \sigma_2 &= C_{12}\epsilon_1 + C_{22}\epsilon_2 + C_{23}\epsilon_3 + C_{24}\gamma_{23} + C_{25}\gamma_{13} + C_{26}\gamma_{12} \\
 \sigma_3 &= C_{13}\epsilon_1 + C_{23}\epsilon_2 + C_{33}\epsilon_3 + C_{34}\gamma_{23} + C_{35}\gamma_{13} + C_{36}\gamma_{12} \\
 \tau_{23} &= C_{14}\epsilon_1 + C_{24}\epsilon_2 + C_{34}\epsilon_3 + C_{44}\gamma_{23} + C_{45}\gamma_{13} + C_{46}\gamma_{12} \\
 \tau_{13} &= C_{15}\epsilon_1 + C_{25}\epsilon_2 + C_{35}\epsilon_3 + C_{45}\gamma_{23} + C_{55}\gamma_{13} + C_{56}\gamma_{12} \\
 \tau_{12} &= C_{16}\epsilon_1 + C_{26}\epsilon_2 + C_{36}\epsilon_3 + C_{46}\gamma_{23} + C_{56}\gamma_{13} + C_{66}\gamma_{12}
 \end{aligned}$$

.... (3-9)

It should be noted that engineering shear strains are equivalent to twice the related tensorial shear strains.

Frequently, it is more convenient to work with matrix algebra for computational purposes. The matrix form of the generalized Hooke's Law (3-9) is

$$\begin{Bmatrix} \sigma_1 \\ \sigma_2 \\ \sigma_3 \\ \sigma_4 \\ \sigma_5 \\ \sigma_6 \end{Bmatrix} = \begin{bmatrix} C_{11} & C_{12} & C_{13} & C_{14} & C_{15} & C_{16} \\ C_{12} & C_{22} & C_{23} & C_{24} & C_{25} & C_{26} \\ C_{13} & C_{23} & C_{33} & C_{34} & C_{35} & C_{36} \\ C_{14} & C_{24} & C_{34} & C_{44} & C_{45} & C_{46} \\ C_{15} & C_{25} & C_{35} & C_{45} & C_{55} & C_{56} \\ C_{16} & C_{26} & C_{36} & C_{46} & C_{56} & C_{66} \end{bmatrix} \begin{Bmatrix} \epsilon_1 \\ \epsilon_2 \\ \epsilon_3 \\ \epsilon_4 \\ \epsilon_5 \\ \epsilon_6 \end{Bmatrix} \quad (3-10)$$

or simply

$$\{\sigma\} = [C] \{\epsilon\} \quad (3-11)$$

where

$$\left. \begin{aligned} \sigma_4 &= \tau_{23} & \epsilon_4 &= \gamma_{23} \\ \sigma_5 &= \tau_{13} & \epsilon_5 &= \gamma_{13} \\ \sigma_6 &= \tau_{12} & \epsilon_6 &= \gamma_{12} \end{aligned} \right\} \quad (3-12)$$

A similar expression which relates strain to stress can be derived:

$$\begin{Bmatrix} \epsilon_1 \\ \epsilon_2 \\ \epsilon_3 \\ \epsilon_4 \\ \epsilon_5 \\ \epsilon_6 \end{Bmatrix} = \begin{bmatrix} S_{11} & S_{12} & S_{13} & S_{14} & S_{15} & S_{16} \\ S_{12} & S_{22} & S_{23} & S_{24} & S_{25} & S_{26} \\ S_{13} & S_{23} & S_{33} & S_{34} & S_{35} & S_{36} \\ S_{14} & S_{24} & S_{34} & S_{44} & S_{45} & S_{46} \\ S_{15} & S_{25} & S_{35} & S_{45} & S_{55} & S_{56} \\ S_{16} & S_{26} & S_{36} & S_{46} & S_{56} & S_{66} \end{bmatrix} \begin{Bmatrix} \sigma_1 \\ \sigma_2 \\ \sigma_3 \\ \sigma_4 \\ \sigma_5 \\ \sigma_6 \end{Bmatrix} \quad (3-13)$$

or

$$\{\epsilon\} = [S]\{\sigma\} \quad (3-14)$$

In this instance, the coefficients of the stress components are termed the elastic compliances.

An inspection of the matrix equations (3-11) and (3-14) reveals that the elastic compliance matrix $[S]$ is simply the inverse of the elastic stiffness matrix $[C]$.

That is to say,

$$[S] = [C]^{-1} \quad (3-15)$$

or

$$[C] = [S]^{-1} \quad (3-16)$$

Therefore, a knowledge of the terms in either the stiffness or compliance matrix enables computation of the other through a simple matrix inversion procedure.

Constitutive relationships, (3-10) and (3-13), interrelate stress and strain in an anisotropic material subjected to a three-dimensional state of stress; the number of independent elastic constants in this most general case is twenty-one.

3.2 TRANSFORMATION OF PROPERTIES

3.2.1 Transformation of Stress Components

The component stresses at a point, defined with reference to a co-ordinate system (x, y, z) , are related to those referenced to a second co-ordinate system $(1, 2, 3)$

with a common origin by the cosines of the angles between the six co-ordinate axes (29). In Figure 3.2, typical relative positions of the two co-ordinate systems are illustrated along with a table of direction cosines.

The specific relationships between the component stresses in the two systems are given by:

$$\begin{aligned}
 \sigma_1 &= l_1^2 \sigma_x + m_1^2 \sigma_y + n_1^2 \sigma_z + 2m_1 n_1 \tau_{yz} + 2n_1 l_1 \tau_{xz} + 2l_1 m_1 \tau_{xy} \\
 \sigma_2 &= l_2^2 \sigma_x + m_2^2 \sigma_y + n_2^2 \sigma_z + 2m_2 n_2 \tau_{yz} + 2n_2 l_2 \tau_{xz} + 2l_2 m_2 \tau_{xy} \\
 \sigma_3 &= l_3^2 \sigma_x + m_3^2 \sigma_y + n_3^2 \sigma_z + 2m_3 n_3 \tau_{yz} + 2n_3 l_3 \tau_{xz} + 2l_3 m_3 \tau_{xy} \\
 \tau_{23} &= l_2 l_3 \sigma_x + m_2 m_3 \sigma_y + n_2 n_3 \sigma_z + (m_2 n_3 + m_3 n_2) \tau_{yz} + (l_2 n_3 + l_3 n_2) \tau_{xz} + (l_2 m_3 + l_3 m_2) \tau_{xy} \\
 \tau_{13} &= l_1 l_3 \sigma_x + m_1 m_3 \sigma_y + n_1 n_3 \sigma_z + (m_1 n_3 + m_3 n_1) \tau_{yz} + (l_1 n_3 + l_3 n_1) \tau_{xz} + (l_1 m_3 + l_3 m_1) \tau_{xy} \\
 \tau_{12} &= l_1 l_2 \sigma_x + m_1 m_2 \sigma_y + n_1 n_2 \sigma_z + (m_1 n_2 + m_2 n_1) \tau_{yz} + (l_1 n_2 + l_2 n_1) \tau_{xz} + (l_1 m_2 + l_2 m_1) \tau_{xy} \\
 &\dots (3-17)
 \end{aligned}$$

which can also be expressed in matrix notation by

$$\begin{Bmatrix} \sigma_1 \\ \sigma_2 \\ \sigma_3 \\ \tau_{23} \\ \tau_{13} \\ \tau_{12} \end{Bmatrix} = \begin{bmatrix} l_1^2 & m_1^2 & n_1^2 & 2m_1 n_1 & 2n_1 l_1 & 2l_1 m_1 \\ l_2^2 & m_2^2 & n_2^2 & 2m_2 n_2 & 2n_2 l_2 & 2l_2 m_2 \\ l_3^2 & m_3^2 & n_3^2 & 2m_3 n_3 & 2n_3 l_3 & 2l_3 m_3 \\ l_2 l_3 & m_2 m_3 & n_2 n_3 & m_2 n_3 + m_3 n_2 & l_2 n_3 + l_3 n_2 & l_2 m_3 + l_3 m_2 \\ l_1 l_3 & m_1 m_3 & n_1 n_3 & m_1 n_3 + m_3 n_1 & l_1 n_3 + l_3 n_1 & l_1 m_3 + l_3 m_1 \\ l_1 l_2 & m_1 m_2 & n_1 n_2 & m_1 n_2 + m_2 n_1 & l_1 n_2 + l_2 n_1 & l_1 m_2 + l_2 m_1 \end{bmatrix} \begin{Bmatrix} \sigma_x \\ \sigma_y \\ \sigma_z \\ \tau_{yz} \\ \tau_{xz} \\ \tau_{xy} \end{Bmatrix}$$

.... (3-18)

or

$$\{\sigma\} = [T] \{\sigma'\} \quad (3-19)$$

3.2.2 Transformation of Strain Components

Strain transformation relationships are quite similar to those for stress; the tensorial strain relationships are, in fact, identical in form:

$$\begin{aligned}
 \epsilon_1 &= l_1^2 \epsilon_x + m_1^2 \epsilon_y + n_1^2 \epsilon_z + 2m_1 n_1 \epsilon_{yz} + 2n_1 l_1 \epsilon_{xz} + 2l_1 m_1 \epsilon_{xy} \\
 \epsilon_2 &= l_2^2 \epsilon_x + m_2^2 \epsilon_y + n_2^2 \epsilon_z + 2m_2 n_2 \epsilon_{yz} + 2n_2 l_2 \epsilon_{xz} + 2l_2 m_2 \epsilon_{xy} \\
 \epsilon_3 &= l_3^2 \epsilon_x + m_3^2 \epsilon_y + n_3^2 \epsilon_z + 2m_3 n_3 \epsilon_{yz} + 2n_3 l_3 \epsilon_{xz} + 2l_3 m_3 \epsilon_{xy} \\
 \epsilon_{23} &= l_2 l_3 \epsilon_x + m_2 m_3 \epsilon_y + n_2 n_3 \epsilon_z + (m_2 n_3 + m_3 n_2) \epsilon_{yz} + (l_2 n_3 + l_3 n_2) \epsilon_{xz} + (l_2 m_3 + l_3 m_2) \epsilon_{xy} \\
 \epsilon_{13} &= l_1 l_3 \epsilon_x + m_1 m_3 \epsilon_y + n_1 n_3 \epsilon_z + (m_1 n_3 + m_3 n_1) \epsilon_{yz} + (l_1 n_3 + l_3 n_1) \epsilon_{xz} + (l_1 m_3 + l_3 m_1) \epsilon_{xy} \\
 \epsilon_{12} &= l_1 l_2 \epsilon_x + m_1 m_2 \epsilon_y + n_1 n_2 \epsilon_z + (m_1 n_2 + m_2 n_1) \epsilon_{yz} + (l_1 n_2 + l_2 n_1) \epsilon_{xz} + (l_1 m_2 + l_2 m_1) \epsilon_{xy} \\
 &\dots (3-20)
 \end{aligned}$$

Since engineering strains and tensorial strains are not always the same, however, (see equation (3-8)) the engineering strain transformation relationships assume a slightly different form:

$$\begin{aligned}
 \epsilon_1 &= l_1^2 \epsilon_x + m_1^2 \epsilon_y + n_1^2 \epsilon_z + m_1 n_1 \gamma_{yz} + n_1 l_1 \gamma_{xz} + l_1 m_1 \gamma_{xy} \\
 \epsilon_2 &= l_2^2 \epsilon_x + m_2^2 \epsilon_y + n_2^2 \epsilon_z + m_2 n_2 \gamma_{yz} + n_2 l_2 \gamma_{xz} + l_2 m_2 \gamma_{xy} \\
 \epsilon_3 &= l_3^2 \epsilon_x + m_3^2 \epsilon_y + n_3^2 \epsilon_z + m_3 n_3 \gamma_{yz} + n_3 l_3 \gamma_{xz} + l_3 m_3 \gamma_{xy} \\
 \gamma_{23} &= 2l_2 l_3 \epsilon_x + 2m_2 m_3 \epsilon_y + 2n_2 n_3 \epsilon_z + (m_2 n_3 + m_3 n_2) \gamma_{yz} + (l_2 l_3 + l_3 l_2) \gamma_{xz} + (l_2 m_3 + l_3 m_2) \gamma_{xy} \\
 \gamma_{13} &= 2l_1 l_3 \epsilon_x + 2m_1 m_3 \epsilon_y + 2n_1 n_3 \epsilon_z + (m_1 n_3 + m_3 n_1) \gamma_{yz} + (l_1 l_3 + l_3 l_1) \gamma_{xz} + (l_1 m_3 + l_3 m_1) \gamma_{xy} \\
 \gamma_{12} &= 2l_1 l_2 \epsilon_x + 2m_1 m_2 \epsilon_y + 2n_1 n_2 \epsilon_z + (m_1 n_2 + m_2 n_1) \gamma_{yz} + (l_1 l_2 + l_2 l_1) \gamma_{xz} + (l_1 m_2 + l_2 m_1) \gamma_{xy} \\
 &\dots (3-21)
 \end{aligned}$$

This can also be expressed in matrix notation:

$$\begin{Bmatrix} \epsilon_1 \\ \epsilon_2 \\ \epsilon_3 \\ \gamma_{23} \\ \gamma_{13} \\ \gamma_{12} \end{Bmatrix} = \begin{bmatrix} l_1^2 & m_1^2 & n_1^2 & m_1 n_1 & n_1 l_1 & l_1 m_1 \\ l_2^2 & m_2^2 & n_2^2 & m_2 n_2 & n_2 l_2 & l_2 m_2 \\ l_3^2 & m_3^2 & n_3^2 & m_3 n_3 & n_3 l_3 & l_3 m_3 \\ 2l_2 l_3 & 2m_2 m_3 & 2n_2 n_3 & m_2 n_3 + m_3 n_2 & l_2 n_3 + l_3 n_2 & l_2 m_3 + l_3 m_2 \\ 2l_1 l_3 & 2m_1 m_3 & 2n_1 n_3 & m_1 n_3 + m_3 n_1 & l_1 n_3 + l_3 n_1 & l_1 m_3 + l_3 m_1 \\ 2l_1 l_2 & 2m_1 m_2 & 2n_1 n_2 & m_1 n_2 + m_2 n_1 & l_1 n_2 + l_2 n_1 & l_1 m_2 + l_2 m_1 \end{bmatrix} \begin{Bmatrix} \epsilon_x \\ \epsilon_y \\ \epsilon_z \\ \gamma_{yz} \\ \gamma_{xz} \\ \gamma_{xy} \end{Bmatrix}$$

.... (3-22)

or

$$\{\epsilon\} = [T'] \{\epsilon'\} \quad (3-23)$$

3.2.3 Transformation of Stiffnesses and Compliances

The matrix form of the generalized Hooke's Law relating stresses and strains in the (1, 2, 3) co-ordinate system is

$$\{\sigma\} = [C] \{\epsilon\} \quad (3-24)$$

Also, within the (x, y, z) co-ordinate system

$$\{\sigma'\} = [C'] \{\epsilon'\} \quad (3-25)$$

Substitution of relations (3-19) and (3-23) into equation (3-24) yields

$$[T] \{\sigma'\} = [C] [T'] \{\epsilon'\} \quad (3-26)$$

and by premultiplying both sides of this equation by $[T]^{-1}$

a new expression for $\{\sigma'\}$ is obtained:

$$\{\sigma'\} = [T]^{-1} [C] [T'] \{\epsilon'\} \quad (3-27)$$

By comparing equations (3-25) and (3-27), it can readily be seen that stiffnesses can be transformed according to the expression:

$$[C'] = [T]^{-1} [C] [T'] \quad (3-28)$$

In a similar way, it can be shown that the compliance transformation equation is

$$[S'] = [T']^{-1} [S] [T] \quad (3-29)$$

3.3 EFFECTS OF MATERIAL SYMMETRY

Few materials are completely anisotropic and, in most structural materials, special kinds of symmetry exist, i.e., the elastic constants remain invariant under certain co-ordinate transformations.

3.3.1 Materials Possessing One Plane of Elastic Symmetry

In certain structural materials, the elastic constants remain invariant under a co-ordinate transformation $1 \rightarrow x, 2 \rightarrow -y, 3 \rightarrow -z$. These materials are said to possess one plane of elastic symmetry. The direction cosines for this transformation are:

$$\begin{aligned}
 l_1 &= 1 \\
 m_2 &= n_3 = -1 \\
 l_2 &= l_3 = m_1 = m_3 = n_1 = n_2 = 0
 \end{aligned}
 \tag{3-30}$$

and the stress and strain transformation matrices, $[T]$ and $[T']$, defined by equations (3-18) and (3-22), are:

$$[T] = [T'] = \begin{bmatrix} 1 & 0 & 0 & 0 & 0 & 0 \\ 0 & 1 & 0 & 0 & 0 & 0 \\ 0 & 0 & 1 & 0 & 0 & 0 \\ 0 & 0 & 0 & 1 & 0 & 0 \\ 0 & 0 & 0 & 0 & -1 & 0 \\ 0 & 0 & 0 & 0 & 0 & -1 \end{bmatrix}
 \tag{3-31}$$

The transformed elastic constants can then be determined by operating on the original stiffness matrix in accordance with equation (3-28). Thus,

$$[C] = \begin{bmatrix} C_{11} & C_{12} & C_{13} & C_{14} & -C_{15} & -C_{16} \\ C_{12} & C_{22} & C_{23} & C_{24} & -C_{25} & -C_{26} \\ C_{13} & C_{23} & C_{33} & C_{34} & -C_{35} & -C_{36} \\ C_{14} & C_{24} & C_{34} & C_{44} & -C_{45} & -C_{46} \\ -C_{15} & -C_{25} & -C_{35} & -C_{45} & C_{55} & C_{56} \\ -C_{16} & -C_{26} & -C_{36} & -C_{46} & C_{56} & C_{66} \end{bmatrix}
 \tag{3-32}$$

In addition, if the material is rotated 180° about the 1 axis, the new co-ordinate axes (x, y, z) will coincide with the original system (1, 2, 3). Due to the symmetry, the

material response characteristics will then be identical to those defined for the material in its original position by equation (3-24), i.e., $[C'] = [C]$.

A comparison of the two stiffness matrices reveals that this is possible only when

$$\left. \begin{array}{ll} C'_{15} = -C_{15} = C_{15} = 0 & C'_{16} = -C_{16} = C_{16} = 0 \\ C'_{25} = -C_{25} = C_{25} = 0 & C'_{26} = -C_{26} = C_{26} = 0 \\ C'_{35} = -C_{35} = C_{35} = 0 & C'_{36} = -C_{36} = C_{36} = 0 \\ C'_{45} = -C_{45} = C_{45} = 0 & C'_{46} = -C_{46} = C_{46} = 0 \end{array} \right\} (3-33)$$

Therefore, the elastic constants for a material possessing a plane of elastic symmetry are summarized by the matrix.

$$[C] = \begin{bmatrix} C_{11} & C_{12} & C_{13} & C_{14} & 0 & 0 \\ C_{12} & C_{22} & C_{23} & C_{24} & 0 & 0 \\ C_{13} & C_{23} & C_{33} & C_{34} & 0 & 0 \\ C_{14} & C_{24} & C_{34} & C_{44} & 0 & 0 \\ 0 & 0 & 0 & 0 & C_{55} & C_{56} \\ 0 & 0 & 0 & 0 & C_{56} & C_{66} \end{bmatrix} \quad (3-34)$$

3.3.2 Two Planes of Elastic Symmetry

In the foregoing, it has been shown that the stiffness matrix for a material possessing one plane of elastic symmetry, i.e., the (1, 2) plane, is comprised of the elements shown in expression (3-34). Had the plane of symmetry been the (2, 3) plane instead of the (1, 2) plane,

it could just as easily have been shown, following the identical procedure, that the elastic constant matrix would have reduced to

$$[C] = \begin{bmatrix} C_{11} & C_{12} & C_{13} & 0 & 0 & C_{16} \\ C_{12} & C_{22} & C_{23} & 0 & 0 & C_{26} \\ C_{13} & C_{23} & C_{33} & 0 & 0 & C_{36} \\ 0 & 0 & 0 & C_{44} & C_{45} & 0 \\ 0 & 0 & 0 & C_{45} & C_{55} & 0 \\ C_{16} & C_{26} & C_{36} & 0 & 0 & C_{66} \end{bmatrix} \quad (3-35)$$

Clearly, if the material possesses both of these planes of elastic symmetry, the matrix relating the stress and strain components will be comprised of only the non-zero elements common to the two matrices described by expressions (3-34) and (3-35):

$$[C] = \begin{bmatrix} C_{11} & C_{12} & C_{13} & 0 & 0 & 0 \\ C_{12} & C_{22} & C_{23} & 0 & 0 & 0 \\ C_{13} & C_{23} & C_{33} & 0 & 0 & 0 \\ 0 & 0 & 0 & C_{44} & 0 & 0 \\ 0 & 0 & 0 & 0 & C_{55} & 0 \\ 0 & 0 & 0 & 0 & 0 & C_{66} \end{bmatrix} \quad (3-36)$$

The same arguments may be employed to establish the validity of this matrix construction, regardless of which two planes of elastic symmetry the material possesses. In general, therefore, any material possessing two mutually orthogonal

planes of symmetry responds according to the relationship

$$\begin{Bmatrix} \sigma_1 \\ \sigma_2 \\ \sigma_3 \\ \tau_{23} \\ \tau_{13} \\ \tau_{12} \end{Bmatrix} = \begin{bmatrix} C_{11} & C_{12} & C_{13} & 0 & 0 & 0 \\ C_{12} & C_{22} & C_{23} & 0 & 0 & 0 \\ C_{13} & C_{23} & C_{33} & 0 & 0 & 0 \\ 0 & 0 & 0 & C_{44} & 0 & 0 \\ 0 & 0 & 0 & 0 & C_{55} & 0 \\ 0 & 0 & 0 & 0 & 0 & C_{66} \end{bmatrix} \begin{Bmatrix} \epsilon_1 \\ \epsilon_2 \\ \epsilon_3 \\ \gamma_{23} \\ \gamma_{13} \\ \gamma_{12} \end{Bmatrix} \quad (3-37)$$

The number of independent elastic constants in this case is reduced to nine.

A corresponding strain-stress relationship can be obtained by utilizing equations (3-13) and (3-15). Since

$$[S] = [C]^{-1}$$

then

$$\begin{Bmatrix} \epsilon_1 \\ \epsilon_2 \\ \epsilon_3 \\ \gamma_{23} \\ \gamma_{13} \\ \gamma_{12} \end{Bmatrix} = \begin{bmatrix} S_{11} & S_{12} & S_{13} & 0 & 0 & 0 \\ S_{12} & S_{22} & S_{23} & 0 & 0 & 0 \\ S_{13} & S_{23} & S_{33} & 0 & 0 & 0 \\ 0 & 0 & 0 & S_{44} & 0 & 0 \\ 0 & 0 & 0 & 0 & S_{55} & 0 \\ 0 & 0 & 0 & 0 & 0 & S_{66} \end{bmatrix} \begin{Bmatrix} \sigma_1 \\ \sigma_2 \\ \sigma_3 \\ \tau_{23} \\ \tau_{13} \\ \tau_{12} \end{Bmatrix} \quad (3-38)$$

3.3.3 Three Planes of Elastic Symmetry - Orthotropic Materials

Materials which have three mutually perpendicular planes of elastic symmetry are termed orthotropic. The matrix of elastic constants for such materials assumes a

form identical to that for materials possessing only two planes of symmetry.

The underlying reason for this was provided in the previous section. It was pointed out that, regardless of which pair of mutually orthogonal planes is symmetrical, the matrix of elastic constants remains the same. Therefore, it is obvious that the number of independent elastic constants is the same for orthotropic materials as it is for materials possessing only two planes of elastic symmetry.

3.4 THE PLANE STRESS ASSUMPTION

3.4.1 The Stress-Strain Relationships for a Specially Orthotropic Layer

The lateral dimensions of fibre-reinforced laminates are generally large in comparison with the thickness, and a state of stress which is approximately plane can be assumed, i.e.,

$$\sigma_3 = \tau_{23} = \tau_{13} = 0 \quad (3-39)$$

through the thickness of the material.

Most lamina materials are orthotropic and behave according to the special forms of the generalized Hooke's Law given in equations (3-37) and (3-38). These constitutive relationships can be simplified further when a state of plane stress is assumed. Introduction of relations (3-39) into (3-38) yields

$$\begin{Bmatrix} \epsilon_1 \\ \epsilon_2 \\ \epsilon_3 \\ \gamma_{23} \\ \gamma_{13} \\ \gamma_{12} \end{Bmatrix} = \begin{bmatrix} S_{11} & S_{12} & S_{13} & 0 & 0 & 0 \\ S_{12} & S_{22} & S_{23} & 0 & 0 & 0 \\ S_{13} & S_{23} & S_{33} & 0 & 0 & 0 \\ 0 & 0 & 0 & S_{44} & 0 & 0 \\ 0 & 0 & 0 & 0 & S_{55} & 0 \\ 0 & 0 & 0 & 0 & 0 & S_{66} \end{bmatrix} \begin{Bmatrix} \sigma_1 \\ \sigma_2 \\ 0 \\ 0 \\ 0 \\ \tau_{12} \end{Bmatrix} \quad (3-40)$$

which can be simplified to

$$\begin{Bmatrix} \epsilon_1 \\ \epsilon_2 \\ \gamma_{12} \end{Bmatrix} = \begin{bmatrix} S_{11} & S_{12} & 0 \\ S_{12} & S_{22} & 0 \\ 0 & 0 & S_{66} \end{bmatrix} \begin{Bmatrix} \sigma_1 \\ \sigma_2 \\ \tau_{12} \end{Bmatrix} \quad (3-41)$$

and

$$\epsilon_3 = S_{13}\sigma_1 + S_{23}\sigma_2 \quad (3-42)$$

since

$$\gamma_{23} = \gamma_{13} = 0 \quad (3-43)$$

Due to the fact that the in-plane stresses, σ_1 and σ_2 , are independent of ϵ_3 , equation (3-42) can generally be ignored in plane-stress analyses.

In terms of engineering constants

$$\begin{aligned} S_{11} &= \frac{1}{E_{11}} \\ S_{12} &= -\frac{\nu_{21}}{E_{22}} = -\frac{\nu_{12}}{E_{11}} \\ S_{22} &= \frac{1}{E_{22}} \\ S_{66} &= \frac{1}{G_{12}} \end{aligned} \quad (3-44)$$

Therefore,

$$\begin{aligned}\epsilon_1 &= \frac{1}{E_{11}} \sigma_1 - \frac{\nu_{21}}{E_{22}} \sigma_2 \\ \epsilon_2 &= -\frac{\nu_{12}}{E_{11}} \sigma_1 + \frac{1}{E_{22}} \sigma_2 \\ \gamma_{12} &= \frac{1}{G_{12}} \tau_{12}\end{aligned}\quad (3-45)$$

From equations (3-45), it can be shown that

$$\begin{aligned}\sigma_1 &= \frac{E_{11}}{1 - \nu_{12}\nu_{21}} \epsilon_1 + \frac{\nu_{12}E_{22}}{1 - \nu_{12}\nu_{21}} \epsilon_2 \\ \sigma_2 &= \frac{\nu_{21}E_{11}}{1 - \nu_{12}\nu_{21}} \epsilon_1 + \frac{E_{22}}{1 - \nu_{12}\nu_{21}} \epsilon_2 \\ \tau_{12} &= G_{12} \gamma_{12}\end{aligned}\quad (3-46)$$

or, in matrix form,

$$\begin{Bmatrix} \sigma_1 \\ \sigma_2 \\ \tau_{12} \end{Bmatrix} = \begin{bmatrix} \bar{C}_{11} & \bar{C}_{12} & 0 \\ \bar{C}_{12} & \bar{C}_{22} & 0 \\ 0 & 0 & \bar{C}_{66} \end{bmatrix} \begin{Bmatrix} \epsilon_1 \\ \epsilon_2 \\ \gamma_{12} \end{Bmatrix}\quad (3-47)$$

where

$$\begin{aligned}\bar{C}_{11} &= \frac{E_{11}}{1 - \nu_{12}\nu_{21}} \\ \bar{C}_{12} &= \frac{\nu_{12}E_{22}}{1 - \nu_{12}\nu_{21}} = \frac{\nu_{21}E_{11}}{1 - \nu_{12}\nu_{21}} \\ \bar{C}_{22} &= \frac{E_{22}}{1 - \nu_{12}\nu_{21}} \\ \bar{C}_{66} &= G_{12}\end{aligned}\quad (3-48)$$

It should be particularly noted that the new matrix coefficients are not the material stiffness coefficients, i.e.,

$$\bar{C}_{ij} \neq C_{ij} \quad (3-49)$$

though they are directly related:

$$\begin{aligned} \bar{C}_{11} &= C_{11} - \frac{(C_{13})^2}{C_{33}} \\ \bar{C}_{12} &= C_{12} - \frac{C_{13}C_{23}}{C_{33}} \\ \bar{C}_{22} &= C_{22} - \frac{(C_{23})^2}{C_{33}} \\ \bar{C}_{66} &= C_{66} \end{aligned} \quad (3-50)$$

Since the plane-stress assumption is adopted, however, fundamental material stiffnesses are no longer utilized in the analysis. Thus, it is possible to revert to the use of C_{ij} for the effective stiffness matrix coefficients. This simplifies equation (3-47) to

$$\begin{Bmatrix} \sigma_1 \\ \sigma_2 \\ \tau_{12} \end{Bmatrix} = \begin{bmatrix} C_{11} & C_{12} & 0 \\ C_{12} & C_{22} & 0 \\ 0 & 0 & C_{66} \end{bmatrix} \begin{Bmatrix} \epsilon_1 \\ \epsilon_2 \\ \gamma_{12} \end{Bmatrix} \quad (3-51)$$

where

$$\begin{aligned} C_{11} &= \frac{E_{11}}{1 - \nu_{12}\nu_{21}} \\ C_{12} &= \frac{\nu_{12}E_{22}}{1 - \nu_{12}\nu_{21}} = \frac{\nu_{21}E_{11}}{1 - \nu_{12}\nu_{21}} \end{aligned}$$

$$C_{22} = \frac{E_{22}}{1 - \nu_{12}\nu_{21}}$$

$$C_{66} = G_{12}$$

.... (3-52)

Equation (3-51) describes the in-plane stress-strain behaviour of a specially orthotropic lamina and is the foundation upon which laminate analysis is built.

3.4.2 The Reduced Stress and Strain Transformation Matrices

The assumption of plane stress also leads to substantial simplification of the stress and strain transformation matrices. The direction cosines of transformation when a state of plane stress exists in the (1,2) plane (refer to Figure 3.3) are:

$$l_1 = m_2 = \cos \theta = m$$

$$l_2 = -\sin \theta = -n$$

$$m_1 = \sin \theta = n$$

(3-53)

$$n_3 = 1$$

$$n_1 = n_2 = l_3 = m_3 = 0$$

Consequently, the stress and strain transformation matrices given in expressions (3-18) and (3-22) become, respectively,

$$[T] = \begin{bmatrix} m^2 & n^2 & 0 & 0 & 0 & 2mn \\ n^2 & m^2 & 0 & 0 & 0 & -2mn \\ 0 & 0 & 1 & 0 & 0 & 0 \\ 0 & 0 & 0 & m & -n & 0 \\ 0 & 0 & 0 & n & m & 0 \\ -mn & mn & 0 & 0 & 0 & (m^2 - n^2) \end{bmatrix} \quad (3-54)$$

and

$$[T'] = \begin{bmatrix} m^2 & n^2 & 0 & 0 & 0 & mn \\ n^2 & m^2 & 0 & 0 & 0 & -mn \\ 0 & 0 & 1 & 0 & 0 & 0 \\ 0 & 0 & 0 & m & -n & 0 \\ 0 & 0 & 0 & n & m & 0 \\ -2mn & 2mn & 0 & 0 & 0 & (m^2 - n^2) \end{bmatrix} \quad (3-55)$$

Since the only transformation coefficients of interest in this case are those interrelating in-plane stresses and strains, these matrices can be reduced to

$$[T] = \begin{bmatrix} m^2 & n^2 & 2mn \\ n^2 & m^2 & -2mn \\ -mn & mn & (m^2 - n^2) \end{bmatrix} \quad (3-56)$$

and

$$[T'] = \begin{bmatrix} m^2 & n^2 & mn \\ n^2 & m^2 & -mn \\ -2mn & 2mn & (m^2 - n^2) \end{bmatrix} \quad (3-57)$$

Thus, the reduced stress and strain transformation equations for planar analysis are:

$$\begin{Bmatrix} \sigma_1 \\ \sigma_2 \\ \tau_{12} \end{Bmatrix} = \begin{bmatrix} m^2 & n^2 & 2mn \\ n^2 & m^2 & -2mn \\ -mn & mn & (m^2 - n^2) \end{bmatrix} \begin{Bmatrix} \sigma_x \\ \sigma_y \\ \tau_{xy} \end{Bmatrix} \quad (3-58)$$

and

$$\begin{Bmatrix} \epsilon_1 \\ \epsilon_2 \\ \gamma_{12} \end{Bmatrix} = \begin{bmatrix} m^2 & n^2 & mn \\ n^2 & m^2 & -mn \\ -2mn & 2mn & (m^2 - n^2) \end{bmatrix} \begin{Bmatrix} \epsilon_x \\ \epsilon_y \\ \gamma_{xy} \end{Bmatrix} \quad (3-59)$$

3.4.3 The Generalized Hooke's Law for an Orthotropic Layer

Quite often, the natural axes (1,2) of the layers within a laminate do not coincide with those chosen for analysis of the laminate. For example, in Figure 3.4, the principal material directions in the helically wound layers are at angles of $\pm \theta$ relative to the co-ordinate system which would normally be chosen for structural analysis. It is therefore essential that stress-strain relationships be established which describe the response of the layer materials in the structural co-ordinate system.

The transformed stress-strain relationship, (3-25), and the coefficient transformation equation, (3-28), apply not only to completely anisotropic materials but also to planar orthotropic orthotropic materials, though in the

planar case, the transformation and elastic constant matrices are in their reduced forms. Now, since

$$[T(\theta)] = [T(-\theta)] \quad (3-60)$$

then

$$\begin{bmatrix} C'_{11} & C'_{12} & C'_{16} \\ C'_{12} & C'_{22} & C'_{26} \\ C'_{16} & C'_{26} & C'_{66} \end{bmatrix} = \begin{bmatrix} m^2 & n^2 & -2mn \\ n^2 & m^2 & 2mn \\ mn & -mn & (m^2 - n^2) \end{bmatrix} \begin{bmatrix} C_{11} & C_{12} & 0 \\ C_{12} & C_{22} & 0 \\ 0 & 0 & C_{66} \end{bmatrix} \begin{bmatrix} m^2 & n^2 & mn \\ n^2 & m^2 & -mn \\ -2mn & 2mn & (m^2 - n^2) \end{bmatrix} \quad \dots (3-61)$$

and hence it can readily be shown that

$$\begin{aligned} C'_{11} &= m^4 C_{11} + n^4 C_{22} + m^2 n^2 (2C_{12} + 4C_{66}) \\ C'_{12} &= m^2 n^2 (C_{11} + C_{22} - 4C_{66}) + (m^4 + n^4) C_{12} \\ C'_{16} &= m^3 n (C_{11} - C_{12} - 2C_{66}) - mn^3 (C_{22} - C_{12} - 2C_{66}) \\ C'_{22} &= n^4 C_{11} + m^4 C_{22} + m^2 n^2 (2C_{12} + 4C_{66}) \\ C'_{26} &= mn^3 (C_{11} - C_{12} - 2C_{66}) - m^3 n (C_{22} - C_{12} - 2C_{66}) \\ C'_{66} &= m^2 n^2 (C_{11} + C_{22} - 2C_{12}) + (m^2 - n^2)^2 C_{66} \end{aligned} \quad \dots (3-62)$$

These expressions are identical to those derived separately by Hearmon (27) and Faupel (22) when account is taken of the difference in sign convention for angular rotation adopted by these authors.

Therefore, in the case of general orthotropy, i.e., off-axis loading,

$$\begin{Bmatrix} \sigma_x \\ \sigma_y \\ \tau_{xy} \end{Bmatrix} = \begin{bmatrix} C'_{11} & C'_{12} & C'_{16} \\ C'_{12} & C'_{22} & C'_{26} \\ C'_{16} & C'_{26} & C'_{66} \end{bmatrix} \begin{Bmatrix} \epsilon_x \\ \epsilon_y \\ \gamma_{xy} \end{Bmatrix} \quad (3-63)$$

or, in algebraic form,

$$\left. \begin{aligned} \sigma_x &= C'_{11} \epsilon_x + C'_{12} \epsilon_y + C'_{16} \gamma_{xy} \\ \sigma_y &= C'_{12} \epsilon_x + C'_{22} \epsilon_y + C'_{26} \gamma_{xy} \\ \tau_{xy} &= C'_{16} \epsilon_x + C'_{26} \epsilon_y + C'_{66} \gamma_{xy} \end{aligned} \right\} \quad (3-64)$$

where the elastic constants, C'_{ij} , are related to the principal elastic constants, C_{ij} , and the co-ordinate system rotation, by equations (3-62). Both of these equations describe the stress-strain behaviour of a homogeneous generally orthotropic layer.

3.4.4 Simplifications in Stress-Strain Relationships

Resulting from Material Isotropy

Before leaving the subject of layer stress-strain relationships, it will prove interesting to investigate the special case of material isotropy. In an isotropic material,

$$\left. \begin{aligned} E_{11} &= E_{22} = E \\ \nu_{12} &= \nu_{21} = \nu \\ G_{12} &= G = \frac{E}{2(1+\nu)} \end{aligned} \right\} \quad (3-65)$$

Therefore, from relations (3-52),

$$\left. \begin{aligned} C_{11} &= C_{22} = \frac{E}{1-\nu^2} \\ C_{12} &= \nu \frac{E}{1-\nu^2} \\ C_{66} &= G_{12} = G = \frac{E}{2(1+\nu)} \end{aligned} \right\} \quad (3-66)$$

Substitution of these expressions for C_{ij} in equations (3-62) yields

$$\left. \begin{aligned} C'_{11} &= C_{11} = \frac{E}{1-\nu^2} \\ C'_{12} &= C_{12} = \frac{\nu E}{1-\nu^2} \\ C'_{16} &= C_{16} = 0 \\ C'_{22} &= C_{22} = \frac{E}{1-\nu^2} \\ C'_{26} &= C_{26} = 0 \\ C'_{66} &= C_{66} = \frac{E}{2(1+\nu)} = G \end{aligned} \right\} \quad (3-67)$$

Hence, equation (3-63) becomes

$$\begin{Bmatrix} \sigma_x \\ \sigma_y \\ \tau_{xy} \end{Bmatrix} = \begin{bmatrix} C_{11} & C_{12} & 0 \\ C_{12} & C_{22} & 0 \\ 0 & 0 & C_{66} \end{bmatrix} \begin{Bmatrix} \epsilon_x \\ \epsilon_y \\ \gamma_{xy} \end{Bmatrix} \quad (3-68)$$

or, in algebraic form,

$$\left. \begin{aligned} \sigma_x &= \frac{E}{1-\nu^2} (\epsilon_x + \nu \epsilon_y) \\ \sigma_y &= \frac{E}{1-\nu^2} (\nu \epsilon_x + \epsilon_y) \\ \tau_{xy} &= G \gamma_{xy} \end{aligned} \right\} \quad (3-69)$$

Relations (3-69) are, as will be readily recognized, the well-known stress-strain relationships for an isotropic material in a state of plane stress. It is apparent, therefore, that equation (3-63) is equally valid for both orthotropic and isotropic layer materials.

3.5 FAILURE CRITERIA

It was pointed out earlier (Section 2.1.1) that laminate failure can originate in any of the layers. Thus, the strength of a laminated composite is necessarily related to the failure of an individual ply (or lamina).

The most accepted lamina failure criterion at the present time appears to be the distortional energy condition which, as applied to a composite lamina, is a variation of the original condition proposed for isotropic materials by Von Mises. Hill (30) postulated a generalized form for anisotropic materials in 1948 and Tsai (31) subsequently adapted this to the special case of an orthotropic lamina in a state of plane stress. The reduced condition, according to Tsai, is

$$\left(\frac{\sigma_1}{X}\right)^2 - \frac{1}{r} \frac{\sigma_1}{X} \frac{\sigma_2}{Y} + \left(\frac{\sigma_2}{Y}\right)^2 + \left(\frac{\tau_{12}}{S}\right)^2 = 1 \quad (3-70)$$

where

$$\frac{1}{r} = \frac{X}{Y}$$

σ_1 , σ_2 and τ_{12} are the applied stresses in the natural

co-ordinate system of the lamina.

X and Y are the tensile or compressive yield strengths of the lamina in the 1 and 2 directions, respectively. Tensile values are employed when the corresponding applied stress is tensile and compressive values when it is compressive.

S is the allowable lamina shear stress.

Lamina failure is assumed to occur when the sum of the terms on the left side of the equation becomes equal to one.

Unfortunately, as Grinius and Noyes (32) have pointed out, this criterion provides no indication of the manner in which a layer has failed. To overcome this limitation, they suggested that an indirect determination of the type of failure could be made by comparing the ratios of longitudinal and transverse stresses in a layer at failure. Specifically, if the inequalities

$$\tan^{-1}\left(\frac{\sigma_2}{\sigma_1}\right) < \tan^{-1}\left(\frac{Y}{X}\right) \quad (3-71)$$

and

$$\tan^{-1}\left(\frac{\tau_{12}}{\sigma_1}\right) < \tan^{-1}\left(\frac{S}{X}\right) \quad (3-72)$$

are not satisfied simultaneously, then either transverse tension or compression, or longitudinal shear failure will be indicated.

Another failure criterion, which is quite similar

to the distortional energy condition, takes the form:

$$\left. \begin{aligned} \left(\frac{\sigma_1}{X}\right)^2 - \frac{\sigma_1}{X} \frac{\sigma_2}{Y} + \left(\frac{\sigma_2}{Y}\right)^2 + \left(\frac{\tau_{12}}{S}\right)^2 &= 1 \\ \left(\frac{\sigma_1}{X}\right)^2 &= 1 \\ \left(\frac{\sigma_2}{Y}\right)^2 &= 1 \end{aligned} \right\} \quad (3-73)$$

This criterion, developed by Norris (33) and commonly called the "Interaction Formula", has two restrictions:

1) no distinction is made between homogeneous and laminated composites, and 2) shear strength is not treated as an independent strength property. Neither of these restrictions applies in the case of the distortional energy criterion.

Stowell and Liu (34) have suggested a three mode maximum stress failure criterion associated with (a) fibre failure, (b) matrix shear failure, and (c) transverse matrix failure. This criterion has received only limited verification to date, however, and is not widely used.

Finally, the maximum strain yield criterion is based upon the use of the maximum principal strain properties of a composite lamina (35). By inserting the principal yield strains of the lamina (which are determined experimentally) into equations (3-41), an envelope of the stresses which produce the yield strains can be produced. For example, if it is assumed that $\tau_{12} = 0$,

$$\left. \begin{aligned} \epsilon_{1y} &= S_{11} \sigma_1 + S_{12} \sigma_2 \\ \epsilon_{2y} &= S_{12} \sigma_1 + S_{22} \sigma_2 \end{aligned} \right\} \quad (3-74)$$

or, by rearranging,

$$\left. \begin{aligned} \sigma_2 &= \frac{\epsilon_{1y}}{S_{12}} - \frac{S_{11}}{S_{12}} \sigma_1 \\ \sigma_2 &= \frac{\epsilon_{2y}}{S_{22}} - \frac{S_{12}}{S_{22}} \sigma_1 \end{aligned} \right\} \quad (3-75)$$

These equations can then be plotted in the $\sigma_1 - \sigma_2$ co-ordinate system to obtain a yield surface similar to the one shown in Figure 3.5. The principal problem with this method appears to be the substantial amount of testing required to account fully for the effects of shear strain, i.e., for cases where $\tau_{12} \neq 0$.

3.6 DETERMINATION OF LAMINA PROPERTIES

It has been shown that the elastic response of an orthotropic lamina to applied loads and conditions of failure are completely predictable as long as four elastic constants, E_{11} , E_{22} , ν_{12} and G_{12} , and five allowable stresses, σ_1^t , σ_2^t , σ_1^c , σ_2^c and τ_{12} , are known. The question at this point is how best to determine these properties for the commonly used lamina or ply materials.

Though considerable effort has been expended in the development of theories for predicting lamina properties, they continue to be determined primarily by testing. There

are numerous reasons for this, but perhaps the most important is that too many unrealistic simplifications of the physical state of the materials have to be made in order to arrive at a mathematically viable model.

Numerous micromechanics theories for predicting the thermoelastic properties of unidirectional composites have been proposed in recent years (35). Unfortunately, however, as Chamis and Sendeckyj (36) have stated in their excellent critique on the subject, "until a breakthrough in the statistical approach is made, where all possible factors influencing ply thermoelastic behaviour are properly accounted for, the ply thermoelastic properties can be described most reliably by semiempirical equations." The need for testing in order to determine properties is implicit in this statement.

Far less effort has gone into the development of theories for predicting the thermoelastic properties of randomly reinforced or woven material plies probably because of the increased difficulties in arriving at a workable model. As a result, the need for testing of these materials is even greater.

The situation is not much better when it comes to the prediction of strength properties. Some of the techniques employed in the prediction of elastic properties, e.g., exact methods (elasticity) (37, 38) and the discrete element method (39), also yield strength predictions.

Unfortunately, these are based upon rather questionable assumptions from a strength standpoint, such as (a) no voids in the matrix, or (b) perfect adhesion between the fibre and the matrix, which can lead to quite substantial errors. Strength predictions are therefore generally less reliable than those for elastic constants.

When one considers the foregoing factors, it is really not surprising that ply properties are still determined primarily by testing. A further advantage of testing is that full stress-strain curves can be obtained for the various types of loading and these are most valuable to a designer attempting to achieve an optimum design.

Five tests are required to characterize a lamina or ply material. Two separate tensile tests conducted on samples cut from the composite lamina at 0° and 90° relative to the principal direction of reinforcement yield E_{11}^t , ν_{12}^t and σ_1^t , and E_{22}^t and σ_2^t respectively. Compression tests on similarly prepared samples, i.e., cut from lamina at 0° and 90° , provide equivalent compressive data, E_{11}^c , ν_{12}^c and σ_1^c , and E_{22}^c and σ_2^c . Finally, the in-plane shear properties are obtained by conducting some form of in-plane shear test, e.g., the rail shear test, again on samples cut from the lamina in both of the principal directions.

Actual testing procedures are generally quite similar to those used in measuring the comparable

properties of conventional isotropic materials. There are, however, numerous fine points associated with the testing of composite materials which cannot be discussed herein. References (40, 41 and 42) are all excellent sources of additional information on this subject.

The use of tests to determine composite lamina response characteristics is not so different from the case of metals. What is different, however, is that there are no industrial standards for composite materials. Each fabricator must therefore himself determine the properties of those combinations of resin and reinforcement with which he will be working. Until the FRP industry develops workable standards comparable to those which exist in, for example, the iron and steel industry, the determination of material properties will remain as a most serious problem.

3.7 CLOSING

A computer program which calculates the principal lamina stiffness coefficients through the use of equations (3-52) and then transforms them to any other co-ordinate system by employing equations (3-62) is included as Appendix A.

SECTION 4

LAMINATE CONSTITUTIVE EQUATIONS

Laminate constitutive equations are obtained by following derivational procedures that are virtually identical to those used in the development of force and moment resultant equations in plate and shell theory. The only significant difference is that material stress-strain relationships generally vary through the thickness of a laminate while they remain invariant in isotropic plates or shells.

4.1 LAMINATE DISPLACEMENT RELATIONSHIPS

As in plate and shell theory, the surface that bisects the thickness of the laminate is called the middle surface or midplane. The entire geometry of the laminate can then be defined by specifying the form of the middle surface and the thickness of the laminate at each point.

Consider the infinitely small element of a deformed laminate shown in Figure 4.1. It is formed by two adjacent planes which are normal to the middle surface of the laminate and which contain its principal curvatures. A co-ordinate axis system can be established whereby x and y are tangent, at O , to the lines of principal curvature and

the z axis is normal to the middle surface.

In Figure 4.2, the x - z plane of the laminate before and after deformation due to a particular loading condition is illustrated. It is assumed that as a result of loading the point M at the middle surface of the material is displaced by a distance u_0 in the x direction and that the normal to the middle surface, BMC , undergoes a rotation relative to the normal axis, z . It is also assumed, as in plate and shell theory, that the normal, BMC , remains straight and normal to the deformed midplane which is equivalent to neglecting the shearing deformations, γ_{xz} and γ_{yz} .

The displacement of a point P on the normal BMC , in the x direction, can therefore be expressed simply by

$$u_p = u_0 - z_p \alpha \quad (4-1)$$

where z is the z co-ordinate of the point P measured from the midplane, and

α is the angular rotation of BMC relative to the z axis.

It is readily apparent from the geometry, however, that α is the change in slope of the midplane with respect to the z co-ordinate axis, or

$$\alpha = \frac{\partial w}{\partial x} \quad (4-2)$$

Hence, by combining equations (4-1) and (4-2),

$$u_p = u_0 - z_p \frac{\partial w}{\partial x} \quad (4-3)$$

or, in general,

$$u = u_0 - z \frac{\partial w}{\partial x} \quad (4-4)$$

A similar relationship,

$$v = v_0 - z \frac{\partial w}{\partial x} \quad (4-5)$$

can be obtained through an equivalent study of deformations in the y-z plane of the laminate. In this case, v is the displacement, in the y direction, of any arbitrary point at a distance z from the midplane.

4.2 STRAIN-DISPLACEMENT RELATIONSHIPS

Tensorial strains have been previously defined in terms of displacements (equation 3-2):

$$\epsilon_{ij} = \frac{1}{2} \left(\frac{\partial u_i}{\partial x_j} + \frac{\partial u_j}{\partial x_i} \right) \quad (4-6)$$

where $i, j = 1, 2, 3$

Thus, in a cartesian co-ordinate system (x,y,z) in which the co-ordinates and displacements are respectively:

$$\left. \begin{aligned} x &= x_1 \\ y &= x_2 \\ z &= x_3 \end{aligned} \right\} \quad (4-7)$$

and

$$\left. \begin{aligned} u &= u_1 \\ v &= u_2 \\ w &= u_3 \end{aligned} \right\} \quad (4-8)$$

the tensorial strains are:

$$\left. \begin{aligned}
 \epsilon_{xx} &= \frac{\partial u}{\partial x} \\
 \epsilon_{yy} &= \frac{\partial v}{\partial y} \\
 \epsilon_{zz} &= \frac{\partial w}{\partial z} \\
 \epsilon_{yz} &= \frac{1}{2} \left(\frac{\partial v}{\partial z} + \frac{\partial w}{\partial y} \right) \\
 \epsilon_{xz} &= \frac{1}{2} \left(\frac{\partial u}{\partial z} + \frac{\partial w}{\partial x} \right) \\
 \epsilon_{xy} &= \frac{1}{2} \left(\frac{\partial u}{\partial y} + \frac{\partial v}{\partial x} \right)
 \end{aligned} \right\} (4-9)$$

and the engineering strains are:

$$\left. \begin{aligned}
 \epsilon_x &= \frac{\partial u}{\partial x} \\
 \epsilon_y &= \frac{\partial v}{\partial y} \\
 \epsilon_z &= \frac{\partial w}{\partial z} \\
 \gamma_{yz} &= \left(\frac{\partial v}{\partial z} + \frac{\partial w}{\partial y} \right) \\
 \gamma_{xz} &= \left(\frac{\partial u}{\partial z} + \frac{\partial w}{\partial x} \right) \\
 \gamma_{xy} &= \left(\frac{\partial u}{\partial y} + \frac{\partial v}{\partial x} \right)
 \end{aligned} \right\} (4-10)$$

Expressions (4-3), (4-4), (4-5) and (4-10) enable strain definition in terms of the midplane displacements, u_0 , v_0 and w , for any point in the laminate. However, since it has already been assumed that the effects of the strains ϵ_z , γ_{yz} and γ_{xz} are negligible, only those relating to deformation in the x-y plane need be considered

any further.

Substitution of equation (4-3) into the first of the relationships given in (4-10) yields

$$\begin{aligned}
 \epsilon_x &= \frac{\partial u}{\partial x} \\
 &= \frac{\partial}{\partial x} \left(u_0 - z \frac{\partial w}{\partial x} \right) \\
 &= \frac{\partial u_0}{\partial x} - z \frac{\partial^2 w}{\partial x^2}
 \end{aligned} \tag{4-11}$$

Similarly,

$$\begin{aligned}
 \epsilon_y &= \frac{\partial v}{\partial y} \\
 &= \frac{\partial}{\partial y} \left(v_0 - z \frac{\partial w}{\partial y} \right) \\
 &= \frac{\partial v_0}{\partial y} - z \frac{\partial^2 w}{\partial y^2}
 \end{aligned} \tag{4-12}$$

and

$$\begin{aligned}
 \gamma_{xy} &= \frac{\partial u}{\partial y} + \frac{\partial v}{\partial x} \\
 &= \frac{\partial}{\partial y} \left(u_0 - z \frac{\partial w}{\partial x} \right) + \frac{\partial}{\partial x} \left(v_0 - z \frac{\partial w}{\partial y} \right) \\
 &= \left(\frac{\partial u_0}{\partial y} + \frac{\partial v_0}{\partial x} \right) - 2z \frac{\partial^2 w}{\partial x \partial y}
 \end{aligned} \tag{4-13}$$

The displacement terms in these last three equations are directly related to the midplane strains, however:

$$\left. \begin{aligned}
 \epsilon_x^0 &= \frac{\partial u_0}{\partial x} \\
 \epsilon_y^0 &= \frac{\partial v_0}{\partial y} \\
 \gamma_{xy}^0 &= \frac{\partial u_0}{\partial y} + \frac{\partial v_0}{\partial x}
 \end{aligned} \right\} \tag{4-14}$$

Also, by definition,

$$\left. \begin{aligned} K_x &= -\frac{\partial^2 w}{\partial x^2} \\ K_y &= -\frac{\partial^2 w}{\partial y^2} \\ K_{xy} &= -2\frac{\partial^2 w}{\partial x \partial y} \end{aligned} \right\} \quad (4-15)$$

where K_x , K_y and K_{xy} denote changes of the plate curvature. Thus, the strain-displacement relationships can be expressed:

$$\left. \begin{aligned} \epsilon_x &= \epsilon_x^\circ + z K_x \\ \epsilon_y &= \epsilon_y^\circ + z K_y \\ \gamma_{xy} &= \gamma_{xy}^\circ + z K_{xy} \end{aligned} \right\} \quad (4-16)$$

The equivalent matrix forms of these equations are:

$$\begin{Bmatrix} \epsilon_x \\ \epsilon_y \\ \gamma_{xy} \end{Bmatrix} = \begin{Bmatrix} \epsilon_x^\circ \\ \epsilon_y^\circ \\ \gamma_{xy}^\circ \end{Bmatrix} + z \begin{Bmatrix} K_x \\ K_y \\ K_{xy} \end{Bmatrix} \quad (4-17)$$

and

$$\{\epsilon\} = \{\epsilon^\circ\} + z \{K\} \quad (4-18)$$

4.3 FORCE AND MOMENT RESULTANTS

Stresses acting on the plane faces of an elemental cube cut from a laminate can be resolved in the directions of the co-ordinate axes as has been described previously in Section 3.1. In the most general case, the stress components are: σ_x , σ_y , σ_z , τ_{xy} , τ_{xz} and τ_{yz} . However,

since it is generally assumed that laminates are in a state of plane stress, only the components σ_x , σ_y and τ_{xy} ($= \tau_{yx}$) need be considered in this analysis.

In Figure 4.3, another view of the x-z plane of a deformed laminate is provided. As a result of deformation, a stress, σ_x , is induced on an infinitesimal area, dA , of the laminate cross section at a distance z from the geometric midplane. If a unit width is assumed for the laminate in the y-direction, this can be replaced by a force,

$$\begin{aligned} dN_x &= \sigma_x dA \\ &= \sigma_x dz \end{aligned} \quad (4-19)$$

and a bending moment

$$\begin{aligned} dM_x &= \sigma_x z dA \\ &= \sigma_x z dz \end{aligned} \quad (4-20)$$

acting at the geometric midplane.

Clearly, then, the entire stress distribution can be replaced by an equivalent force and bending moment acting at the midplane. The equivalent force, N_x , is the integral, or sum, of all the elemental forces, dN_x :

$$\begin{aligned} N_x &= \int_{-h/2}^{h/2} dN_x \\ &= \int_{-h/2}^{h/2} \sigma_x dz \end{aligned} \quad (4-21)$$

and the equivalent bending moment is obtained by integrating the elemental bending moments, dM :

$$\begin{aligned} M_x &= \int_{-h/2}^{h/2} dM_x \\ &= \int_{-h/2}^{h/2} \sigma_x z \, dz \end{aligned} \quad (4-22)$$

Similarly, it can be shown that

$$N_y = \int_{-h/2}^{h/2} \sigma_y \, dz \quad (4-23)$$

$$M_y = \int_{-h/2}^{h/2} \sigma_y z \, dz \quad (4-24)$$

$$N_{xy} = \int_{-h/2}^{h/2} \tau_{xy} \, dz \quad (4-25)$$

$$M_{xy} = \int_{-h/2}^{h/2} \tau_{xy} z \, dz \quad (4-26)$$

The stresses, σ_x , σ_y and τ_{xy} , which are generated within a laminate during deformation can therefore be replaced (for analytical purposes) by a system of three forces and three moments acting at the geometric midplane, as is shown in Figure 4.4.

4.4 CONSTITUTIVE EQUATIONS

4.4.1 Force Resultant Considerations

Consider initially the force resultant, N_x . From equation (4-21),

$$N_x = \int_{-h/2}^{h/2} \sigma_x d\bar{z}$$

However, the stress in a laminate does not vary linearly across the thickness as it does in the case of isotropic materials. There may, in fact, be substantial variation in the stress pattern from one layer, or lamina, to the next. For example, in a laminate containing a high modulus material immediately adjacent to another of low modulus, the stresses would have to be much higher in the higher modulus material since the strains at the interface would have to be identical (strain compatibility condition). Accordingly, since the stress variation cannot be described by a single continuous function, the integration must be carried out in parts, i.e.,

$$N_x = \int_{-h/2}^{h_1} \sigma_x^{(1)} d\bar{z} + \int_{h_1}^{h_2} \sigma_x^{(2)} d\bar{z} + \dots + \int_{h_{k-1}}^{h_k} \sigma_x^{(k)} d\bar{z} + \dots + \int_{h_{n-1}}^{h/2} \sigma_x^{(n)} d\bar{z}$$

(= h_n)

or

$$N_x = \sum_{k=1}^n \int_{h_{k-1}}^{h_k} \sigma_x^{(k)} d\bar{z} \quad (4-27)$$

where $\sigma_x^{(k)}$ is the stress in the k th layer of the laminate which can be described by a continuous function.

From equations (3-64), the stress, $\sigma_x^{(k)}$, in the k th layer is related to the strains in that layer by the expression

$$\sigma_x^{(k)} = C_{11}'^{(k)} \epsilon_x + C_{12}'^{(k)} \epsilon_y + C_{16}'^{(k)} \gamma_{xy} \quad (4-28)$$

Also from equations (4-16),

$$\begin{aligned} \epsilon_x &= \epsilon_x^{\circ} + z \chi_x \\ \epsilon_y &= \epsilon_y^{\circ} + z \chi_y \\ \gamma_{xy} &= \gamma_{xy}^{\circ} + z \chi_{xy} \end{aligned}$$

hence,

$$\sigma_x^{(k)} = C_{11}'^{(k)} \epsilon_x^{\circ} + C_{12}'^{(k)} \epsilon_y^{\circ} + C_{16}'^{(k)} \gamma_{xy}^{\circ} + C_{11}'^{(k)} z \chi_x + C_{12}'^{(k)} z \chi_y + C_{16}'^{(k)} z \chi_{xy} \quad \dots (4-29)$$

Substitution of this expression into equation (4-27) then yields

$$N_x = \sum_{k=1}^n \int_{h_{k-1}}^{h_k} \left(C_{11}'^{(k)} \epsilon_x^{\circ} + C_{12}'^{(k)} \epsilon_y^{\circ} + C_{16}'^{(k)} \gamma_{xy}^{\circ} + C_{11}'^{(k)} z \chi_x + C_{12}'^{(k)} z \chi_y + C_{16}'^{(k)} z \chi_{xy} \right) dz \quad \dots (4-30)$$

or, by rearranging terms,

$$N_x = \sum_{k=1}^n \int_{h_{k-1}}^{h_k} \left(C_{11}'^{(k)} \epsilon_x^{\circ} + C_{12}'^{(k)} \epsilon_y^{\circ} + C_{16}'^{(k)} \gamma_{xy}^{\circ} \right) dz + \sum_{k=1}^n \int_{h_{k-1}}^{h_k} \left(C_{11}'^{(k)} z \chi_x + C_{12}'^{(k)} z \chi_y + C_{16}'^{(k)} z \chi_{xy} \right) dz \quad \dots (4-31)$$

In the range of integration, however, $C_{11}'^{(k)}$, $C_{12}'^{(k)}$ and $C_{16}'^{(k)}$

are constants. Further, the midplane strains, ϵ_x° , ϵ_y° , γ_{xy}° , and the plate curvatures, κ_x , κ_y , κ_{xy} , are also independent of z . Hence,

$$N_x = \sum_{k=1}^n \left(C_{11}'^{(k)} \epsilon_x^\circ + C_{12}'^{(k)} \epsilon_y^\circ + C_{16}'^{(k)} \gamma_{xy}^\circ \right) \int_{h_{k-1}}^{h_k} dz + \sum_{k=1}^n \left(C_{11}'^{(k)} z \kappa_x + C_{12}'^{(k)} z \kappa_y + C_{16}'^{(k)} z \kappa_{xy} \right) \int_{h_{k-1}}^{h_k} z dz \quad (4-32)$$

Then,

$$N_x = \sum_{k=1}^n \left(C_{11}'^{(k)} \epsilon_x^\circ + C_{12}'^{(k)} \epsilon_y^\circ + C_{16}'^{(k)} \gamma_{xy}^\circ \right) [z]_{h_{k-1}}^{h_k} + \sum_{k=1}^n \left(C_{11}'^{(k)} z \kappa_x + C_{12}'^{(k)} z \kappa_y + C_{16}'^{(k)} z \kappa_{xy} \right) \left[\frac{z^2}{2} \right]_{h_{k-1}}^{h_k} \quad (4-33)$$

and

$$N_x = \sum_{k=1}^n \left(C_{11}'^{(k)} \epsilon_x^\circ + C_{12}'^{(k)} \epsilon_y^\circ + C_{16}'^{(k)} \gamma_{xy}^\circ \right) (h_k - h_{k-1}) + \sum_{k=1}^n \left(C_{11}'^{(k)} z \kappa_x + C_{12}'^{(k)} z \kappa_y + C_{16}'^{(k)} z \kappa_{xy} \right) \frac{1}{2} (h_k^2 - h_{k-1}^2) \quad (4-34)$$

By rewriting equation (4-34) in the form

$$N_x = \left[\sum_{k=1}^n C_{11}'^{(k)} (h_k - h_{k-1}) \right] \epsilon_x^\circ + \left[\sum_{k=1}^n C_{12}'^{(k)} (h_k - h_{k-1}) \right] \epsilon_y^\circ + \left[\sum_{k=1}^n C_{16}'^{(k)} (h_k - h_{k-1}) \right] \gamma_{xy}^\circ + \left[\sum_{k=1}^n C_{11}'^{(k)} \frac{1}{2} (h_k^2 - h_{k-1}^2) \right] \kappa_x + \left[\sum_{k=1}^n C_{12}'^{(k)} \frac{1}{2} (h_k^2 - h_{k-1}^2) \right] \kappa_y + \left[\sum_{k=1}^n C_{16}'^{(k)} \frac{1}{2} (h_k^2 - h_{k-1}^2) \right] \kappa_{xy} \dots \quad (4-35)$$

it becomes apparent that the bracketed terms are constants,

dependent only upon the constituent elastic constants and the laminate geometry. The equation can therefore be expressed in the relatively simple form:

$$N_x = A_{11} \epsilon_x^\circ + A_{12} \epsilon_y^\circ + A_{16} \gamma_{xy}^\circ + B_{11} \kappa_x + B_{12} \kappa_y + B_{16} \kappa_{xy} \quad (4-36)$$

where

$$\left. \begin{aligned} A_{11} &= \sum_{k=1}^n C'_{11}{}^{(k)} (h_k - h_{k-1}) \\ A_{12} &= \sum_{k=1}^n C'_{12}{}^{(k)} (h_k - h_{k-1}) \\ A_{16} &= \sum_{k=1}^n C'_{16}{}^{(k)} (h_k - h_{k-1}) \\ B_{11} &= \sum_{k=1}^n C'_{11}{}^{(k)} \frac{1}{2} (h_k^2 - h_{k-1}^2) \\ B_{12} &= \sum_{k=1}^n C'_{12}{}^{(k)} \frac{1}{2} (h_k^2 - h_{k-1}^2) \\ B_{16} &= \sum_{k=1}^n C'_{16}{}^{(k)} \frac{1}{2} (h_k^2 - h_{k-1}^2) \end{aligned} \right\} \quad (4-37)$$

Similar relationships can be developed for N_y and N_{xy} by starting with the relationships

$$N_y = \int_{-h/2}^{h/2} \sigma_y dz$$

$$N_{xy} = \int_{-h/2}^{h/2} \tau_{xy} dz$$

and repeating the procedure outlined in the foregoing.

The resulting laminate constitutive relationships

are:

$$\left. \begin{aligned} N_x &= A_{11} \epsilon_x^0 + A_{12} \epsilon_y^0 + A_{16} \gamma_{xy}^0 + B_{11} \kappa_x + B_{12} \kappa_y + B_{16} \kappa_{xy} \\ N_y &= A_{12} \epsilon_x^0 + A_{22} \epsilon_y^0 + A_{26} \gamma_{xy}^0 + B_{12} \kappa_x + B_{22} \kappa_y + B_{26} \kappa_{xy} \\ N_{xy} &= A_{16} \epsilon_x^0 + A_{26} \epsilon_y^0 + A_{66} \gamma_{xy}^0 + B_{16} \kappa_x + B_{26} \kappa_y + B_{66} \kappa_{xy} \end{aligned} \right\} (4-38)$$

where

$$A_{ij} = \sum_{k=1}^n C'_{ij}{}^{(k)} (h_k - h_{k-1}) \quad (4-39)$$

and

$$B_{ij} = \sum_{k=1}^n C'_{ij}{}^{(k)} \frac{1}{2} (h_k^2 - h_{k-1}^2) \quad (4-40)$$

4.4.2 Moment Resultant Considerations

Equations relating the moment resultants, M_x , M_y and M_{xy} to the laminate midplane strains and plate curvatures are obtained in a similar way to the force resultant relationships.

In this case, the starting point is the moment resultant-planar stress relationships

$$\left. \begin{aligned} M_x &= \int_{-h/2}^{h/2} \sigma_x z \, dz \\ M_y &= \int_{-h/2}^{h/2} \sigma_y z \, dz \\ M_{xy} &= \int_{-h/2}^{h/2} \tau_{xy} z \, dz \end{aligned} \right\} (4-41)$$

Following the procedure outlined in the previous section, it can be shown that the equivalent expressions for

equations (4-27) and (4-32) are, respectively,

$$M_x = \sum_{k=1}^n \int_{-h/2}^{h/2} \sigma_x^{(k)} z \, dz \quad (4-42)$$

and

$$M_x = \sum_{k=1}^n (C_{11}^{(k)} \epsilon_x^{\circ} + C_{12}^{(k)} \epsilon_y^{\circ} + C_{16}^{(k)} \gamma_{xy}^{\circ}) \int_{h_{k-1}}^{h_k} z \, dz \\ + \sum_{k=1}^n (C_{11}^{(k)} \chi_x + C_{12}^{(k)} \chi_y + C_{16}^{(k)} \chi_{xy}) \int_{h_k}^{h_{k-1}} z^2 \, dz \quad (4-43)$$

Integration of this expression then yields an equation similar in form to (4-36):

$$M_x = \left[\sum_{k=1}^n C_{11}^{(k)} \frac{1}{2} (h_k^2 - h_{k-1}^2) \right] \epsilon_x^{\circ} + \left[\sum_{k=1}^n C_{12}^{(k)} \frac{1}{2} (h_k^2 - h_{k-1}^2) \right] \epsilon_y^{\circ} + \left[\sum_{k=1}^n C_{16}^{(k)} \frac{1}{2} (h_k^2 - h_{k-1}^2) \right] \gamma_{xy}^{\circ} \\ + \left[\sum_{k=1}^n C_{11}^{(k)} \frac{1}{3} (h_k^3 - h_{k-1}^3) \right] \chi_x + \left[\sum_{k=1}^n C_{12}^{(k)} \frac{1}{3} (h_k^3 - h_{k-1}^3) \right] \chi_y + \left[\sum_{k=1}^n C_{16}^{(k)} \frac{1}{3} (h_k^3 - h_{k-1}^3) \right] \chi_{xy} \\ \dots (4-44)$$

Once again, it is readily apparent that the bracketed terms are constants, dependent only upon the constituent layer elastic and geometric properties. Thus,

$$M_x = B_{11} \epsilon_x^{\circ} + B_{12} \epsilon_y^{\circ} + B_{16} \gamma_{xy}^{\circ} + D_{11} \chi_x + D_{12} \chi_y + D_{16} \chi_{xy} \quad (4-45)$$

Similarly,

$$M_y = B_{12} \epsilon_x^{\circ} + B_{22} \epsilon_y^{\circ} + B_{26} \gamma_{xy}^{\circ} + D_{12} \chi_x + D_{22} \chi_y + D_{66} \chi_{xy} \quad (4-46)$$

and

$$M_{xy} = B_{16}\epsilon_x^{\circ} + B_{26}\epsilon_y^{\circ} + B_{66}\gamma_{xy}^{\circ} + D_{16}K_x + D_{26}K_y + D_{66}K_{xy} \quad (4-47)$$

Therefore, the moment resultant constitutive equations are:

$$\left. \begin{aligned} M_x &= B_{11}\epsilon_x^{\circ} + B_{12}\epsilon_y^{\circ} + B_{16}\gamma_{xy}^{\circ} + D_{11}K_x + D_{12}K_y + D_{16}K_{xy} \\ M_y &= B_{12}\epsilon_x^{\circ} + B_{22}\epsilon_y^{\circ} + B_{26}\gamma_{xy}^{\circ} + D_{12}K_x + D_{22}K_y + D_{26}K_{xy} \\ M_{xy} &= B_{16}\epsilon_x^{\circ} + B_{26}\epsilon_y^{\circ} + B_{66}\gamma_{xy}^{\circ} + D_{16}K_x + D_{26}K_y + D_{66}K_{xy} \end{aligned} \right\} \quad (4-48)$$

where

$$D_{ij} = \sum_{k=1}^n C_{ij}^{(k)} \frac{1}{3} (h_k^3 - h_{k-1}^3) \quad (4-49)$$

and B_{ij} was defined previously in equation (4-40).

The response of a laminate to externally applied loads is fully described by equations (4-38) and (4-48).

Thus, the full set of laminate constitutive equations is:

$$\left. \begin{aligned} N_x &= A_{11}\epsilon_x^{\circ} + A_{12}\epsilon_y^{\circ} + A_{16}\gamma_{xy}^{\circ} + B_{11}K_x + B_{12}K_y + B_{16}K_{xy} \\ N_y &= A_{12}\epsilon_x^{\circ} + A_{22}\epsilon_y^{\circ} + A_{26}\gamma_{xy}^{\circ} + B_{12}K_x + B_{22}K_y + B_{26}K_{xy} \\ N_{xy} &= A_{16}\epsilon_x^{\circ} + A_{26}\epsilon_y^{\circ} + A_{66}\gamma_{xy}^{\circ} + B_{16}K_x + B_{26}K_y + B_{66}K_{xy} \\ M_x &= B_{11}\epsilon_x^{\circ} + B_{12}\epsilon_y^{\circ} + B_{16}\gamma_{xy}^{\circ} + D_{11}K_x + D_{12}K_y + D_{16}K_{xy} \\ M_y &= B_{12}\epsilon_x^{\circ} + B_{22}\epsilon_y^{\circ} + B_{26}\gamma_{xy}^{\circ} + D_{12}K_x + D_{22}K_y + D_{26}K_{xy} \\ M_{xy} &= B_{16}\epsilon_x^{\circ} + B_{26}\epsilon_y^{\circ} + B_{66}\gamma_{xy}^{\circ} + D_{16}K_x + D_{26}K_y + D_{66}K_{xy} \end{aligned} \right\} \quad (4-50)$$

which can also be expressed in matrix form:

$$\begin{Bmatrix} N_x \\ N_y \\ N_{xy} \\ M_x \\ M_y \\ M_{xy} \end{Bmatrix} = \begin{bmatrix} A_{11} & A_{12} & A_{16} & B_{11} & B_{12} & B_{16} \\ A_{12} & A_{22} & A_{26} & B_{12} & B_{22} & B_{26} \\ A_{16} & A_{26} & A_{66} & B_{16} & B_{26} & B_{66} \\ B_{11} & B_{12} & B_{16} & D_{11} & D_{12} & D_{16} \\ B_{12} & B_{22} & B_{26} & D_{12} & D_{22} & D_{26} \\ B_{16} & B_{26} & B_{66} & D_{16} & D_{26} & D_{66} \end{bmatrix} \begin{Bmatrix} \epsilon_x^0 \\ \epsilon_y^0 \\ \gamma_{xy}^0 \\ \chi_x \\ \chi_y \\ \chi_{xy} \end{Bmatrix} \quad (4-51)$$

or, simply,

$$\begin{Bmatrix} N \\ M \end{Bmatrix} = \begin{bmatrix} A & | & B \\ \hline B & | & D \end{bmatrix} \begin{Bmatrix} \epsilon^0 \\ \chi \end{Bmatrix} \quad (4-52)$$

By inverting this equation, another form of the constitutive equations, particularly useful in plate and shell analysis, is obtained:

$$\begin{Bmatrix} \epsilon^0 \\ M \end{Bmatrix} = \begin{bmatrix} A^* & | & B^* \\ \hline H^* & | & D^* \end{bmatrix} \begin{Bmatrix} N \\ \chi \end{Bmatrix} \quad (4-53)$$

where

$$\begin{aligned} [A^*] &= [A]^{-1} \\ [B^*] &= -[A]^{-1} [B] \\ [H^*] &= [B] [A]^{-1} \\ [D^*] &= [D] - [B] [A]^{-1} [B] \end{aligned} \quad (4-54)$$

Finally, the fully inverted form of equation (4-52)

is:

$$\begin{Bmatrix} \epsilon^0 \\ \chi \end{Bmatrix} = \begin{bmatrix} A' & | & B' \\ \hline B' & | & D' \end{bmatrix} \begin{Bmatrix} N \\ M \end{Bmatrix} \quad (4-55)$$

where

$$\begin{aligned} [A'] &= [A^*] - [B^*] [D^*]^{-1} [H^*] \\ [B'] &= [B^*] [D^*]^{-1} \\ [D'] &= [D^*]^{-1} \end{aligned} \quad (4-56)$$

It is commonly utilized in the determination of midplane strains and curvatures when the applied laminate loads, N and M , are known.

4.5 COUPLING BETWEEN BENDING AND STRETCHING

It is interesting to note from equations (4-53) that coupling may exist between bending and stretching in fibre-reinforced composite laminates. That is to say, for certain laminate constructions, the application of stretching loads (N) will result in bending moments (M) being induced in the laminate (or vice versa), since

$$\{M\} = [H^*] \{N\} + [D^*] \{\kappa\} \quad (4-57)$$

The degree of coupling, as indicated by this equation, is dependent upon the value of the terms in the matrix $[H^*]$. However, from equations (4-54), it is also clear that these terms are in turn dependent upon the values of the terms of the $[A]$ and $[B]$ matrices. It will therefore be necessary to study some of the effects of laminate construction of the value of $[A]$ and $[B]$ in order to obtain a better understanding of the coupling phenomenon.

It is evident from equations (3-62) that C'_{11} , C'_{12} , C'_{22} ,

and C'_{66} are always positive and greater than zero. Thus, according to equation (4-39), A_{11} , A_{12} , A_{22} and A_{66} must also be similarly valued since the lamina thickness terms $(h_k - h_{k-1})$ can never be less than or equal to zero. The situation is quite different for the A_{16} and A_{26} terms, however. Depending upon lamina orientation, C'_{16} and C'_{26} can be negative, zero or positive according to equations (3-62). Thus, A_{16} and A_{26} are not limited in value as are the other A_{ij} .

Consider a laminate constructed in such a way that for each lamina with a positive orientation, there is another with similar properties at an identical negative orientation. It can readily be shown through equation (4-39) that in this special case, $A_{16} = A_{26} = 0$. Such laminates are generally termed specially orthotropic.

Of far more importance are laminates which are midplane symmetric. In these, for every lamina above the midplane, there is another of similar properties and orientation located at an identical distance below it. Coupling is eliminated in laminates constructed in this way as can be shown from equations (4-40) and (4-54) since all B_{ij} and hence $H_{ij}^* = 0$. There are two principal advantages to constructing midplane symmetric laminates:

- 1) laminate analysis is considerably simplified, and
- 2) warping due to inplane loads, particularly thermal forces, is avoided.

Through judicious laminate design, therefore, it is possible to produce a laminate with constitutive equations which are identical in form to those for an isotropic plate or shell:

$$\begin{Bmatrix} N_x \\ N_y \\ N_{xy} \end{Bmatrix} = \begin{bmatrix} A_{11} & A_{12} & 0 \\ A_{12} & A_{22} & 0 \\ 0 & 0 & A_{66} \end{bmatrix} \begin{Bmatrix} \epsilon_x^o \\ \epsilon_y^o \\ \gamma_{xy}^o \end{Bmatrix} \quad (4-58)$$

and

$$\begin{Bmatrix} M_x \\ M_y \\ M_{xy} \end{Bmatrix} = \begin{bmatrix} D_{11} & D_{12} & 0 \\ D_{12} & D_{22} & 0 \\ 0 & 0 & D_{66} \end{bmatrix} \begin{Bmatrix} \chi_x \\ \chi_y \\ \chi_{xy} \end{Bmatrix} \quad (4-59)$$

where, in the isotropic case,

$$\left. \begin{aligned} A_{11} &= A_{22} = \frac{Eh}{1-\nu^2} \\ A_{12} &= \nu A_{11} \\ A_{66} &= \frac{Eh}{2(1+\nu)} \\ D_{11} &= D_{22} = \frac{Eh^3}{12(1-\nu^2)} \\ D_{12} &= \nu D_{11} \\ D_{66} &= \frac{Eh^3}{24(1+\nu)} \end{aligned} \right\} \quad (4-60)$$

and, in the orthotropic case, all A_{ij} and D_{ij} are as previously defined.

4.6 LAMINATE FAILURE ANALYSIS

Laminate failure is usually associated with the initial failure of a constituent layer. It is therefore necessary to ascertain individual layer strains and/or stresses before an appropriate failure criterion can be applied to determine structural adequacy.

The first step in a failure analysis is to determine the midplane strains and curvatures for the particular loading condition under consideration. This is usually accomplished by employing equations (4-55). Next, individual layer strain components in the co-ordinate system of the structure are obtained through the use of equations (4-17). These are in turn transformed into strain components in the natural co-ordinate system of the layer materials in accordance with the strain transformation relationships (3-59). The principal layer stresses can then be computed, if necessary, from the lamina constitutive equations (3-51). The final step in the analysis is to substitute the principal layer strains or stresses (whichever is appropriate) into the selected failure criterion to find out whether or not any of the layers, and hence the laminate, has failed.

Although most structural design is based upon the initial failure condition, the ultimate load carrying capability of a laminate is also an important consideration, especially in the case of life critical structures, e.g.,

aircraft. A degradation-of-layers approach (31, 43, 46) is usually employed to determine the ultimate strength of a laminate. In this approach, as a layer fails, the type of failure is observed and its effect on the components of the stiffness matrix of that layer determined. New effective laminate stiffnesses are then established and the failure analysis is repeated to resolve which layer or layers will fail next and at what load. The process is then repeated until all layers have failed.

4.7 CLOSING

Occasionally, it is necessary to go through a full plate or shell analysis in order to ascertain structural behaviour. In such cases, as was indicated in Section 2.2, the analysis closely follows conventional plate or shell analysis procedures, the only difference being that laminate constitutive equations are used in place of the conventional force and moment resultant equations. This procedure is fully demonstrated in the next section which deals with a specific shell problem: the analysis of a laminated composite liquid storage tank.

SECTION 5

CYLINDRICAL TANK ANALYSIS

The problem of a cylindrical tank subjected to the action of internal pressure, as shown in Figure 5.1, has been studied previously by Timoshenko and Woinowsky-Krieger (44). Unfortunately, their analysis is applicable only in cases where isotropic materials of construction are employed. In this section, revised deflection, strain and stress equations are developed for laminated composite tanks.

Displacement equations are derived first by following the approach outlined previously, i.e., by substituting laminate constitutive relationships for the usual force and moment resultant equations in the conventional shell analysis and re-solving the equations. Once these have been obtained, it becomes a relatively simple matter to use the strain-displacement relationships to determine mid-plane strains and shell curvatures and hence individual lamina strains and stresses (see Section 4.6). Full details of the theoretical development are included in order to demonstrate thoroughly this new approach to the analysis of laminated composite plate or shell structures.

5.1 STRAIN-DISPLACEMENT RELATIONSHIPS

According to Timoshenko and Woinowsky-Krieger (44), components at a point are related to the middle surface strains and changes in shell curvature by the expressions

$$\left. \begin{aligned} \epsilon_x &= \epsilon_x^\circ - z \chi_x \\ \epsilon_\theta &= \epsilon_\theta^\circ - z \chi_\theta \\ \gamma_{x\theta} &= \gamma_{x\theta}^\circ - 2z \chi_{x\theta} \end{aligned} \right\} \quad (5-1)$$

where $\epsilon_x, \epsilon_\theta, \gamma_{x\theta}$ are the component strains at the point,
 $\epsilon_x^\circ, \epsilon_\theta^\circ, \gamma_{x\theta}^\circ$ are the middle surface strains,
 $\chi_x, \chi_\theta, \chi_{x\theta}$ are the changes in shell curvature.

Also, the middle surface strains and the changes in curvature can be represented in terms of the displacements in the $x, \theta,$ and z directions, i.e., u, v and w , respectively, as follows:

$$\left. \begin{aligned} \epsilon_x^\circ &= \frac{\partial u^\circ}{\partial x} \\ \epsilon_\theta^\circ &= \frac{1}{r} \frac{\partial v^\circ}{\partial \theta} - \frac{w}{r} \\ \gamma_{x\theta}^\circ &= \frac{1}{r} \frac{\partial u^\circ}{\partial \theta} + \frac{\partial v^\circ}{\partial x} \\ \chi_x &= \frac{\partial^2 w}{\partial x^2} \\ \chi_\theta &= \frac{1}{r^2} \left(\frac{\partial v^\circ}{\partial \theta} + \frac{\partial^2 w}{\partial \theta^2} \right) \\ \chi_{x\theta} &= \frac{1}{r} \left(\frac{\partial v^\circ}{\partial x} + \frac{\partial^2 w}{\partial x \partial \theta} \right) \end{aligned} \right\} \quad (5-2)$$

Hence, the generalized strain-displacement relationships

are:

$$\left. \begin{aligned} \epsilon_x &= \frac{\partial u^{\circ}}{\partial x} - z \frac{\partial^2 w}{\partial x^2} \\ \epsilon_{\theta} &= \frac{1}{r} \left(\frac{\partial v^{\circ}}{\partial \theta} - w \right) - z \frac{1}{r^2} \left(\frac{\partial v^{\circ}}{\partial \theta} + \frac{\partial^2 w}{\partial \theta^2} \right) \\ \gamma_{x\theta} &= \frac{1}{r} \frac{\partial u^{\circ}}{\partial \theta} + \frac{\partial v^{\circ}}{\partial x} - 2z \frac{1}{r} \left(\frac{\partial v^{\circ}}{\partial x} + \frac{\partial^2 w}{\partial x \partial \theta} \right) \end{aligned} \right\} (5-3)$$

or

$$\left. \begin{aligned} \epsilon_x &= \frac{\partial u^{\circ}}{\partial x} - z \frac{\partial^2 w}{\partial x^2} \\ \epsilon_{\theta} &= \frac{1}{r} \left(1 - \frac{z}{r} \right) \frac{\partial v^{\circ}}{\partial \theta} - \frac{w}{r} - z \frac{1}{r^2} \frac{\partial^2 w}{\partial \theta^2} \\ \gamma_{x\theta} &= \frac{1}{r} \frac{\partial u^{\circ}}{\partial \theta} + \left(1 - \frac{2z}{r} \right) \frac{\partial v^{\circ}}{\partial x} - z \frac{2}{r} \frac{\partial^2 w}{\partial x \partial \theta} \end{aligned} \right\} (5-4)$$

Neglecting the small quantities $\frac{z}{r}$, $\frac{2z}{r}$ in comparison with unity,

$$\left. \begin{aligned} \epsilon_x &= \frac{\partial u^{\circ}}{\partial x} - z \frac{\partial^2 w}{\partial x^2} \\ \epsilon_{\theta} &= \frac{1}{r} \frac{\partial v^{\circ}}{\partial \theta} - \frac{w}{r} - z \frac{1}{r^2} \frac{\partial^2 w}{\partial \theta^2} \\ \gamma_{x\theta} &= \frac{1}{r} \frac{\partial u^{\circ}}{\partial \theta} + \frac{\partial v^{\circ}}{\partial x} - z \frac{2}{r} \frac{\partial^2 w}{\partial x \partial \theta} \end{aligned} \right\} (5-5)$$

Due to the general form of the laminate constitutive relationship, however, it will be more convenient to use a slightly different form of equation (5-1), i.e.,

$$\left. \begin{aligned} \epsilon_x &= \epsilon_x^{\circ} + z \chi_x \\ \epsilon_{\theta} &= \epsilon_{\theta}^{\circ} + z \chi_{\theta} \\ \gamma_{x\theta} &= \gamma_{x\theta}^{\circ} + z \chi_{x\theta} \end{aligned} \right\} (5-6)$$

where

$$\left. \begin{aligned} \chi_x &= -\chi_x = 0 \\ \chi_\theta &= -\chi_\theta = 0 \\ \chi_{x\theta} &= -2\chi_{x\theta} = 0 \end{aligned} \right\} \quad (5-7)$$

In the particular problem at hand, the strain-displacement relationships can be simplified somewhat since, due to symmetry,

$$\left. \begin{aligned} \frac{\partial u^\circ}{\partial \theta} &= \frac{\partial v^\circ}{\partial \theta} = \frac{\partial w}{\partial \theta} = 0 \\ \frac{\partial^2 w}{\partial \theta^2} &= \frac{\partial^2 w}{\partial x \partial \theta} = 0 \end{aligned} \right\} \quad (5-8)$$

hence,

$$\left. \begin{aligned} \epsilon_x^\circ &= \frac{\partial u^\circ}{\partial x} \\ \chi_x &= -\frac{\partial^2 w}{\partial x^2} \\ \epsilon_\theta^\circ &= -\frac{w}{r} \\ \chi_\theta &= 0 \\ \gamma_{x\theta}^\circ &= \frac{\partial v^\circ}{\partial x} \\ \chi_{x\theta} &= 0 \end{aligned} \right\} \quad (5-9)$$

Thus, the strain-displacement relationships (5-6) simplify to

$$\left. \begin{aligned} \epsilon_x &= \frac{du^\circ}{dx} - z \frac{d^2 w}{dx^2} \\ \epsilon_\theta &= -\frac{w}{r} \\ \gamma_{x\theta} &= \frac{dv^\circ}{dx} \end{aligned} \right\} \quad (5-10)$$

5.2 THE EQUATIONS OF EQUILIBRIUM

Typical loads encountered by an element of a cylindrical shell are indicated in Figure 5.2. Force and moment equilibrium considerations, in the most general case, yield three equations of equilibrium (44):

$$\tau \frac{\partial N_x}{\partial x} + \frac{\partial N_{x\theta}}{\partial \theta} = 0 \quad (5-11)$$

$$\frac{\partial N_\theta}{\partial \theta} + r \frac{\partial N_{x\theta}}{\partial x} = 0 \quad (5-12)$$

$$N_\theta + \frac{\partial^2 M_{\theta x}}{\partial x \partial \theta} + r \frac{\partial^2 M_x}{\partial x^2} - \frac{\partial^2 M_{x\theta}}{\partial x \partial \theta} + \frac{1}{r} \frac{\partial^2 M_\theta}{\partial \theta^2} + Zr = 0 \quad (5-13)$$

Due to symmetry, however, the force and moment resultants are independent of θ ; therefore, these equations reduce to

$$\frac{dN_x}{dx} = 0 \quad (5-14)$$

$$\frac{dN_{x\theta}}{dx} = 0 \quad (5-15)$$

and

$$N_\theta + r \frac{d^2 M_x}{dx^2} + Zr = 0 \quad (5-16)$$

Equations (5-14) and (5-15) indicate that both N_x and $N_{x\theta}$ have constant values and, since it has been assumed that there is no external loading at the top of the tank, it must be concluded that

$$N_x = N_{x\theta} = 0 \quad (5-17)$$

Equilibrium can therefore be represented by the single equation

$$\frac{d^2 M_x}{d x^2} + \frac{1}{r} N_\theta = -Z \quad (5-18)$$

The lateral load Z in this problem is defined by the equation

$$Z = -\rho(d-x) \quad (5-19)$$

where ρ is the density of the contained liquid

d is the overall height of the tank

x is the distance from the base of the tank.

In cases where N_x and/or $N_{x\theta}$ are different from zero, the deformations and stresses corresponding to such constant forces can be calculated separately and superposed on the deformations and stresses determined in this analysis (44).

5.3 LAMINATE CONSTITUTIVE RELATIONSHIPS

The constitutive relationships for thin laminated cylindrical shells are developed in an identical manner to those for flat plates. The only significant change in the final equations is the subscript notation, i.e., cylindrical co-ordinate system notation is adopted in place of cartesian. Thus, their normal form is:

$$\begin{Bmatrix} N_x \\ N_\theta \\ N_{x\theta} \\ M_x \\ M_\theta \\ M_{x\theta} \end{Bmatrix} = \begin{bmatrix} A_{11} & A_{12} & A_{16} & B_{11} & B_{12} & B_{16} \\ A_{12} & A_{22} & A_{26} & B_{12} & B_{22} & B_{26} \\ A_{16} & A_{26} & A_{66} & B_{16} & B_{26} & B_{66} \\ B_{11} & B_{12} & B_{16} & D_{11} & D_{12} & D_{16} \\ B_{12} & B_{22} & B_{26} & D_{12} & D_{22} & D_{26} \\ B_{16} & B_{26} & B_{66} & D_{16} & D_{26} & D_{66} \end{bmatrix} \begin{Bmatrix} \epsilon_x^\circ \\ \epsilon_\theta^\circ \\ \gamma_{x\theta}^\circ \\ \chi_x \\ \chi_\theta \\ \chi_{x\theta} \end{Bmatrix} \quad (5-20)$$

In this analysis, however, it will be more convenient to start with the partially inverted form of the constitutive relationships:

$$\begin{Bmatrix} \epsilon_x^\circ \\ \epsilon_\theta^\circ \\ \gamma_{x\theta}^\circ \\ M_x \\ M_\theta \\ M_{x\theta} \end{Bmatrix} = \begin{bmatrix} A_{11}^* & A_{12}^* & A_{16}^* & B_{11}^* & B_{12}^* & B_{16}^* \\ A_{12}^* & A_{22}^* & A_{26}^* & B_{12}^* & B_{22}^* & B_{26}^* \\ A_{16}^* & A_{26}^* & A_{66}^* & B_{16}^* & B_{26}^* & B_{66}^* \\ H_{11}^* & H_{12}^* & H_{16}^* & D_{11}^* & D_{12}^* & D_{16}^* \\ H_{12}^* & H_{22}^* & H_{26}^* & D_{12}^* & D_{22}^* & D_{26}^* \\ H_{16}^* & H_{26}^* & H_{66}^* & D_{16}^* & D_{26}^* & D_{66}^* \end{bmatrix} \begin{Bmatrix} N_x \\ N_\theta \\ N_{x\theta} \\ \chi_x \\ \chi_\theta \\ \chi_{x\theta} \end{Bmatrix} \quad (5-21)$$

By introducing relations (5-9) and (5-17),

$$\begin{Bmatrix} \epsilon_x^\circ \\ \epsilon_\theta^\circ \\ \gamma_{x\theta}^\circ \\ M_x \\ M_\theta \\ M_{x\theta} \end{Bmatrix} = \begin{bmatrix} A_{11}^* & A_{12}^* & A_{16}^* & B_{11}^* & B_{12}^* & B_{16}^* \\ A_{12}^* & A_{22}^* & A_{26}^* & B_{12}^* & B_{22}^* & B_{26}^* \\ A_{16}^* & A_{26}^* & A_{66}^* & B_{16}^* & B_{26}^* & B_{66}^* \\ H_{11}^* & H_{12}^* & H_{16}^* & D_{11}^* & D_{12}^* & D_{16}^* \\ H_{12}^* & H_{22}^* & H_{26}^* & D_{12}^* & D_{22}^* & D_{26}^* \\ H_{16}^* & H_{26}^* & H_{66}^* & D_{16}^* & D_{26}^* & D_{66}^* \end{bmatrix} \begin{Bmatrix} 0 \\ N_\theta \\ 0 \\ \chi_x \\ 0 \\ 0 \end{Bmatrix} \quad (5-22)$$

and hence the constitutive equations finally reduce to:

$$\begin{aligned}
 \epsilon_x^\circ &= A_{12}^* N_\theta + B_{11}^* \chi_x \\
 \epsilon_\theta^\circ &= A_{22}^* N_\theta + B_{21}^* \chi_x \\
 \gamma_{x\theta} &= A_{26}^* N_\theta + B_{61}^* \chi_x \\
 M_x &= H_{12}^* N_\theta + D_{11}^* \chi_x \\
 M_\theta &= H_{22}^* N_\theta + D_{12}^* \chi_x \\
 M_{x\theta} &= H_{26}^* N_\theta + D_{16}^* \chi_x
 \end{aligned}
 \tag{5-23}$$

5.4 THE COMPATIBILITY CONDITION

The compatibility condition in the case of general deformation of a cylindrical shell is:

$$\frac{1}{r^2} \frac{\partial^2 \epsilon_x}{\partial \theta^2} + \frac{\partial^2 \epsilon_\theta}{\partial x^2} + \frac{1}{r} \frac{\partial^2 w}{\partial x^2} = \frac{1}{r} \frac{\partial^2 \gamma_{x\theta}}{\partial x \partial \theta}
 \tag{5-24}$$

However, due to symmetry in the problem under consideration, ϵ_x and $\gamma_{x\theta}$ are both independent of θ . Thus, the equation is considerably simplified to:

$$\frac{d^2 \epsilon_\theta}{dx^2} + \frac{1}{r} \frac{d^2 w}{dx^2} = 0
 \tag{5-25}$$

5.5 THE GOVERNING DIFFERENTIAL EQUATION OF DISPLACEMENT

The governing equation of displacement is obtained by utilizing the compatibility condition, equation (5-25), in conjunction with the final form of the partially inverted constitutive relationships (5-23), the strain-displacement relationships (5-9) and (5-10) and the equation of equilibrium (5-18).

From the strain-displacement relationships (5-9)

and (5-10) and the reduced form of the constitutive equations (5-23), it can be shown that

$$\epsilon_{\theta}^{\circ} = \epsilon_{\theta} = -\frac{w}{r} = A_{22}^* N_{\theta} - B_{21}^* \frac{d^2 w}{dx^2} \quad (5-26)$$

and

$$M_x = H_{12}^* N_{\theta} - D_{11}^* \frac{d^2 w}{dx^2} \quad (5-27)$$

Therefore, by differentiating,

$$\frac{d^2 \epsilon_{\theta}}{dx^2} = A_{22}^* \frac{d^2 N_{\theta}}{dx^2} - B_{21}^* \frac{d^4 w}{dx^4} \quad (5-28)$$

and

$$\frac{d^2 M_x}{dx^2} = H_{12}^* \frac{d^2 N_{\theta}}{dx^2} - D_{11}^* \frac{d^4 w}{dx^4} \quad (5-29)$$

Also, from equation (5-26),

$$N_{\theta} = -\frac{1}{A_{22}^*} \frac{w}{r} + \frac{B_{21}^*}{A_{22}^*} \frac{d^2 w}{dx^2} \quad (5-30)$$

Substitution of equation (5-28) into the compatibility equation (5-25) then yields

$$A_{22}^* \frac{d^2 N_{\theta}}{dx^2} - B_{21}^* \frac{d^4 w}{dx^4} + \frac{1}{r} \frac{d^2 w}{dx^2} = 0 \quad (5-31)$$

and hence

$$\frac{d^2 N_{\theta}}{dx^2} = \frac{B_{21}^*}{A_{22}^*} \frac{d^4 w}{dx^4} - \frac{1}{A_{22}^*} \frac{1}{r} \frac{d^2 w}{dx^2} \quad (5-32)$$

Accordingly, equation (5-29) can be rewritten in the form:

$$\frac{d^2 M_x}{dx^2} = \frac{B_{21}^* H_{12}^*}{A_{22}^*} \frac{d^4 w}{dx^4} - \frac{H_{12}^*}{A_{22}^*} \frac{1}{r} \frac{d^2 w}{dx^2} - D_{11}^* \frac{d^4 w}{dx^4} \quad (5-33)$$

hence

$$\frac{d^2 M_x}{dx^2} = - \left(D_{11}^* - \frac{B_{21}^* H_{12}^*}{A_{22}^*} \right) \frac{d^4 w}{dx^4} - \frac{H_{12}^*}{A_{22}^*} \frac{1}{r} \frac{d^2 w}{dx^2} \quad (5-34)$$

Equations (5-19), (5-30) and (5-34) can then be combined with the equation of equilibrium (5-18) to yield

$$- \left(D_{11}^* - \frac{B_{21}^* H_{12}^*}{A_{22}^*} \right) \frac{d^4 w}{dx^4} + \left(\frac{B_{21}^* - H_{12}^*}{A_{22}^*} \right) \frac{1}{r} \frac{d^2 w}{dx^2} - \frac{1}{A_{22}^*} \frac{1}{r^2} = \rho(d-x) \quad (5-35)$$

hence

$$\begin{aligned} \frac{d^4 w}{dx^4} - \left(\frac{B_{21}^* - H_{12}^*}{A_{22}^* D_{11}^* - B_{21}^* H_{12}^*} \right) \frac{1}{r} \frac{d^2 w}{dx^2} + \frac{1}{A_{22}^* D_{11}^* - B_{21}^* H_{12}^*} \frac{w}{r^2} \\ = - \frac{A_{22}^*}{A_{22}^* D_{11}^* - B_{21}^* H_{12}^*} \rho(d-x) \end{aligned} \quad (5-36)$$

Furthermore, from equations (4-54),

$$B_{21}^* = - H_{12}^* \quad (5-37)$$

thus

$$\begin{aligned} \frac{d^4 w}{dx^4} + \frac{2 H_{12}^*}{A_{22}^* D_{11}^* + (H_{12}^*)^2} \frac{1}{r} \frac{d^2 w}{dx^2} + \frac{1}{A_{22}^* D_{11}^* + (H_{12}^*)^2} \frac{w}{r^2} \\ = - \frac{A_{22}^*}{A_{22}^* D_{11}^* + (H_{12}^*)^2} \rho(d-x) \end{aligned} \quad (5-38)$$

This is the governing differential equation of a cylindrical tank subjected to the action of uniformly varying hydrostatic pressure in the axial direction.

5.6 GENERAL SOLUTION OF THE GOVERNING DIFFERENTIAL EQUATION

Equation (5-39) is a standard fourth order linear differential equation which can readily be solved by the technique indicated in Appendix C. The general solution of the equation, as determined in the Appendix, is:

$$w = e^{\alpha x}(C_1 \sin \beta x + C_2 \cos \beta x) + e^{-\alpha x}(C_3 \sin \beta x + C_4 \cos \beta x) + w_p \quad \dots (5-39)$$

where

$$\alpha = \left[-\frac{1}{2\tau} \frac{H_{12}^*}{A_{22}^* D_{11}^* + (H_{12}^*)^2} + \frac{1}{2\tau} \left(\frac{1}{A_{22}^* D_{11}^* + (H_{12}^*)^2} \right)^{1/2} \right]^{1/2} \quad (5-40)$$

$$\beta = \left[\frac{1}{2\tau} \frac{H_{12}^*}{A_{22}^* D_{11}^* + (H_{12}^*)^2} + \frac{1}{2\tau} \left(\frac{1}{A_{22}^* D_{11}^* + (H_{12}^*)^2} \right)^{1/2} \right]^{1/2} \quad (5-41)$$

C_1 , C_2 , C_3 and C_4 are constants of integration which must be determined from boundary conditions, and w_p is a "particular" solution of the governing differential equation.

One particular solution of equation (5-38) is

$$w_p = -A_{22}^* \tau^2 \rho (d-x) \quad (5-42)$$

which represents the radial expansion of a cylindrical shell with free edges under the action of a uniform internal pressure. Accordingly, the complete general solution is:

$$w = e^{\alpha x}(C_1 \sin \beta x + C_2 \cos \beta x) + e^{-\alpha x}(C_3 \sin \beta x + C_4 \cos \beta x) - A_{22}^* \tau^2 \rho (d-x) \quad (5-43)$$

In most cases, however, the wall thickness is small

compared to the structure dimensions r and d , and the shell can be considered to be infinitely long. Thus, C_1 and C_2 are equal to zero (44) and equation (5-43) reduces to

$$w = e^{-\alpha x} (C_3 \sin \beta x + C_4 \cos \beta x) - A_{22}^* r^2 \rho (d - x) \quad (5-44)$$

The remaining constants of integration, C_3 and C_4 , are determined from the boundary conditions.

5.7 APPLICATION OF BOUNDARY CONDITIONS

In this study, it is assumed that the base of the tank is rigidly constrained; thus, the boundary conditions are:

$$w = 0 \quad \text{at} \quad x = 0 \quad (5-45)$$

and

$$\frac{dw}{dx} = 0 \quad \text{at} \quad x = 0 \quad (5-46)$$

From equation (5-44), when $x = 0$,

$$0 = C_4 - A_{22}^* r^2 \rho d \quad (5-47)$$

Also,

$$\begin{aligned} \frac{dw}{dx} = & -\alpha e^{-\alpha x} (C_3 \sin \beta x + C_4 \cos \beta x) + \\ & \beta e^{-\alpha x} (C_3 \cos \beta x + C_4 \sin \beta x) + A_{22}^* r^2 \rho \end{aligned} \quad (5-48)$$

and hence

$$0 = -\alpha C_4 + \beta C_3 + A_{22}^* r^2 \rho \quad (5-49)$$

By solving equations (5-47) and (5-48), it can be determined that:

$$C_3 = A_{22}^* r^2 \rho \left(\frac{\alpha}{\beta} d - \frac{1}{\beta} \right) \quad (5-50)$$

and

$$C_4 = A_{22}^* r^2 \rho d \quad (5-51)$$

Therefore, equation (5-44) becomes

$$w = -A_{22}^* \rho r^2 \left\{ d - x - e^{-\alpha x} \left[d \cos \beta x + \left(\frac{\alpha}{\beta} d - \frac{1}{\beta} \right) \sin \beta x \right] \right\} \quad (5-52)$$

This is the deflection equation for a laminated composite vertical storage tank. It is obviously quite similar to that derived by Timoshenko and Woinowsky-Krieger (44) for tanks constructed of isotropic materials:

$$w = -\frac{1}{Eh} \rho r^2 \left\{ d - x - e^{-\beta x} \left[d \cos \beta x + \left(d - \frac{1}{\beta} \right) \sin \beta x \right] \right\} \quad (5-53)$$

It can in fact be shown that for the special case of a laminate comprised of a number of similar isotropic layers, i.e., in the isotropic case,

$$A_{22}^* = \frac{1}{Eh} \quad (5-54)$$

and

$$\alpha = \beta = \left[\frac{3(1-\nu^2)}{r^2 h^2} \right]^{1/4} \quad (5-55)$$

Therefore, equation (5-52) is actually a more general solution to the problem.

5.8 FAILURE ANALYSIS

As was indicated in Section 4.6, the first step in a laminate failure analysis is to determine mid-plane strains and shell curvatures. From equations (5-9),

$$\begin{aligned}\epsilon_{\theta} &= -\frac{W}{r} \\ \kappa_x &= -\frac{d^2W}{dx^2} \\ \kappa_{\theta} &= 0 \\ \kappa_{x\theta} &= 0\end{aligned}\quad (5-56)$$

and, from equations (5-23) and (5-30),

$$\epsilon_x^{\circ} = -\frac{A_{12}^*}{A_{22}^*} \frac{W}{r} - \left(B_{11}^* - \frac{A_{12}^* B_{21}^*}{A_{22}^*} \right) \frac{d^2W}{dx^2} \quad (5-57)$$

and

$$\gamma_{x\theta}^{\circ} = -\frac{A_{26}^*}{A_{22}^*} \frac{W}{r} - \left(B_{61}^* - \frac{A_{26}^* B_{21}^*}{A_{22}^*} \right) \frac{d^2W}{dx^2} \quad (5-58)$$

Thus, the mid-plane strains and shell curvatures are functions solely of the tank wall deflection, w , and the wall curvature in the axial direction, $\frac{d^2W}{dx^2}$.

By differentiating equation (5-52),

$$\frac{dw}{dx} = A_{22}^* p r^2 \left\{ 1 - e^{-\alpha x} \left[\cos \beta x + \left(\frac{\alpha^2 + \beta^2}{\beta} d - \frac{\alpha}{\beta} \right) \sin \beta x \right] \right\} \quad (5-59)$$

and

$$\begin{aligned}\frac{d^2W}{dx^2} &= -A_{22}^* p r^2 e^{-\alpha x} \left\{ \left[(\alpha^2 + \beta^2) d - 2\alpha \right] \cos \beta x \right. \\ &\quad \left. - \left[\frac{\alpha (\alpha^2 + \beta^2)}{\beta} d + \frac{\beta^2 - \alpha^2}{\beta} \right] \sin \beta x \right\} \dots (5-60)\end{aligned}$$

Therefore, all of the mid-plane strains and shell curvatures at a given point (defined by x) can be determined by applying equations (5-52), (5-56), (5-57), (5-58) and (5-60). Once these values have been established, the failure analysis proceeds as outlined previously in Section 4.6.

5.9 COMPUTER PROGRAM

The theory presented in the foregoing provided the basis for a computer program which was developed for analyzing laminated composite storage tanks. A listing of this program, code-named CYLTAN, is provided in Appendix D. The distortional energy condition was adopted as the criterion of failure.

5.10 GUN-LAUNCHED ROCKET MOTOR CASE ANALYSIS

5.10.1 Background Information

As a gun-launched rocket exits the barrel, the motor case wall is subjected to internal pressures which are due to extremely high inertial forces acting upon the structurally weak solid rocket propellant. As can be seen from Figure 5.3, the rocket motor case may therefore be assumed to perform instantaneously as a storage tank filled with an enormously dense fluid. The effect of this loading on the case wall can be predicted by utilizing

the tank analysis developed earlier in this section.

O'Connell (1), in his analysis of the HARP seven inch fibreglass rocket motor case, adopted the storage tank model but did not use the theory of laminated composites (it was not then available to him). Instead, he assumed that the analysis developed by Timoshenko for isotropic tanks could be modified to take into account the orthotropy of the fibreglass simply by substituting orthotropic elastic constants for the equivalent isotropic properties at the appropriate places in the equations.

It was therefore decided that this problem would provide an ideal test for the newly developed analytical procedure. By utilizing O'Connell's input data, the results of the two approaches can be directly compared and, hopefully, some direct evaluation made of the newly derived equations.

Rocket motor case, i.e., "tank" data utilized in the analysis was as follows:

- 1) r = tank radius = 3.412 inches
- 2) d = tank depth = 43.00 inches
- 3) ρ = fluid density = 98.0 lb./ cu. in.
- 4) t = wall thickness = 0.325 inches
- 5) laminate construction:
 - a) outer layer (hoop wound)
 - i) $t^{(1)}$ = thickness = 0.1625 inches
 - ii) $\theta^{(1)}$ = orientation = 90°

- b) inner layer (helically wound)
- i) $t^{(2)} = 0.1625$ inches
 - ii) $\theta^{(2)} = 33^\circ$
- 6) lamina elastic properties ($V_f = 0.8$):
- a) $E_1 = 8.88 \times 10^6$ psi
 - b) $E_2 = 1.75 \times 10^6$ psi
 - c) $G_{12} = 0.66 \times 10^6$ psi
 - d) $\nu_{12} = 0.244$
- 7) Allowable lamina stresses, required for the failure analysis, were taken from a report by Tsai (O'Connell did not analyze for failure).
- a) $\sigma_1^t = +150,000$ psi
 - b) $\sigma_1^c = -150,000$ psi
 - c) $\sigma_2^t = +12,000$ psi
 - d) $\sigma_2^c = -20,000$ psi
 - e) $\tau_{12} = 10,000$ psi

5.10.2 Computational Procedure

Computations were carried out in three phases.

First, lamina stiffness coefficients were determined from the known elastic constants and layer orientations through the use of computer program STIFCO. Next, the laminate constants A_{12}^* , A_{22}^* , A_{26}^* , B_{11}^* , B_{61}^* , H_{12}^* and D_{11}^* were determined by employing program MN CM. Finally, program CYLTAN was run to complete the analysis. The outputs from all three programs are provided in Appendices A, B

and D respectively. Unfortunately, due to its volume, the tank analysis program output had to be limited to the two main points of interest:

a) the base

and

b) the point of maximum deflection

5.10.3 Results of Initial Study

The predicted tank, i.e., rocket motor case, deflection curve is illustrated graphically in Figure 5.4. This plot tends to exaggerate the tank curvatures, however, and it was deemed necessary to provide also a full scale representation - Figure 5.5 - of the bottom five inches of the deformed structure to put the deflection pattern into proper perspective.

The computed maximum wall deflection is 0.0285 inches which compares favourably with that predicted by O'Connell - 0.0281 inches; the location of the point of maximum deflection is not the same, however. Computer results indicate that it is 2.0 inches from the base of the tank compared with O'Connell's value of 2.5 inches. This could perhaps be construed as an indication of the existence of more severe curvatures near the base of the tank than would be predicted by the approximate method used by O'Connell. However, since he calculated neither curvatures nor stresses due to bending, this cannot be

verified.

Laminate bending stresses due to curvature at the base of the cylinder are nevertheless a primary design consideration. In both the $90^{\circ}/+33^{\circ}$ and $90^{\circ}/\pm 33^{\circ}$ laminate analyses, the laminates were much more highly stressed (failure criterion ≈ 4.5) due to bending at the cylinder base than they were due to the maximum radial deflection (failure criterion ≈ 1.05). In particular, the hoop layers on the outside of the cylinder were found to be critically stressed in the transverse direction (approximately 42,000 psi compressive stress versus 20,000 psi allowable).

The only other direct comparison possible between the two approaches pertains to the predicted stresses in the wall at the point of maximum deflection. These are tabulated in Table 5.1 along with those determined when a more typical $90^{\circ}/\pm 33^{\circ}$ laminate is assumed. In general, they appear to be quite comparable although the revised analysis does indicate that the critical transverse tensile stress in the helically wound layer(s) is 20 to 42 percent higher than was predicted by O'Connell's method.

5.10.4 Additional Parametric Studies

To further illustrate the value of the newly developed composite tank analysis, three additional computer studies were made to investigate the effects of:

- 1) layer sequence

TABLE 5.1

COMPARISON OF STRESSES AT MAXIMUM DEFLECTION

	O'CONNELL (90/+33)	CASE 1 (90/+33)	CASE 2 (90/+33)
MAXIMUM DEFLECTION (INCHES)	0.0281	0.0285	0.0285
LOCATION OF MAXIMUM DEFLECTION (INCHES ABOVE BASE)	2.5	2.0	2.0
LAYER STRESSES:			
OUTSIDE - LAYER 1			
$\sigma_1 (= \sigma_y)$ - KSI	74.01	74.69	74.59
$\sigma_2 (= \sigma_x)$ - KSI	-0.52	-1.59	-1.50
$\tau_{12} (= \tau_{xy})$ - KSI	-2.78	-0.30	-0.03
MIDPLANE - LAYER 1			
$\sigma_1 (= \sigma_y)$ - KSI	74.01	74.17	74.03
$\sigma_2 (= \sigma_x)$ - KSI	-0.52	-0.54	-0.77
$\tau_{12} (= \tau_{xy})$ - KSI	-2.78	0.30	0.03
MIDPLANE - LAYER 2			
σ_x - KSI	0.52	2.68	2.93
σ_y - KSI	13.22	15.05	15.17
τ_{xy} - KSI	2.78	1.69	2.28
σ_1 - KSI	(6.83)*	7.90	8.65
σ_2 - KSI	(6.91)	9.83	9.46
τ_{12} - KSI	(6.93)	6.34	6.52
INSIDE - LAYER**			
σ_x - KSI	0.52	3.72	-3.66
σ_y - KSI	13.22	12.70	12.78
τ_{xy} - KSI	2.78	-1.09	0.47
σ_1 - KSI	(6.83)	0.15	0.79
σ_2 - KSI	(6.91)	8.83	8.33
τ_{12} - KSI	(6.93)	7.06	-7.32

* Bracketed numbers indicate transformed stresses not presented in original work.

** The inside layer is layer 2 in the 90/+33 laminates and layer 11 in the 90/+33 laminate.

- 2) the hoop layer thickness, and
- 3) the wind angle of the helical layers

on the structural performance of the rocket motor case wall constant wall thickness was maintained throughout.

The elastic properties assumed originally by O'Connell and used heretofore were unrealistically high. In these latter studies, more representative lamina properties were adopted (37). The revised elastic constants are:

- a) $E_1 = 7.80 \times 10^6$ psi
- b) $E_2 = 2.60 \times 10^6$ psi
- c) $G_{12} = 1.25 \times 10^6$ psi
- d) $\nu_{12} = 0.25$

A summary of the various wall constructions investigated is provided in Table 5.2. Cases 1 and 2 indicate the wall constructions assumed in the comparative study described previously. The next three pertain to the layer sequence study and cases 6 through 11 comprise the hoop layer thickness investigation. The remaining cases constitute the wind angle study.

Critical layer principal stresses and failure criteria values at the point of maximum deflection and at the base of the structure are tabulated in Tables 5.3a and 5.3b respectively. Maximum deflections are also included in Table 5.3a as are axial curvatures in Table 5.3b. In addition, relevant laminate information is provided in both tables for ready reference.

TABLE 5.2

SUMMARY OF LAMINATES ANALYZED

CASE NUMBER	OF LAYERS	LAMINATE CONSTRUCTION	HELIX	PERCENT	LAYER THICKNESSES	
			ANGLE	HOOP	HOOP	HELICAL
			(DEG)		(INCHES)	(INCHES)
1	2	90 / +33	33	50	0.16250	0.16250
2	11	90 /+/-/+/-/+/-/+/-/+/-	33	50	0.16250	0.01625
3	11	90 /+/-/+/-/+/-/+/-/+/-	33	50	0.16250	0.01625
4	12	+/-/ 90 /+/-/+/-/+/-/ 90 /+/-	33	50	0.08125	0.01625
5	12	+/-/+/-/ 90 /+/-/ 90 /+/-/+/-	33	50	0.08125	0.01625
6	20	+/-/+/-/+/-/+/-/+/-/+/-/+/-/+/-/+/-/+/-/+/-/+/-	33	0	-	0.01625
7	17	+/-/+/-/+/-/+/-/+/-/ 90 /-/+/-/+/-/+/-/+	33	20	0.06500	0.01625
8	13	+/-/+/-/+/-/+/-/ 90 /-/+/-/+/-/+	33	40	0.13000	0.01625
9	9	+/-/+/-/ 90 /-/+/-/+	33	60	0.19500	0.01625
10	5	+/-/ 90 /-/+	33	80	0.26000	0.01625
11	1	90	-	100	0.32500	-
12	12	+/-/+/-/ 90 /+/-/ 90 /+/-/+/-	75	50	0.08125	0.01625
13	12	+/-/+/-/ 90 /+/-/ 90 /+/-/+/-	60	50	0.08125	0.01625
14	12	+/-/+/-/ 90 /+/-/ 90 /+/-/+/-	45	50	0.08125	0.01625
15	12	+/-/+/-/ 90 /+/-/ 90 /+/-/+/-	15	50	0.08125	0.01625
16	12	+/-/+/-/ 90 /+/-/ 90 /+/-/+/-	0	50	0.08125	0.01625

TABLE 5.3-a

SUMMARY OF RESULTS - THE POINT OF MAXIMUM DEFLECTION

CASE NUMBER	NUMBER OF LAYERS	HELIX ANGLE (DEG)	PERCENT HOOP	A_{22}^* ($\times 10^{-6}$ IN/LB)	MAXIMUM DEFLECTION (INCHES)	CRITICAL LAYER	PRINCIPAL LAYER STRESSES			VALUE OF FAILURE CRITERION
							σ_1 (KSI)	σ_2 (KSI)	τ_{12} (KSI)	
1	2	33	50	0.5823	0.0285	2 o*	-3.78	7.97	7.53	1.072
2	11	33	50	0.5812	0.0285	2 o	8.65	9.46	6.52	1.046
3	11	33	50	0.5754	0.0280	11 i	6.37	13.27	-12.72	2.839
4	12	33	50	0.5754	0.0279	12 i	5.06	12.96	-12.95	2.840
5	12	33	50	0.5754	0.0279	12 i	4.35	12.77	-13.05	2.835
6	20	33	0	1.064	0.0510	20 i	10.72	24.03	23.29	9.429
7	17	33	20	0.7942	0.0382	17 i	6.83	17.76	17.70	5.318
8	13	33	40	0.6336	0.0306	13 i	6.66	14.47	13.93	3.393
9	9	33	60	0.5271	0.0256	9 i	4.38	11.84	11.87	2.381
10	5	33	80	0.4512	0.0219	5 i	2.42	9.88	10.46	1.771
11	1	-	100	0.3945	0.0193	1 o	43.41	-3.12	0.00	0.151
12	12	75	50	0.4148	0.0203	12 i	40.95	-2.95	-5.62	0.417
13	12	60	50	0.4727	0.0231	12 i	33.14	0.52	-11.00	1.260
14	12	45	50	0.5414	0.0263	12 i	18.44	7.06	-13.96	2.303
15	12	15	50	0.5887	0.0284	1 o	5.36	20.56	5.54	3.240
16	12	0	50	0.5886	0.0284	1 o	3.69	21.94	0.00	3.338

* i - denotes inside of layer
o - denotes outside of layer

TABLE 5.3-b

SUMMARY OF RESULTS - THE BASE OF THE STRUCTURE

CASE NUMBER	OF LAYERS	HELIX ANGLE (DEG)	PERCENT HOOP	$\left(\frac{A_{22}^*}{D_{11}^*}\right)^{1/2}$ ($\times 10^{-5} \text{ LB}^{-1}$)	$\frac{d^2 w}{d x^2}$ AT BASE (INCHES ⁻¹)	CRITICAL LAYER	PRINCIPAL LAYER STRESSES			VALUE OF FAILURE CRITERION
							σ_1 (KSI)	σ_2 (KSI)	τ_{12} (KSI)	
1	2	33	50	0.878	-0.1243	1 o	-10.12	-41.48	3.72	4.425
2	11	33	50	0.841	-0.1190	1 o	-10.45	-42.82	-0.52	4.571
3	11	33	50	0.737	-0.1042	1 o	-13.20	-52.79	-0.50	6.946
4	12	33	50	0.699	-0.0988	10 i	8.52	34.10	-0.48	8.066
5	12	33	50	0.642	-0.0906	1 i	84.25	18.79	17.00	5.586
6	20	33	0	0.823	-0.1157	20 i	109.05	23.59	-21.47	8.888
7	17	33	20	0.712	-0.1003	17 i	94.58	20.46	18.62	6.685
8	13	33	40	0.645	-0.0911	13 i	85.83	18.56	16.90	5.505
9	9	33	60	0.614	-0.0868	9 i	81.79	17.69	-16.10	4.999
10	5	33	80	0.625	-0.0884	3 i	7.63	30.50	-0.00	6.453
11	1	-	100	0.721	-0.1021	1 i	11.02	44.07	-0.00	13.474
12	12	75	50	0.730	-0.1034	12 i	19.26	42.40	10.43	13.552
13	12	60	50	0.734	-0.1039	12 i	41.49	36.59	18.18	12.611
14	12	45	50	0.688	-0.0972	12 i	68.01	26.87	20.02	9.144
15	12	15	50	0.570	-0.0804	8 i	5.20	20.80	-0.33	3.003
16	12	0	50	0.549	-0.0774	8 i	5.01	20.03	-0.00	2.784

It is immediately apparent from these tables that (a) the wall thickness is inadequate for the assumed loading and (b) the bending stresses induced at the base of the cylinder must be the primary design consideration. In all cases but three (6, 15 and 16), the layer stresses are considerably more critical at the base than they are at the point of maximum deflection. However, since there were cases in which the critical point in the structure was the point of maximum deflection, layer stresses at this location must also be carefully considered.

A closer scrutiny of the results reveals that failure is primarily related to layer transverse and shear stresses rather than to the stresses in the direction of the reinforcing fibres. Only in cases 11 and 12 do the principal stresses represent more than ten percent of the failure criterion value. In these cases, at the point of maximum deflection, the fibres are largely aligned in the primary direction of loading, i.e., in the hoop direction, which explains why they are substantially stressed. Even then, the principal stress represents less than sixty percent of the value of the failure criterion, however. At the base, where bending is the primary consideration, the principal stress never represents more than six percent of this value.

It is also interesting to note that in cases 15 and 16 the most severely stressed layer in the twelve layer

laminate is the eighth. This confirms the statements made earlier on this subject in Section 2.1.1, i.e., that even in the case of pure bending, the most critically stressed layer in an orthotropic laminate is not always at one of the outer surfaces.

A comparison of the results of cases 2 and 3 reveals that the individual layer stiffness properties substantially effect the structural performance of the complete laminate. By introducing lower material constants (case 3), the values for the failure criterion at the point of maximum deflection rose from 1.046 to 2.839 and at the base from 4.571 to 6.946 even though an identical laminate construction was assumed in both cases.

Layer sequence is shown to have a most significant effect on the flexural load carrying capabilities of a laminate in cases 3, 4 and 5. At the base of the structure, where flexure is the sole consideration, the value of the failure criterion is lowest when the hoop layers are located closest to the centre of the laminate. It is also clear from the results that the layer sequence has virtually no effect on the ability of the laminate to withstand tensile loads, e.g., hoop stresses. Although both of these conclusions seem entirely logical and obvious now, such was certainly not the case at the time of the development of the HARP rocket motor case. Little consideration was given to the effect of layer sequence on structural performance at

that time and the sequence was in fact determined by manufacturing considerations: it was easier to wind first all of the helical layers and then the hoop layers. This example clearly points out the significance of "thinking composites" and how lamination theory helps us do this.

In Figure 5.6, computed maximum wall deflections are plotted against related values of the laminate stiffness coefficient A_{22}^* . From this graph, which includes data from all of the cases analyzed, it is clear that an almost perfectly linear relationship exists between the maximum deflection and the laminate constant. This is somewhat surprising, perhaps, since it has already been demonstrated (Figure 5.4) that the deflection pattern is substantially affected by end constraint. The fact that the graph is linear cannot be ignored, however; indeed, this can actually be an advantage from an analytical standpoint. Since the slope of the curve is within three percent of the value that would be obtained by assuming that the base was unconstrained, the maximum wall deflection can be quite accurately predicted simply by employing the relationship

$$w_{\text{MAX}} = -A_{22}^* \rho r^2 d \quad (5-61)$$

where all symbols are as defined previously.

By ignoring cross-coupling stiffness coefficients, it can also be shown, from equations (5-40), (5-41) and

(5-52), that when $x = 0$, i.e., at the base of the tank,

$$\frac{d^2 w}{dx^2} = - \left(\frac{A_{22}^*}{D_{11}^*} \right)^{1/2} \rho r d \quad (5-62)$$

This approximate relationship is demonstrated to be quite accurate in Figure 5.7 where the computed axial curvatures at the base (all cases) are plotted against their related laminate constants $(A_{22}^*/D_{11}^*)^{1/2}$. The calculated slope of the graph is within one percent of the value of $(\rho r d)$. It would therefore seem possible, once the formula has been experimentally verified, to use it to predict axial curvature and hence lamina strains and stresses at the base of the tank without going through a full scale tank analysis.

The results of the study into the effect of the hoop wound layer thickness on structural performance (cases 6 through 11) are presented graphically in Figures 5.8 and 5.9. In Figure 5.8, the laminate elastic properties A_{22}^* and $(A_{22}^*/D_{11}^*)^{1/2}$ are plotted against the thickness of the hoop wound layer (presented as a percentage of the total wall thickness) which is in all cases located at the centre of the laminate. Figure 5.9 shows the effect of hoop wound layer thickness on the values of the distortional energy failure criterion at both the base and the point of maximum deflection. It is quite clear from Figure 5.9 that the best structural performance is obtained when approximately

60 percent of the wall thickness is hoop wound. Further, according to Figure 5.8, this percentage very nearly coincides with the minimum value of the laminate constant $(A_{zz}^* / D_{11}^*)^{1/2}$.

The two distinct portions of the failure criterion "at base" curve reflect two quite different modes of laminate failure. From zero to approximately 72 percent, the maximum value of the failure criterion is found to be at the inner surface of the cylinder. Beyond this point, the most critically stressed point is the inner surface of the hoop layer. Once again it is demonstrated that failure in a fibre-reinforced composite laminate does not necessarily occur at the extreme fibres.

The effect of the helical wind angle on the elastic properties of a laminate in which one half of the thickness is hoop wound (cases 11 through 16) is shown in Figure 5.10. In addition, its effects on the structural performance of the laminate are shown in Figures 5.11-a and 5.11-b. It should be noted that, due to filament winding limitations, the hoop wound layers in all of these cases are located close to but not at the centre of the laminate (see Table 5.2).

From Figure 5.11-a and -b, it is clear that any one of three different failure modes may be encountered depending upon the angle at which the helical layers are wound. When wind angles of between 0 and approximately 20

degrees are employed, the analysis indicates that the initial failure will occur at the outer surface of the shell in the vicinity of the point of maximum deflection. Next, in motor cases with helical layers wound in the 20 to 25 degree range, failure is initiated at the inner surface of the eighth layer of the laminate at the base of the structure. Finally, for larger helix angles the initial failure is also at the base of the structure. However, this time it is at the inner surface of the shell. It is also apparent that the value of the failure criterion is lowest when the helical wind angle is approximately 20 degrees. Thus the study shows that, for a motor case in which one half the wall thickness is hoop wound, the most effective laminate is one in which the helical layers are wound at an angle of approximately 20 degrees.

5.10.5 Closing Remarks

The foregoing studies have amply demonstrated the advantages of using lamination theory in conjunction with conventional shell theory. In addition to providing a much clearer picture of the inter-relationship between bending and stretching, they also showed the vital role of bending at the base of the structure and the significance of layer sequence, hoop layer thickness and the helical layer wind angle.

The studies also provided an indication of the

validity of the newly derived deflection equation (5-52) for a laminated composite storage tank. In particular, it was shown (in study 1) that the computed maximum deflection was within two percent of the value determined separately by O'Connell (1) in his investigation of this same problem. Theoretical studies still leave some measure of doubt, however; only through an experimental program can the validity of these equations be properly confirmed.

Finally, some new guidelines relative to the design of the wall of a gun-launched FRP rocket motor case have evolved as a result of these investigations. It was shown that the wall of the structure should consist of a hoop layer, located between two identical helical layers. Although the optimum combination of hoop layer thickness and wind angle was not established for the particular case analysed, the results indicated that in all likelihood, between fifty to seventy percent of the total wall thickness should be hoop wound and that the helical layers should be wound at a relatively shallow angle, probably less than thirty degrees. These guidelines appear to be equally applicable to the design of fibre-reinforced cylindrical storage tanks.

SECTION 6

CONCLUSION

The original object of the study has been realized. An extensive literature survey has unearthed a recently developed theory which provides the basis for a new rational approach to the analysis of laminated composite structures. This objective was not easily achieved, however.

The initial phase of the literature survey proved to be most disappointing. Although numerous books, reports and papers were encountered on the fundamentals and general uses of reinforcement, relatively few could be found dealing specifically with the design or analysis of composite material structures. Further, those which did invariably pertained to one of the approaches outlined in Section 2; none seemed to offer any hope of a significant analytical breakthrough.

Fortunately, the theory of laminated composites was discovered a few months later. It became immediately apparent that this was the breakthrough that had been anticipated and the theory was promptly utilized to resolve the composite tank analysis problem (Section 5).

The literature also indicated that no single publication adequately covered all phases of composite

structural analysis. Accordingly, since the average designer has little time for searching out references, it is felt that this thesis is a significant contribution as it is a comprehensive, self-contained introduction to the subject.

Another important contribution of this work is the cylindrical tank analysis revision which enables a thorough stress analysis of tanks constructed of laminated orthotropic and/or isotropic materials. The revised deflection equation appears to be correct in form and does, in fact, simplify down to the equation derived by Timoshenko (44) for the isotropic case. An extensive test program is essential, however, before this equation, and others developed in the analysis, can be verified.

Two computer programs were developed during the course of the study. The first of these computes the stiffness coefficients of a generally orthotropic layer in accordance with the theory presented in Section 3. The second, which is based upon the theoretical equations developed in Section 5, performs a complete stress analysis at any number of points in a composite cylindrical storage tank.

The value of the tank analysis program was realized in a series of studies conducted on a H.A.R.P. gun-launched rocket. As a result of these studies, some new guidelines

for the design of filament wound storage tanks were established (for the loading condition considered):

- 1) The cylinder wall should consist of three filament wound layers: a hoop wound layer sandwiched between two identical helical layers. Further, though no attempt was made to optimize, the results suggest that the helical layers should be wound at a relatively shallow angle, e.g., 20 degrees and that approximately 60 percent of the total wall thickness should be hoop wound.
- 2) The maximum wall deflection is strongly dependent upon the laminate elastic constant, A_{22}^* . According to the results, the maximum tank deflection can be approximated to within three percent by using the relationship

$$w_{MAX} = -A_{22}^* p r^2 d \quad (6-1)$$

A_{22}^* is approximately inversely proportional to the effective modulus of the laminate in the hoop direction and is comparable to the term $(1/Eh)$ commonly encountered in the analysis of isotropic plates or shells.

- 3) The curvature at the base of the tank can be closely estimated from the expression

$$\frac{d^2 w}{dx^2} = - \left(\frac{A_{22}^*}{D_{11}^*} \right)^{1/2} p r d \quad (6-2)$$

where D_{11}^* is effectively, the flexural rigidity of the wall in the axial direction. This suggests that the laminate should be constructed in such a way that the value of the laminate constant $(A_{22}^*/D_{11}^*)^{1/2}$ is minimized. In this way, the stresses due to bending, at the base, should also be minimized.

In addition, two conclusions were drawn concerning the design of laminates generally.

- 1) Layer sequence has a substantial effect on the load carrying capabilities of a laminate in flexure but has little effect on simple tension, compression or in-plane shear performance. This suggests that where possible, laminates should be balanced and symmetrical with the outer layers oriented according to the particular stiffness requirements of the application.
- 2) Failure can be expected to originate within the matrix in most instances. It is usually due to the transverse and/or in-plane shear stresses within a particular layer; seldom is the stress in the direction of the fibres the primary factor.

Though obviously superior to any of the analytical approaches previously available, the theory of laminated composites does have some limitations. In particular, it does not take into account either interlaminar shear or transverse (out of plane) stresses. In some instances,

e.g. laminates containing woven materials, these limitations can be quite serious as delamination is a fairly common mode of failure. For the most part, however, these stresses are of secondary importance and the theory can be employed with a much higher degree of confidence than was possible with any of the methods previously available.

The limitations in the theory, noted above, suggest one potentially fertile area for future work. Of more concern, however, is the industrial need for new analytical solutions to the many fundamental plate and shell problems which have previously been considered from an isotropic standpoint only. It is suggested that, by introducing the theory of laminated composites into the conventional plate or shell analysis (as was done in the cylindrical tank analysis presented herein) many of these problems can quite readily be re-solved. Further work is also needed relative to the design of cylindrical tanks. In particular, studies could be undertaken to consider:

- a) new boundary conditions at the base of the tank (rigid constraint is not commonly encountered in practice).
- b) tapered wall construction
- c) the effect of circumferential stiffening rings
(or joints)
- d) buckling

and, finally

e) structural optimization

Hopefully, this thesis will prove to be of use in some of these future studies.

APPENDIX A

COMPUTER PROGRAM FOR DETERMINING

LAMINA STIFFNESS COEFFICIENTS

A.1 DESCRIPTION OF PROGRAM

Program STIFCO computes lamina stiffness coefficients, C'_{ij} , in accordance with the theory presented in Section 3. Coefficients can be determined for any reasonable number of isotropic or orthotropic layers oriented at various angles relative to the co-ordinate axes of the structure.

A.2 INPUT PARAMETER DEFINITION

<u>Parameter</u>	<u>Definition</u>
THETA(K)	is the angle of rotation between the co-ordinate system of interest and the natural axes of the layer material
E11(K)	are the principal elastic properties of the kth layer:
E22(K)	E_{11} , E_{22} , G_{12} and ν_{12} respectively
G12(K)	
ν12(K)	
CIJ(K)	are the lamina stiffness coefficients, C_{ij} , in the natural co-ordinate system of the kth layer
CPIJ(K)	are the transformed lamina stiffness coefficients C'_{ij} of the kth layer.

A.3 TYPICAL INPUT

A data input deck for the determination of the stiffness coefficients of a particular orthotropic layer material at three different orientations is shown below.

<u>Parameter</u>	<u>Value</u>	<u>Format</u>
THETA(1)	33.0	(12F6.0)
THETA(2)	-33.0	
THETA(3)	90.0	
E11(1)	0.888000E+07	(3E12.6,F6.0)
E22(1)	0.175000E+07	
G12(1)	0.660000E+06	
V12(1)	0.244	
E11(2)	0.888000E+07	(3E12.6,F6.0)
E22(2)	0.175000E+07	
G12(2)	0.660000E+06	
V12(2)	0.244	
E11(3)	0.888000E+07	(3E12.6,F6.0)
E22(3)	0.175000E+07	
G12(3)	0.660000E+06	
V12(3)	0.244	

A.4 TYPICAL OUTPUT

The output corresponding to the above input deck is shown in the next two pages.

LAYER NO.	ELASTIC CONSTANTS			
	E11 (10+6 LB./SQ.IN.)	E22 (10+6 LB./SQ.IN.)	G12	V12
K				
1	8.8800	1.7500	0.6600	0.2440
2	8.8800	1.7500	0.6600	0.2440
3	8.8800	1.7500	0.6600	0.2440
LAYER NO.	STIFFNESS COEFFICIENTS (10+6 LB./SQ.IN.)			
	C11	C12	C22	C66
K				
1	8.9854	0.4321	1.7708	0.6600
2	8.9854	0.4321	1.7708	0.6600
3	8.9854	0.4321	1.7708	0.6600

LAYER NO.	ORIENTATION (DEGREES)	TRANSFORMED STIFFNESS COEFFICIENTS (10+6 LB./SQ.IN.)					
	THETA (K)	CP11	CP12	CP16	CP22	CP26	CP66
1	33.00	5.3323	1.9451	2.3214	2.3978	0.9741	2.1731
2	-33.00	5.3323	1.9451	-2.3214	2.3978	-0.9741	2.1731
3	90.00	1.7708	0.4321	-0.0000	8.9854	0.0000	0.6600

A.5 PROGRAM LISTING

A complete listing of the Fortran IV program is included in the following pages.

C PROGRAM STIFCO
 C PROGRAM FOR CALCULATING PRINCIPAL LAYER STIFFNESS COEFFICIENTS AND FOR
 C TRANSFORMING THEM TO OTHER CO-ORDINATE SYSTEMS

C

DIMENSION THETA(25),E11(25),E22(25),G12(25),V12(25),C11(25),C12(25),
 C1(25),C22(25),C66(25),ANGLE(25),CP11(25),CP12(25),CP16(25),CP22(25),CP
 126(25),CP66(25)

C

N = 1

C N IS THE NUMBER OF LAYERS

READ (5,101) (THETA(K),K=1,N)

101 FORMAT (12F6.0)

C THETA(K) IS THE ANGLE OF ROTATION BETWEEN THE CO-ORDINATE SYSTEM INTO
 C WHICH THE STIFFNESS COEFFICIENTS ARE BEING TRANSFORMED AND THE NATURAL
 C MATERIAL AXIS SYSTEM OF THE KTH LAYER

C

READ (5,102) (E11(K),E22(K),G12(K),V12(K),K=1,N)

102 FORMAT (3E12.6,F6.0)

WRITE (6,103)

103 FORMAT (1H1,11X,5HLAYER,18X,17HELASTIC CONSTANTS/13X,3HNO.///14X,1
 1HK,11X,3HE11,7X,3HE22,7X,3HG12,12X,3HV12/29X,17H(10+6 LB./SQ.IN.)/
 1//)

DO 10 K = 1,N

10 WRITE (6,104) K,E11(K),E22(K),G12(K),V12(K)

104 FORMAT (13X,12,6X,-6PF10.4,-6PF10.4,-6PF10.4,5X,0PF10.4)

WRITE (6,105)

105 FORMAT (1HU//12X,5HLAYER/13X,3HNO.,16X,22HSTIFFNESS COEFFICIENTS/3
 15X,17H(10+6 LB./SQ.IN.)/14X,1HK,11X,3HC11,9X,3HC12,9X,3HC22,9X,3H
 1C66///)

DO 20 K = 1,N

V21 = (E22(K) / E11(K)) * V12(K)

C11(K) = E11(K) / (1.0 - (V12(K) * V21))

C12(K) = (V12(K) * E22(K)) / (1.0 - (V12(K) * V21))

C22(K) = E22(K) / (1.0 - (V12(K) * V21))

C66(K) = G12(K)

20 WRITE (6,106) K,C11(K),C12(K),C22(K),C66(K)

106 FORMAT (13X,12,4X,-6PF12.4,-6PF12.4,-6PF12.4,-6PF12.4)

WRITE (6,107)

107 FORMAT (1H1,1X,5HLAYER/5X,3HNO.,5X,11HORIENTATION,13X,34HTRANSFORM
 1ED STIFFNESS COEFFICIENTS/10X,9H(DEGREES),22X,17H(10+6 LB./SQ.IN.)
 1//4X,1HK,5X,8HTHETA(K),5X,4HCP11,6X,4HCP12,6X,4HCP16,6X,4HCP22,6X,
 14HCP26,6X,4HCP66///)

DO 30 K = 1,N

ANGLE(K) = (THETA(K) / 180.0) * 3.1415927

RM = COS (ANGLE(K))

RN = SIN (ANGLE(K))

CP11(K) = ((RM ** 4) * C11(K)) + ((RN ** 4) * C22(K)) + (((RM ** 2
 1) * (RN ** 2)) * ((2.0 * C12(K)) + (4.0 * C66(K))))

CP12(K) = (((RM ** 2) * (RN ** 2)) * (C11(K) + C22(K) - (4.0 * C66
 1(K)))) + (((RM ** 4) + (RN ** 4)) * C12(K))

CP16(K) = (((RM ** 3) * RN) * (C11(K) - C12(K) - (2.0 * C66(K))))
 1- ((RM * (RN ** 3)) * (C22(K) - C12(K) - (2.0 * C66(K))))

CP22(K) = ((RN ** 4) * C11(K)) + ((RM ** 4) * C22(K)) + (((RM ** 2

```
1) * (RN ** 2)) * ((2.0 * C12(K)) + (4.0 * C66(K)))
CP26(K) = ((RM * (RN ** 3)) * (C11(K) - C12(K) - (2.0 * C66(K))))
1- (((RM ** 3) * RN) * (C22(K) - C12(K) - (2.0 * C66(K))))
CP66(K) = (((RM ** 2) * (RN ** 2)) * (C11(K) + C22(K) - (2.0 * C12
1(K)))) + (((RM ** 2) - (RN ** 2)) ** 2) * C66(K))
30 WRITE (6,108) K, THETA(K), CP11(K), CP12(K), CP16(K), CP22(K), CP26(K), C
1P66(K)
108 FORMAT (3X, 12, 5X, 6PF6.2, 2X, -6PF10.4, -6PF10.4, -6PF10.4, -6PF10.4, -6P
1F10.4, -6PF10.4)
WRITE (6,109)
109 FORMAT (1H1//)
STOP
END
```

APPENDIX B

DETERMINATION OF LAMINATE STIFFNESS COEFFICIENTS

B.1 DESCRIPTION OF PROGRAM

A computer program, developed originally by Tsai et al (37), is used in the determination of laminate stiffness coefficients: A_{ij} , B_{ij} , D_{ij} , A_{ij}^* , B_{ij}^* , H_{ij}^* , D_{ij}^* , A'_{ij} , B'_{ij} and D'_{ij} . This program, which consists of two parts MN CM ie, Main Composite Materials, for computing laminate stiffness coefficient matrices, and Subroutine PARTWO for determining laminate load carrying capabilities, is not described in detail herein as full documentation is available in (37). However, sufficient input/output information is provided in the following for normal usage of MN CM. The underlying theory for this part of the program is described in Section 4.

B.2 INPUT PARAMETER DEFINITION

<u>Parameter</u>	<u>Definition</u>
N	is the total number of layers
THTA	is the fibre orientation or lamination angle in degrees (defined for angle-ply composites)
LPP	defines the particular case under consideration: LPP=1 implies a cylinder or a pressure vessel

<u>Parameter</u>	<u>Definition</u>
	LPP=2 implies a plate.
J	is a format control which defines the heading to be printed: J=1 implies cross-ply J=2 implies angle-ply J=3 implies general laminate
RM	is the cross-ply ratio (total thickness of the odd layers divided by that of the even layers).
LKL	is a format control which defines the heading to be printed: LKL=0 implies all layers intact LKL=1 implies all layers degraded
JB	indicates whether or not the laminate under consideration is balanced and symmetric. JB=0 implies laminate is not balanced and symmetric JB=1 implies laminate is balanced and symmetric
H(K)	is the thickness (in.) of the kth layer.
C(I,J,K)	are the transformed stiffness coefficients, C'_{ij} , (psi) of the kth layer.
ALPHA(I,K)	is the thermal coefficient of expansion α_i (in./in./ F) of the kth layer.
THETA(K)	is the fibre orientation or lamination angle (radians) for the kth layer.

B.3 TYPICAL INPUT

A data input deck for computing the stiffness coefficients of a two layer $90^\circ/33^\circ$ laminate is shown below.

<u>Parameter</u>	<u>Value</u>	<u>Format</u>
N	2	(I2,F5.0,2I1,F12.0,2I1)
THTA	0.0	
LPP	2	
J	3	
RM	0.0	
LKL	0	
JB	0	
H(1)	0.1625	(6F12.0)
H(2)	0.1625	
C(1,1,1)	0.177080E+07	(6E12.6)
C(1,2,1)	0.432100E+06	
C(2,2,1)	0.898540E+07	
C(3,1,1)	0.000000E+00	
C(3,2,1)	0.000000E+00	
C(3,3,1)	0.660000E+06	
C(1,1,2)	0.533230E+07	(6E12.6)
C(1,2,2)	0.194510E+07	
C(2,2,2)	0.239780E+07	
C(3,1,2)	0.232140E+07	

<u>Parameter</u>	<u>Value</u>	<u>Format</u>
C(3,2,2)	0.974100E+06	
C(3,3,2)	0.217310E+06	
ALPHA(1,1)	0.000000E+00	(6E12.6)
ALPHA(2,1)	0.000000E+00	
ALPHA(3,1)	0.000000E+00	
ALPHA(1,2)	0.000000E+00	
ALPHA(2,2)	0.000000E+00	
ALPHA(3,2)	0.000000E+00	
THETA(1)	0.157080E+01	
THETA(2)	0.575959E+00	

B.4 TYPICAL OUTPUT

The output corresponding to the foregoing input deck is shown in the following pages.

GENERAL	LAMINATE 2 LAYERS	ALL LAYERS INTACT (N = 2)
---------	----------------------	------------------------------

LAYER NO.	THICKNESS OF LAYERS (INCHES)	COORDINATES OF LAYER SURFACES (INCHES)		COEFS. OF STIFFNESS MATRIX (10+6 LB./IN.SQ.)					
		Z(K)	Z(K+1)	C(1,1)	C(1,2)	C(2,2)	C(6,1)	C(6,2)	C(6,6)
1	0.1625	0.1625	0.0000	1.7708	0.4321	8.9854	0.0000	0.0000	0.6600*
2	0.1625	0.0000	0.1625	5.3323	1.9451	2.3978	2.3214	0.9741	2.1731*

A (LB./IN.)				A* (IN./LB.)			
0.1154E 07	0.3863E 06	0.3772E 06	0.1237E -05	-0.1768E -06	-0.9527E -06		
0.3863E 06	0.1850E 07	0.1583E 06	-0.1768E -06	0.5823E -06	-0.5535E -07		
0.3772E 06	0.1583E 06	0.4604E 06	-0.9527E -06	-0.5535E -07	0.2972E -05		

B (LB.)				B* (IN.)			
0.4702E 05	0.1998E 05	0.3065E 05	-0.2543E -01	-0.2783E -01	-0.1660E -01		
0.1998E 05	-0.8698E 05	0.1286E 05	-0.1622E -02	0.5489E -01	-0.9646E -03		
0.3065E 05	0.1286E 05	0.1998E 05	-0.4518E -01	-0.2400E -01	-0.2946E -01		

COEF. OF THERMAL FORCE (LB./IN. DEG. F.)				H* (IN.)			
N1-T	UUUUUUUUUUUU		0.2543E -01	0.1622E -02	0.4518E -01		
N2-T	UUUUUUUUUUUU		0.2783E -01	-0.5489E -01	0.2400E -01		
N3-T	UUUUUUUUUUUU		0.1660E -01	0.9646E -03	0.2946E -01		

D (LB./IN.)				D* (LB./IN.)			
0.1016E 05	0.3400E 04	0.3320E 04	0.7547E 04	0.2452E 04	0.1618E 04		
0.3400E 04	0.1628E 05	0.1393E 04	0.2452E 04	0.1064E 05	0.7667E 03		
0.3320E 04	0.1393E 04	0.4052E 04	0.1618E 04	0.7667E 03	0.2942E 04		

A PRIME (IN./LB.)			
0.1405E-05	-0.2733E-06	-0.7014E-06	
-0.2733E-06	0.8950E-06	-0.8321E-07	
-0.7014E-06	-0.8321E-07	0.3399E-05	
B PRIME (1/LB.)			
-0.1873E-05	-0.1886E-05	-0.4121E-05	
-0.1886E-05	0.5646E-05	-0.7620E-06	
-0.4121E-05	-0.7620E-06	-0.7547E-05	
COEF. OF THERMAL MOMENT (LB./DEG.F.)			
M1-T UUUUUUUUUUUU			
M2-T UUUUUUUUUUUU			
M3-T UUUUUUUUUUUU			
D PRIME (1/LB.IN.)			
0.1597E-03	-0.3105E-04	-0.7968E-04	
-0.3105E-04	0.1018E-03	-0.9453E-05	
-0.7968E-04	-0.9453E-05	0.3861E-03	

B.5 PROGRAM LISTING

A complete listing of the program, which is written in Fortran IV, is included overleaf.

C PROGRAM MN CM

C

```
COMMON THETA(25),N,THA(3,3),LPP,LL,PCNU(3,25,2),RB(3,25,2),PCNT(3,25,2),PCNTR(3,25,2),PCMU(3,25,2),PCMT(3,25,2),PCMTR(3,25,2),RC(3,25,1,2),PCT(3,25,2),RS(3,3),RD(3,3),XA(25),S(25),XP(25),YA(25),YP(25),ICVS(4),CVP(4),CTS(4),NM,SGL(4,25,2),T(25),SIGMX(2),SIGMY(2),IQUAD(14,25,2),PRB(3,25),CNU(3,25),CNTR(3,25),CNT(3,25),PRC(3,25),CT(3,25,1),TITLE(10),JK,Z(30)
```

C

```
DIMENSION ALPHA(3,25),H(25),A(3,3),B(3,3),D(3,3),C(3,3,25),HS(25),IHC(25),AN(3,6),X(3,3),ASTAR(3,3),BSTAR(3,3),HSTAR(3,3),DSTAR(3,3),IDPRI(3,3),BPRI(3,3),APRI(3,3),SUM(3,25),TSUM(3),TADD(3),RNT(3),RMT1(3),SASK(3),DSUM(3,30),CSUM(3,25,2)
```

C

10 READ (5,101) N,THA,LPP,J,RM,LKL,JB

101 FORMAT (I2,F5.0,2I1,F12.0,2I1)

C N = NO. OF LAYERS

C MAXIMUM VALUE OF N IS N = 25

C THA IMPLIES ANGLE-PLY

C LPP = 1 IMPLIES PRESSURE VESSEL OR CYLINDER

C LPP = 2 IMPLIES PLATE

C J = 1 IMPLIES CROSS-PLY

C J = 2 IMPLIES ANGLE-PLY

C J = 3 IMPLIES GENERAL LAMINATE

C RM = CROSS PLY RATIO

C LKL = 0 IMPLIES ALL LAYERS INTACT

C LKL = 1 IMPLIES ALL LAYERS DEGRADED

C JB = 0 IMPLIES LAMINATE IS NOT BALANCED AND SYMMETRIC

C JB = 1 IMPLIES LAMINATE IS BALANCED AND SYMMETRIC

READ (5,102) (H(K),K=1,N)

102 FORMAT (6F12.0)

READ (5,103) (C(1,1,K),C(1,2,K),C(2,2,K),C(3,1,K),C(3,2,K),C(3,3,K),K=1,N)

103 FORMAT (6E12.6)

READ (5,103) ((ALPHA(I,K),I=1,3),K=1,N)

READ (5,103) (THETA(K),K=1,N)

TOTAL = 0.0

DO 20 K = 1,N

C(2,1,K) = C(1,2,K)

C(1,3,K) = C(3,1,K)

C(2,3,K) = C(3,2,K)

20 TOTAL = TOTAL + H(K)

Z(1) = - TOTAL / 2.0

MM = N + 1

DO 30 K = 2,MM

KM = K - 1

30 Z(K) = Z(KM) + H(KM)

IF (J .EQ. 2) GO TO 40

IF (J .EQ. 3) GO TO 60

WRITE (6,104) RM,N,N

104 FORMAT (1H1,37X,9HCROSS-PLY,4X,3HM =,F5.3,17HALL LAYERS INTACT/50X 1,12,1X,12HLAYERS (N = ,I2,1H))

GO TO 70


```

40 IF (LKL .EQ. 1) GO TO 50
   WRITE (6,105) THTA,N,N
105 FORMAT (1H1,33X,9HANGLE-PLY,4X,8HTHETA = ,F5.2,1X,7HDEGREES,4X,17H
   IALL LAYERS INTACT/52X,12,1X,12HLAYERS (N = ,I2,1H))
   GO TO 70
50 WRITE (6,106) THTA,N,N
106 FORMAT (1H1,33X,9HANGLE-PLY,4X,8HTHETA = ,F5.2,1X,7HDEGREES,4X,19H
   IALL LAYERS DEGRADED/52X,12,1X,12HLAYERS (N = ,I2,1H))
   GO TO 70
60 WRITE (6,107) N,N
107 FORMAT (1H1,41X,16HGENERAL LAMINATE,4X,17HALL LAYERS INTACT/50X,12
   1,1X,12HLAYERS (N = ,I2,1H))
70 WRITE (6,108)
108 FORMAT (1HU//2X,5HLAYER,2X,9HTHICKNESS,2X,14HCOORDINATES OF/3X,3HN
   10.,3X,9HOF LAYERS,2X,14HLAYER SURFACES,15X,26HCUEFS. OF STIFFNESS
   1MATR1X,14X,27HCUEFS. OF THERMAL EXPANSION/9X,8H(INCHES),6X,8H(INCH
   1ES),22X,17H(10+6 LB./IN.SQ.),22X,21H(10-6 IN./IN./DEG.F.))//4X,1HK,
   16X,4HH(K),5X,4HZ(K),4X,6HZ(K+1),3X,6HC(1,1),3X,6HC(1,2),3X,6HC(2,2
   1),3X,6HC(6,1),3X,6HC(6,2),3X,6HC(6,6),2X,8HALPHA(1),1X,8HALPHA(2),
   11X,8HALPHA(6)//)
   DO 75 K = 1,N
   KP = K + 1
75 WRITE (6,109) K,H(K),Z(K),Z(KP),C(1,1,K),C(1,2,K),C(2,2,K),C(3,1,K
   1),C(3,2,K),C(3,3,K),ALPHA(1,K),ALPHA(2,K),ALPHA(3,K)
109 FORMAT (3X,12,3X,F9.4,F9.4,F9.4,-6PF9.4,-6PF9.4,-6PF9.4,-6PF9.4,-6
   1PF9.4,-6PF9.4,6PF9.4,6PF9.4,6PF9.4)
   DO 80 K = 1,N
   KP = K + 1
   HS(K) = (Z(KP) ** 2) - (Z(K) ** 2)
80 HC(K) = (Z(KP) ** 3) - (Z(K) ** 3)
   DO 100 I = 1,3
   DO 100 J = 1,3
   A(1,J) = 0.0
   B(1,J) = 0.0
   D(1,J) = 0.0
   KK=1
   DO 92 K=1,N
   IF(KK.EQ.0) GO TO 90
   KP=(K+1)/2
   KK=0
   GO TO 91
90 KP=N-(K-2)/2
   KK=1
91 A(1,J) = A(1,J)+(C(1,J,KP)*H(KP))
   D(1,J) = D(1,J)+(C(1,J,KP)*HC(KP))
   IF(JB.EQ.1) GO TO 92
   B(1,J) = B(1,J) + (C(1,J,KP)*HS(KP))
92 CONTINUE
   B(1,J) = B(1,J) / 2.0
   D(1,J) = D(1,J) / 3.0
100 CONTINUE
   L = 0
   DO 200 I = 1,3

```

```

DO 200 J = 1,3
200 AN(I,J) = A(I,J)
210 DO 220 I = 1,3
    DO 220 J = 4,6
220 AN(I,J) = 0.0
    DO 230 I = 1,3
        J = I + 3
230 AN(I,J) = 1.0
    IF (L .EQ. 1) GO TO 270
    CALL MATS (AN,X,3,3,MATERR)
    IF (MATERR) 240,240,235
235 WRITE (6,110) ((A(I,J),I=1,3),J=1,3)
110 FORMAT (1H0,20HMATRIX A IS SINGULAR// (3(-6PF8.4)))
    GO TO 10
240 CALL MATMPY (X,B,BSTAR,3,3,3)
    DO 250 I = 1,3
        DO 250 J = 1,3
        ASTAR(I,J) = X(I,J)
250 BSTAR(I,J) = - BSTAR(I,J)
    CALL MATMPY (B,X,HSTAR,3,3,3)
    CALL MATMPY (HSTAR,B,DSTAR,3,3,3)
    CALL MATSBT (D,DSTAR,3,3)
    DO 260 I = 1,3
        DO 260 J = 1,3
260 AN(I,J) = DSTAR(I,J)
    L = 1
    GO TO 210
270 CALL MATS (AN,DPRI,3,3,MATERR)
    IF (MATERR) 290,290,280
280 WRITE (6,111) ((DSTAR(I,J),I=1,3),J=1,3)
111 FORMAT (1H0,24HMATRIX DSTAR IS SINGULAR// (3(-6PF8.4)))
    GO TO 10
290 CALL MATMPY (BSTAR,DPRI,BPRI,3,3,3)
    CALL MATMPY (BPRI,HSTAR,APRI,3,3,3)
    CALL MATSBT (ASTAR,APRI,3,3)
    DO 300 I = 1,3
        DO 300 K = 1,N
        SUM(I,K) = 0.0
    DO 300 J = 1,3
300 SUM(I,K) = SUM(I,K) + (C(I,J,K) * ALPHA(J,K))
    DO 320 I = 1,3
        TSUM(I) = 0.0
        TADD(I) = 0.0
    DO 310 K = 1,N
        TSUM(I) = TSUM(I) + (SUM(I,K) * H(K))
310 TADD(I) = TADD(I) + (SUM(I,K) * HS(K))
        RNT(I) = TSUM(I)
320 RMT(I) = TADD(I) / 2.0
    IF (LPP .EQ. 2) GO TO 370
    DO 330 K = 1,N
        DO 330 I = 1,3
        CNU(I,K) = 0.0
        CNT(I,K) = 0.0

```

```

CNTR(1,K) = 0.0
DO 330 J = 1,3
CND(1,K) = CND(1,K) + (C(1,J,K) * ASTAR(J,1))
CNT(1,K) = CNT(1,K) + (C(1,J,K) * ASTAR(J,2))
330 CNTR(1,K) = CNTR(1,K) + (C(1,J,K) * ASTAR(J,3))
DO 340 I = 1,3
SASR(1) = 0.0
DO 340 J = 1,3
340 SASR(1) = SASR(1) + (ASTAR(I,J) * RNT(J))
DO 360 K = 1,N
DO 360 I = 1,3
CT(1,K) = 0.0
DO 350 J = 1,3
350 CT(1,K) = CT(1,K) + (C(1,J,K) * SASR(J))
360 CT(1,K) = CT(1,K) - SUM(1,K)
GO TO 420
370 DO 375 K = 1,N
DO 375 I = 1,3
DO 375 LR = 1,2
PCND(1,K,LR) = 0.0
PCNT(1,K,LR) = 0.0
PCNTR(1,K,LR) = 0.0
PCMU(1,K,LR) = 0.0
PCMT(1,K,LR) = 0.0
375 PCMTR(1,K,LR) = 0.0
DO 380 K = 1,N
DO 380 I = 1,3
DO 380 J = 1,3
DO 380 LR = 1,2
KP = K
IF (LR .EQ. 2) KP = KP + 1
PCND(1,K,LR) = PCND(1,K,LR) + (C(1,J,K) * (APRI(J,1) + (Z(KP) * BP
LRI(J,1))))
PCNT(1,K,LR) = PCNT(1,K,LR) + (C(1,J,K) * (APRI(J,2) + (Z(KP) * BP
LRI(J,2))))
PCNTR(1,J,LR) = PCNTR(1,K,LR) + (C(1,J,K) * (APRI(J,3) + (Z(KP) *
1BPRI(J,3))))
PCMU(1,K,LR) = PCMU(1,K,LR) + (C(1,J,K) * (BPRI(J,1) + (Z(KP) * DP
LRI(J,1))))
PCMT(1,K,LR) = PCMT(1,K,LR) + (C(1,J,K) * (BPRI(J,2) + (Z(KP) * DP
LRI(J,2))))
380 PCMTR(1,J,LR) = PCMTR(1,K,LR) + (C(1,J,K) * (BPRI(J,3) + (Z(KP) *
1DPRI(J,3))))
MM = N + 1
DO 390 K = 1,MM
DO 390 I = 1,3
DSUM(1,K) = 0.0
DO 390 J = 1,3
390 DSUM(1,K) = DSUM(1,K) + ((APRI(1,J) + (Z(K) * BPRI(1,J))) * RNT(J)
1) + ((BPRI(1,J) + (Z(K) * DPRI(1,J))) * RMT(J))
DO 410 K = 1,N
DO 410 I = 1,3
CSUM(1,K,1) = 0.0

```

```

CSUM(I,K,2) = 0.0
DO 400 J = 1,3
CSUM(I,K,1) = CSUM(I,K,1) + (C(I,J,K) * DSUM(J,K))
KP = K + 1
400 CSUM(I,K,2) = CSUM(I,K,2) + (C(I,J,K) * DSUM(J,KP))
PCT(I,K,1) = CSUM(I,K,1) - SUM(I,K)
410 PCT(I,K,2) = CSUM(I,K,2) - SUM(I,K)
420 WRITE (6,112)
112 FORMAT (1H0///18X,1HA,39X,2HA*,35X,7HA PRIME/14X,9H(LB./IN.),32X,
19H(IN./LB.),30X,9H(IN./LB.)//)
WRITE (6,113) (A(I,1),A(I,2),A(I,3),ASTAR(I,1),ASTAR(I,2),ASTAR(I,
13),APRI(I,1),APRI(I,2),APRI(I,3),I=1,3)
113 FORMAT (1X,3E12.4,4X,3E12.4,4X,3E12.4)
WRITE (6,114)
114 FORMAT (1H0//18X,1HB,39X,2HB*,35X,7HB PRIME/16X,5H(LB.),35X,5H(IN.
1),34X,7H(1/LB.)//)
WRITE (6,115) (B(I,1),B(I,2),B(I,3),BSTAR(I,1),BSTAR(I,2),BSTAR(I,
13),BPRI(I,1),BPRI(I,2),BPRI(I,3),I=1,3)
115 FORMAT (1X,3E12.4,4X,3E12.4,4X,3E12.4)
WRITE (6,116)
116 FORMAT (1H0//8X,22HCDEF. OF THERMAL FORCE,28X,2HH*,28X,23HCDEF. OF
1 THERMAL MOMENT/12X,15H(LB./IN.DEG.F.),29X,5H(IN.),32X,12H(LB./DEG
1.F.)//)
WRITE (6,117) (1,RNT(I),HSTAR(I,1),HSTAR(I,2),HSTAR(I,3),1,RMT(I),
I=1,3)
117 FORMAT (11X,1HN,11,3H-T ,E12.4,13X,3E12.4,14X,1HM,11,3H-T ,E12.4)
WRITE (6,118)
118 FORMAT (1H0//18X,1HD,39X,2HD*,35X,7HD PRIME/15X,8H(LB.IN.),32X,8H(
1LB.IN.),31X,1CH(1/LB.IN.)//)
WRITE (6,119) (D(I,1),D(I,2),D(I,3),DSTAR(I,1),DSTAR(I,2),DSTAR(I,
13),DPRI(I,1),DPRI(I,2),DPRI(I,3),I=1,3)
119 FORMAT (1X,3E12.4,4X,3E12.4,4X,3E12.4)
IF (LPP .EQ. 1) GO TO 450
WRITE (6,120)
120 FORMAT (1H0//7X,1HZ,8X,6HSTRESS,3X,11HCDEF. OF N1,2X,11HCDEF. OF N
12,2X,11HCDEF. OF N6,2X,11HCDEF. OF M1,2X,11HCDEF. OF M2,2X,11HCDEF
1. OF M6,2X,14HCDEF. OF TEMP./5X,5H(IN.),4X,9HCMPONENT,4X,7H(1/IN.
1),6X,7H(1/IN.),6X,7H(1/IN.),4X,10H(1/IN.SQ.),3X,10H(1/IN.SQ.),3X,1
10H(1/IN.SQ.),3X,15H(LB./IN.SQ./F.)//)
DO 430 K = 1,N
KP = K + 1
WRITE (6,121) K
121 FORMAT (50X,9H-- LAYER ,12,3H --//)
WRITE (6,122) Z(K),(PCNU(I,K,1),PCNT(I,K,1),PCNTR(I,K,1),PCMU(I,K,
11),PCMT(I,K,1),PCMTR(I,K,1),PCT(I,K,1),I=1,3),Z(KP),(PCNU(I,K,2),P
1CNT(I,K,2),PCNTR(I,K,2),PCMU(I,K,2),PCMT(I,K,2),PCMTR(I,K,2),PCT(I
1,K,2),I=1,3)
122 FORMAT (3X,F8.4,4X,7HSIGMA 1,4X,F8.4,5F13.4,6X,F8.4/21X,1H2,4X,F8.
14,5F13.4,6X,F8.4/21X,1H6,4X,F8.4,5F13.4,6X,F8.4/)
430 CONTINUE
440 CALL PARTWO
GO TO 470
450 WRITE (6,123)

```

```
123 FORMAT (1H0//31X,6HSTRESS,3X,11HCOEF. OF N1,2X,11HCOEF. OF N2,2X,1
11HCOEF. OF N3,2X,14HCOEF. OF TEMP./29X,9HCOMPONENT,4X,7H(1/IN.),6
1,7H(1/IN.),6X,7H(1/IN.),4X,15H(LB./IN.SQ./F.))//)
DO 460 K = 1,N
WRITE (6,124) K
124 FORMAT (55X,9H-- LAYER ,12,3H --//)
WRITE (6,125) (CNC(I,K),CNT(I,K),CNTR(I,K),CT(I,K),I=1,3)
125 FORMAT (30X,7HSIGMA 1,4X,F8.4,2F13.4,6X,F8.4/36X,1H2,4X,F8.4,2F13.
14,6X,F8.4/36X,1H6,4X,F8.4,2F13.4,6X,F8.4/)
460 CONTINUE
GO TO 440
470 CONTINUE
STOP
END
```

```

SUBROUTINE MATS (A,X,N,M,MATERR)
DIMENSION A(3,6),X(3,3)
MATERR = 0
MM = N + M
DO 50 I = 2,N
  II = I - 1
  DO 50 J = 1,II
    IF (A(I,J) .EQ. 0.0) GO TO 50
    IF ((ABS(A(J,J)) - ABS(A(I,J))) .LT. 0.0) GO TO 10
    R = A(I,J) / A(J,J)
    GO TO 30
  10 R = A(J,J) / A(I,J)
  DO 20 K = 1,MM
    B = A(J,K)
    A(J,K) = A(I,K)
  20 A(I,K) = B
  30 JJ = J + 1
  DO 40 K = JJ,MM
  40 A(I,K) = A(I,K) - (R * A(J,K))
  50 CONTINUE
  IF ((ABS(A(N,N)) - 1.0E-10) .GT. 0.0) GO TO 70
  60 WRITE (6,101) N,N
101 FORMAT (26HC                      ELEMENT(,I2,IH,,I2,IH),38H VERY SMALL
  1. CASE DELETED BY MATS      )
  MATERR = 1
  GO TO 100
  70 DO 90 J = 1,M
    KK = N + J
    X(N,J) = A(N,KK) / A(N,N)
    DO 90 I = 2,N
      JJ = N - I + 1
      B = 0.0
      II = N - I + 2
      DO 80 K = II,N
  80 B = B + (A(JJ,K) * X(K,J))
      IF ((ABS(A(JJ,JJ)) - 1.0E-10) .LE. 0.0) GO TO 60
  90 X(JJ,J) = (A(JJ,KK) - B) / A(JJ,JJ)
100 RETURN
END

```

```
SUBROUTINE MATMPY (A,B,C,L,M,N)
DIMENSION A(3,3),B(3,3),C(3,3)
DO 20 I = 1,L
DO 20 J = 1,N
SUM = 0.0
DO 10 LL = 1,M
10 SUM = SUM + (A(I,LL) * B(LL,J))
20 C(I,J) = SUM
RETURN
END
```

```
SUBROUTINE MATSBT (A,B,M,N)
DIMENSION A(3,3),B(3,3)
DO 10 I = 1,M
DO 10 J = 1,N
C = B(I,J)
10 B(1,J) = A(1,J) - C
RETURN
END
```



```

SUBROUTINE PARTWC
COMMON THETA(25),N,TM(3,3),LPP,LL,PCNG(3,25,2),RB(3,25,2),PCNT(3,2
15,2),PCNTR(3,25,2),PCMU(3,25,2),PCMT(3,25,2),PCMTR(3,25,2),RC(3,25
1,2),PCT(3,25,2),RS(3,3),RD(3,3),XA(25),S(25),XP(25),YA(25),YP(25),
1CVS(4),CVP(4),CTS(4),NM,SOL(4,25,2),T(25),SIGMX(2),SIGMY(2),1QUAD(
14,25,2),PRB(3,25),CND(3,25),CNTR(3,25),CNT(3,25),PRC(3,25),CT(3,25
1),TITLE(10),JK,Z(30)
10 READ (5,101) KQR,LL,JK,NM
101 FORMAT (3I1,I2)
C KQR = 0 IMPLIES SUBROUTINE IS TO CONTINUE READING
C KQR = 1 IMPLIES RETURN TO THE MAIN PROGRAM
C LL IMPLIES CASE UNDER CONSIDERATION
C FOR PLATE
C LL = 1 IMPLIES N1 NOT EQUAL TO 0.0
C LL = 2 IMPLIES N2 NOT EQUAL TO 0.0
C LL = 3 IMPLIES N6 NOT EQUAL TO 0.0
C LL = 4 IMPLIES M1 NOT EQUAL TO 0.0
C LL = 5 IMPLIES M2 NOT EQUAL TO 0.0
C LL = 6 IMPLIES M6 NOT EQUAL TO 0.0
C FOR CYLINDER
C LL = 1 IMPLIES N1 NOT EQUAL TO 0.0
C LL = 2 IMPLIES N6 NOT EQUAL TO 0.0
C LL = 3 IMPLIES 2N1 = N2
C JK = 1 IMPLIES CASES N1 OR M1
C JK = 2 IMPLIES CASES N2 OR M2
C JK = 6 IMPLIES CASES N6 OR M6
C NM = NO. OF INPUT VALUES OF TEMPERATURE
C MAXIMUM VALUE OF NM = 50
IF (KQR .EQ. 1) GO TO 570
READ (5,102) (T(K),K=1,NM)
102 FORMAT (6F12.6)
READ (5,103) (XA(K),K=1,N)
103 FORMAT (6E12.6)
READ (5,103) (YA(K),K=1,N)
READ (5,103) (XP(K),K=1,N)
READ (5,103) (YP(K),K=1,N)
READ (5,103) (S(K),K=1,N)
READ(5,104) TITLE
104 FORMAT (10A6)
20 WRITE (6,105)
105 FORMAT (1H1,1X,1H2,3X,22HAXIAL TENSILE STRENGTH,2X,26HAXIAL COMPRES
ISSIVE STRENGTH,3X,27HTRANSVERSE TENSILE STRENGTH,2X,31HTRANSVERSE
1COMPRESSIVE STRENGTH/1X,4H(IN),9X,5H(PSI),22X,5H(PSI),23X,5H(PSI),
126X,5H(PSI)//)
DO 30 K = 1,N
WRITE (6,106) Z(K),XA(K),XP(K),YA(K),YP(K)
106 FORMAT (F8.4,3X,E13.6,12X,E13.6,16X,E13.6,18X,E13.6)
30 CONTINUE
WRITE (6,107) (S(K),K=1,N)
107 FORMAT (1HC,52X,14HSHEAR STRENGTH/57X,5H(PSI)//(52X,E13.6))
WRITE (6,108) TITLE
108 FORMAT (1H1,47X,7HCASE ,10A6)
TEMP = -1.0E-75

```

```

DO 560 K = 1,N
RM = COS(THETA(K))
RN = SIN(THETA(K))
TM(1,1) = RM * RM
TM(1,2) = RN * RN
RPMN = RM * RN
TM(1,3) = 2.0 * RPMN
TM(2,1) = TM(1,2)
TM(2,2) = TM(1,1)
TM(2,3) = - TM(1,3)
TM(3,1) = - RPMN
TM(3,2) = RPMN
TM(3,3) = TM(1,1) - TM(1,2)
WRITE (6,110) K
110 FORMAT(1H1,53X,9H-- LAYER ,I2,3H --/)
DO 550 J = 1,2
IF (LPP .EQ. 1) GO TO 300
GO TO (50,70,90,210,230,250),LL
50 DO 60 I = 1,3
60 RB(I,K,J) = PCNO(I,K,J)
GO TO 270
70 DO 80 I = 1,3
80 RB(I,K,J) = PCNT(I,K,J)
GO TO 270
90 DO 100 I = 1,3
100 RB(I,K,J) = PCNTR(I,K,J)
GO TO 270
210 DO 220 I = 1,3
220 RB(I,K,J) = PCMG(I,K,J)
GO TO 270
230 DO 240 I = 1,3
240 RB(I,K,J) = PCMT(I,K,J)
GO TO 270
250 DO 260 I = 1,3
260 RB(I,K,J) = PCMTR(I,K,J)
270 DO 280 I = 1,3
280 RC(I,K,J) = PCT(I,K,J)
DO 290 I = 1,3
KS(1,1) = RB(1,K,J)
290 KS(1,2) = RC(1,K,J)
GO TO 400
300 IF (J .EQ. 2) GO TO 550
GO TO (310,330,350),LL
310 DO 320 I = 1,3
320 PRB(I,K) = CNO(I,K)
GO TO 370
330 DO 340 I = 1,3
340 PRB(I,K) = CNTR(I,K)
GO TO 370
350 DO 360 I = 1,3
360 PRB(I,K) = (0.5 * CNO(I,K)) + CNT(I,K)
370 DO 380 I = 1,3
380 PRC(I,K) = CT(I,K)

```

```

DO 390 I = 1,3
RS(I,1) = PRB(1,K)
390 RS(I,2) = PRC(1,K)
400 CALL MATMPY (TM,RS,RD,3,3,2)
S1 = RD(1,1) ** 2
S2 = RD(1,1) * RD(2,1)
S3 = RD(2,1) ** 2
S4 = RD(3,1) ** 2
S5 = 2.0 * RD(1,1) * RD(1,2)
S6 = (RD(1,2) * RD(2,1)) + (RD(1,1) * RD(2,2))
S7 = 2.0 * RD(2,1) * RD(2,2)
S8 = 2.0 * RD(3,1) * RD(3,2)
S9 = RD(1,2) ** 2
S10 = RD(1,2) * RD(2,2)
S11 = RD(2,2) ** 2
S12 = RD(3,2) ** 2
R1 = XA(K) / YA(K)
R2 = XP(K) / YA(K)
R3 = XP(K) / YP(K)
R4 = XA(K) / YP(K)
SQ = S(K) ** 2
YAS = YA(K) ** 2
XAS = XA(K) ** 2
YPS = YP(K) ** 2
XPS = XP(K) ** 2
XY = XA(K) * YA(K)
XPYP = XP(K) * YP(K)
XYP = XA(K) * YP(K)
XPY = XP(K) * YA(K)
CVS(1) = (S1 / XAS) - (S2 / (R1 * XY)) + (S3 / YAS) + (S4 / SQ)
CVS(2) = (S1 / XPS) - (S2 / (R2 * XPY)) + (S3 / YAS) + (S4 / SQ)
CVS(3) = (S1 / XPS) - (S2 / (R3 * XPYP)) + (S3 / YPS) + (S4 / SQ)
CVS(4) = (S1 / XAS) - (S2 / (R4 * XYP)) + (S3 / YPS) + (S4 / SQ)
CVP(1) = (S5 / XAS) - (S6 / (R1 * XY)) + (S7 / YAS) + (S8 / SQ)
CVP(2) = (S5 / XPS) - (S6 / (R2 * XPY)) + (S7 / YAS) + (S8 / SQ)
CVP(3) = (S5 / XPS) - (S6 / (R3 * XPYP)) + (S7 / YPS) + (S8 / SQ)
CVP(4) = (S5 / XAS) - (S6 / (R4 * XYP)) + (S7 / YPS) + (S8 / SQ)
CTS(1) = (S9 / XAS) - (S10 / (R1 * XY)) + (S11 / YAS) + (S12 / SQ)
CTS(2) = (S9 / XPS) - (S10 / (R2 * XPY)) + (S11 / YAS) + (S12 / SQ)
1)
CTS(3) = (S9 / XPS) - (S10 / (R3 * XPYP)) + (S11 / YPS) + (S12 / SQ)
1Q)
CTS(4) = (S9 / XAS) - (S10 / (R4 * XYP)) + (S11 / YPS) + (S12 / SQ)
1)
DO 470 I = 1,4
DO 470 JL = 1,NM
DISC = ((CVP(I) * T(JL)) ** 2) - (4.0 * CVS(I) * (CTS(I) * (T(JL)
1** 2) - 1.0))
410 IF (DISC .LT. 0.0) GO TO 420
SOL(I,JL,1) = (- (CVP(I) * T(JL)) + SQRT(DISC)) / (2.0 * CVS(I))
SOL(I,JL,2) = (- (CVP(I) * T(JL)) - SQRT(DISC)) / (2.0 * CVS(I))
GO TO 430
420 SOL(I,JL,1) = TEMP

```

```

SCL(1,JL,2) = TEMP
430 DO 470 IL = 1,2
    SIGMX(IL) = (RD(1,1) * SCL(1,JL,1L)) + (RD(1,2) * T(JL))
    SIGMY(IL) = (RD(2,1) * SCL(1,JL,1L)) + (RD(2,2) * T(JL))
    IF (SIGMX(IL) .GE. 0.0 .AND. SIGMY(IL) .GE. 0.0) GO TO 440
    IF (SIGMX(IL) .LT. 0.0 .AND. SIGMY(IL) .GT. 0.0) GO TO 450
    IF (SIGMX(IL) .LT. 0.0 .AND. SIGMY(IL) .LT. 0.0) GO TO 460
    IQUAD(1,JL,IL) = 4
    GO TO 470
440 IQUAD(1,JL,1L) = 1
    GO TO 470
450 IQUAD(1,JL,1L) = 2
    GO TO 470
460 IQUAD(1,JL,1L) = 3
470 CONTINUE
    IF (J .EQ. 2) GO TO 480
    IF (LPP .EQ. 1) GO TO 490
    WRITE (6,111) Z(K)
111 FORMAT (4X,4HZ = ,F8.4)
    GO TO 490
480 KP = K + 1
    WRITE (6,112) Z(KP)
112 FORMAT (1H1,3X,4HZ = ,F8.4)
490 DO 540 I = 1,4
    IF (LPP .EQ. 1) GO TO 500
    IF (LL .GT. 3) GO TO 510
500 WRITE (6,113) I,CVS(I),JK,CVP(I),JK,CTS(I)
113 FORMAT (1H0,54X,9HQADRANT ,11//20X,E13.6,2H*N,11,4H**2 ,E13.6,2H*
IN,11,3H*T ,E13.6,13H*T**2 - 1 = 0//)
    GO TO 520
510 WRITE (6,114) I,CVS(I),JK,CVP(I),JK,CTS(I)
114 FORMAT (1H0,54X,9HQADRANT ,11//20X,E13.6,2H*M,11,4H**2 ,E13.6,2H*
IM,11,3H*T ,E13.6,13H*T**2 - 1 = 0//)
520 WRITE (6,115)
115 FORMAT (9X,11HTEMPERATURE,13X,10HSOLUTION 1,8X,8HQADRANT,7X,10HSO
LUTION 2,8X,8HQADRANT/10X,8H(DEG. F)//)
    DO 530 JL = 1,NM
    WRITE (6,116) T(JL),SCL(1,JL,1),IQUAD(1,JL,1),SCL(1,JL,2),IQUAD(1,
1JL,2)
116 FORMAT (11X,F7.1,13X,E13.6,10X,11,9X,E13.6,10X,11)
530 CONTINUE
540 CONTINUE
550 CONTINUE
560 CONTINUE
570 RETURN
    END

```

APPENDIX C

SOLUTION OF THE

GOVERNING DIFFERENTIAL EQUATION OF DISPLACEMENT

The general solution of $\phi(D)w = F(x)$ can be obtained by finding a particular solution, w_p , of this equation and adding it to the complementary solution, w_c , which is the general solution of $\phi(D)w = 0$ (45).

In operator notation, equation (5-38) may be written

$$(D^4 + k_1 D^2 + k_2)w = F(x) \quad (C-1)$$

thus

$$\phi(D)w = (D^4 + k_1 D^2 + k_2)w \quad (C-2)$$

The complementary or reduced differential equation is therefore

$$(D^4 + k_1 D^2 + k_2)w = 0 \quad (C-3)$$

Letting $w = e^{mx}$, the auxiliary equation

$$m^4 + k_1 m^2 + k_2 = 0 \quad (C-4)$$

is obtained. If it is then assumed that this equation has roots of the form

$$\begin{aligned}
 m &= \alpha + \beta i \\
 m &= \alpha - \beta i \\
 m &= -\alpha + \beta i \\
 m &= -\alpha - \beta i
 \end{aligned}
 \tag{C-5}$$

equation (C-4) should be obtainable from

$$m - (\alpha + \beta i) m - (\alpha - \beta i) m - (-\alpha + \beta i) m - (-\alpha - \beta i) = 0$$

.... (C-6)

Multiplication of the factors in equation (C-6) yields .

$$m^4 - 2(\alpha^2 - \beta^2)m^2 + (\alpha^2 + \beta^2) = 0
 \tag{C-7}$$

Then, the roots assumed in (C-5) can only be true roots of the auxiliary equation (C-4) if

$$\begin{aligned}
 k_1 &= -2(\alpha^2 - \beta^2) \\
 k &= (\alpha^2 + \beta^2)^2
 \end{aligned}
 \tag{C-8}$$

or,

$$\begin{aligned}
 \alpha^2 &= \left[-\frac{k_1}{4} + \frac{k_2^{1/2}}{2} \right] \\
 \beta^2 &= \left[\frac{k_1}{4} + \frac{k_2^{1/2}}{2} \right]
 \end{aligned}
 \tag{C-9}$$

Then, since $\alpha \pm \beta i$ and $-\alpha \pm \beta i$ are all roots of the auxiliary equation, $e^{\alpha x}(C_1 \sin \beta x + C_2 \cos \beta x)$ and $e^{-\alpha x}(C_3 \sin \beta x + C_4 \cos \beta x)$ are both valid solutions.

Therefore, the complete solution to the complementary

equation is

$$w_c = e^{\alpha x}(C_1 \sin \beta x + C_2 \cos \beta x) + e^{-\alpha x}(C_3 \sin \beta x + C_4 \cos \beta x) \quad (C-10)$$

and hence the general solution to the governing differential equation is

$$w = w_c + w_p$$

or

$$w = e^{\alpha x}(C_1 \sin \beta x + C_2 \cos \beta x) + e^{-\alpha x}(C_3 \sin \beta x + C_4 \cos \beta x) + w_p$$

.... (C-11)

APPENDIX D

PROGRAM FOR ANALYZING CYLINDRICAL STORAGE TANKS

D.1 DESCRIPTION OF PROGRAM

The computer program, CYLTAN, i.e., Cylindrical Tank Analysis, enables a complete layer-by-layer stress analysis at any number of points in a vertical storage tank constructed of either isotropic or fibre-reinforced composite materials. It is based upon the theoretical analysis presented in Section 5 which assumes that the tank is rigidly constrained at its base.

D.2 INPUT PARAMETER DEFINITIONS

<u>Parameter</u>	<u>Definition</u>
R	is the tank radius (in.).
DPTH	is depth (in.) of the contained fluid.
RHO	is the density (lb./cu.in.) of the contained fluid.
N	is the number of layers within the laminate.
H(K)	is the thickness (in.) of the kth layer.
C(I,J,K)	is the elastic stiffness, C_{ij} (psi), of the kth layer.
ASTR12,ASTR22	are elements of the intermediate in-plane

<u>Parameter</u>	<u>Definition</u>
ASTR26,BSTR11 BSTR61,HSTR12 DSTR11	matrix A^* (in./lb.), the intermediate coupling matrices B^* (in.) and H^* (in.), and the intermediate flexural matrix D^* (lb.-in.).
THETA(K)	is the fibre orientation or lamination angle (degrees) of the kth layer.
XA(K)	is the axial tensile strength (psi) of the kth layer.
YA(K)	is the transverse tensile strength (psi) of the kth layer.
XP(K)	is the axial compressive strength (psi) of the kth layer.
YP(K)	is the transverse compressive strength (psi) of the kth layer.
S(K)	is the in-plane shear strength (psi) of the kth layer.

D.3 TYPICAL INPUT

A data input deck for determining the inertial effects of the contained fuel on a gun-launched rocket motor case as it exits from the muzzle is provided below. The problem is described in detail in Section 5.10.

<u>Parameter</u>	<u>Value</u>	<u>Format</u>
R	3.41	(3F6.0,I3)
DPTH	43.00	

<u>Parameter</u>	<u>Value</u>	<u>Format</u>
RHO	98.00	
N	2	
H(1)	0.1625	(6F12.0)
H(2)	0.1625	
C(1,1,1)	0.898540E+07	(4E12.6)
C(1,2,1)	0.432100E+06	
C(2,2,1)	0.177080E+07	
C(3,3,1)	0.660000E+06	
C(1,1,2)	0.898540E+07	(4E12.6)
C(1,2,2)	0.432100E+06	
C(2,2,2)	0.177080E+07	
C(3,3,2)	0.660000E+06	
ASTR12	-0.176800E-06	(4E12.6)
ASTR22	0.582300E-06	
ASTR26	-0.553500E-07	
BSTR11	-0.254300E-01	
BSTR61	-0.451800E-01	(4E12.6)
HSTR12	0.162200E-02	
DSTR11	0.754700E-04	

<u>Parameter</u>	<u>Value</u>	<u>Format</u>
THETA(1)	20.0	(6F12.0)
THETA(2)	33.0	
XA(1)	150000.0	(6F12.0)
XA(2)	150000.0	
YA(1)	12000.0	(6F12.0)
YA(2)	12000.0	
XP(1)	150000.0	(6F12.0)
XP(2)	150000.0	
YP(1)	20000.0	(6F12.0)
YP(2)	20000.0	
S(1)	10000.0	(6F12.0)
S(2)	10000.0	

D.4 TYPICAL OUTPUT

A typical output, corresponding to the foregoing input deck, is shown in the following pages. Included are complete stress analyses at the two main points of interest: the base and the point of maximum deflection.

CYLINDRICAL TANK ANALYSIS

TANK RADIUS = 3.41 INCHES

TANK HEIGHT = 43.00 INCHES

FLUID DENSITY = 98.0000 LB./CU. IN.

ASTAR12 = -0.1768E-06 IN./LB.

ASTAR22 = 0.5823E-06 IN./LB.

ASTAR26 = -0.5535E-07 IN./LB.

BSTAR11 = -0.2543E-01 INCHES

BSTAR61 = -0.4518E-01 INCHES

HSTAR12 = 0.1622E-02 INCHES

DSTAR11 = 0.7547E 04 LB. IN.

LAYER NO.	THICKNESS OF LAYERS (INCHES)	COORDINATES OF LAYER SURFACES (INCHES)		ORIENTATION (DEGREES)	COEFS. OF STIFFNESS MATRIX (10+6 LB./SQ.IN.)			
		Z (K)	Z (K+1)		THETA (K)	C (1,1)	C (1,2)	(2,2)
K	H (K)	Z (K)	Z (K+1)	THETA (K)	C (1,1)	C (1,2)	(2,2)	C (6,6)
1	0.1625	-0.1625	0.0000	90.00	8.9854	0.4321	1.7708	0.6600
2	0.1625	0.0000	0.1625	33.00	8.9854	0.4321	1.7708	0.6600

ALLOWABLE STRESSES							
Z (IN)	AXIAL TENSILE (KSI)	AXIAL COMPRESSIVE (KSI)	TRANSVERSE TENSILE (KSI)	TRANSVERSE COMPRESSIVE (KSI)	SHEAR (KSI)		
-0.1625	150.00	150.00	12.00	20.00	10.00		
0.0000	150.00	150.00	12.00	20.00	10.00		
0.0000	150.00	150.00	12.00	20.00	10.00		
0.1625	150.00	150.00	12.00	20.00	10.00		

DISTANCE FROM BASE OF TANK = 0.00 INCHES										
RADIAL DEFLECTION = 0.000000 INCHES										
CHANGE OF CURVATURE (X-DIRECTION) = -0.124307E 00										
LAYER NO.	LAYER STRAINS (PERCENT)						PRINCIPAL LAYER STRESSES (10+3 LB./SQ. IN.)			FAILURE CRITERIA
K	EPSX	EPSY	GAMXY	EPS1	EPS2	GAM12	S1	S2	S12	
1	-2.342	-00.000	-0.564	-0.000	-2.342	0.564	-10.12	-41.48	3.72	4.425
1	-0.322	-00.000	-0.564	-0.000	-0.322	0.564	-1.39	-5.71	3.72	0.219
2	-0.322	-00.000	-0.564	-0.484	0.162	0.065	-42.80	0.77	0.43	0.089
2	1.698	-00.000	-0.564	0.937	0.761	-1.780	87.46	17.52	-11.75	3.785

DISTANCE FROM BASE OF TANK = 2.00 INCHES										
RADIAL DEFLECTION = -0.028548 INCHES										
CHANGE OF CURVATURE (X-DIRECTION) = 0.739925E-02										
LAYER NO.	LAYER STRAINS (PERCENT)						PRINCIPAL LAYER STRESSES (10+3 LB./SQ. IN.)			FAILURE CRITERIA
K	EPSX	EPSY	GAMXY	EPS1	EPS2	GAM12	S1	S2	S12	
1	-0.115	0.837	-0.046	0.837	-0.115	0.046	74.69	1.59	0.30	0.261
1	-0.235	0.837	-0.046	0.837	-0.235	0.046	74.17	-0.54	0.30	0.248
2	-0.235	0.837	-0.046	0.062	0.540	0.960	7.90	9.83	6.34	1.072
2	-0.355	0.837	-0.046	-0.023	0.504	1.070	0.15	8.83	7.06	1.040

D.5 PROGRAM LISTING

A complete listing of the program CYLTAN, which is written in FORTRAN IV language, follows.

```

C PROGRAM CYLTAN
C
C STRESS ANALYSIS OF A VERTICAL CYLINDRICAL TANK CONTAINING LIQUID
C
C MATERIAL OF CONSTRUCTION CAN BE ORTHOTROPIC OR ISOTROPIC
C
C THE TANK IS ASSUMED TO BE RIGIDLY CONSTRAINED AT ITS BASE
C
      DIMENSION H(25),C(3,3,25),THETA(25),XA(25),YA(25),XP(25),YP(25),S(
      125),Z(30),W(431),D2W(431),TM(3,3)
C
C INPUT
C
      READ (5,101) R,DPTH,RHD,N
      101 FORMAT (3F6.0,I3)
C R IS THE TANK RADIUS
C DPTH IS THE DEPTH OF THE TANK
C RHD IS THE DENSITY OF THE CONTAINED LIQUID
C N = NUMBER OF LAYERS
      WRITE (6,102) R,DPTH,RHD
      102 FORMAT (1H1//23X,25HCYLINDRICAL TANK ANALYSIS//10X,17HTANK RADIUS
      1 = ,F6.2,1X,6HINCHES//10X,17HTANK HEIGHT = ,F6.2,1X,6HINCHES
      1//10X,16HFLUID DENSITY = ,F7.4,1X,10HLB./CU.IN.//)
      READ (5,103) (H(K),K=1,N)
      103 FORMAT (6F12.0)
      READ (5,104) (C(1,1,K),C(1,2,K),C(2,2,K),C(3,3,K),K=1,N)
      104 FORMAT (4E12.6)
      READ (5,104) ASTR12,ASTR22,ASTR26,BSTR11,BSTR61,HSTR12,DSTR11
C ASTR12, ASTR22, ASTR26, BSTR11, BSTR61, HSTR12 AND DSTR11 ARE OBTAINED
C FROM THE ELASTIC CONSTANT MATRIX ASSOCIATED WITH THE PARTIALLY
C INVERTED FORM OF THE LAMINATE CONSTITUTIVE EQUATION
      WRITE (6,105) ASTR12,ASTR22,ASTR26,BSTR11,BSTR61,HSTR12,DSTR11
      105 FORMAT (1H0//10X,11HASTAR12 = ,E12.4,2X,7HIN./LB.//10X,11HASTAR22
      1 = ,E12.4,2X,7HIN./LB.//10X,11HASTAR26 = ,E12.4,2X,7HIN./LB.//10X
      1,11HBSTAR11 = ,E12.4,2X,6HINCHES//10X,11HBSTAR61 = ,E12.4,2X,6HI
      INCHES//10X,11HHSTAR12 = ,E12.4,2X,6HINCHES//10X,11HDSTAR11 = ,E1
      12.4,2X,6HLB.IN.//)
      READ (5,103) (THETA(K),K=1,N)
C THETA(K) INPUT VALUES ARE IN DEGREES
      READ (5,103) (XA(K),K=1,N)
      READ (5,103) (YA(K),K=1,N)
      READ (5,103) (XP(K),K=1,N)
      READ (5,103) (YP(K),K=1,N)
      READ (5,103) (S(K),K=1,N)
C XA(K), YA(K), XP(K), YP(K), S(K) ARE ALLOWABLE PRINCIPLE STRESSES
      TOTAL = 0.0
C
      DO 10 K = 1,N
      10 TOTAL = TOTAL + H(K)
      Z(1) = - (TOTAL / 2.0)
      MM = N + 1
C
      DO 20 K = 2, MM

```



```

      KM = K - 1
20  Z(K) = Z(KM) + H(KM)
      WRITE (6,106)
106  FORMAT (1H0///2X,5H LAYER,2X,9H THICKNESS,2X,14H COORDINATES OF/3X,3H
      INU.,3X,9H OF LAYERS,2X,14H LAYER SURFACES,3X,11H ORIENTATION,7X,26H CO
      LEFS. OF STIFFNESS MATRIX/9X,8H (INCHES),6X,8H (INCHES),7X,9H (DEGREES
      1),13X,17H (10+6 LB./SQ. IN.)/4X,1HK,6X,4HH(K),6X,4HZ(K),4X,6HZ(K+1)
      1,4X,8H THETA(K),5X,6HC(1,1),4X,6HC(1,2),4X,6H(2,2),4X,6HC(6,6)///)
C
      DO 30 K = 1,N
      KP = K + 1
      30  WRITE (6,107) K,H(K),Z(K),Z(KP),THETA(K),C(1,1,K),C(1,2,K),C(2,2,K),
      1),C(3,3,K)
107  FORMAT (3X,12,2X,F9.4,1X,F9.4,F9.4,2X,F9.2,2X,-6PF10.4,-6PF10.4,-6
      1PF10.4,-6PF10.4)
      WRITE (6,108)
108  FORMAT (1H1///34X,18H ALLOWABLE STRESSES//13X,1HZ,6X,5H AXIAL,7X,5H A
      1XIAL,6X,10H TRANSVERSE,4X,10H TRANSVERSE,5X,5H SHEAR/19X,7H TENSILE,3X
      1,11H COMPRESSIVE,4X,7H TENSILE,5X,11H COMPRESSIVE/11X,4H (IN),5X,5H (KS
      11),7X,5H (KSI),8X,5H (KSI),9X,5H (KSI),8X,5H (KSI)///)
C
      DO 70 K = 1,N
      DO 60 J = 1,2
      IF (J .EQ. 1) GO TO 40
      KP = K + 1
      GO TO 50
40  KP = K
      50  WRITE (6,109) Z(KP),XA(K),XP(K),YA(K),YP(K),S(K)
109  FORMAT (8X,F8.4,2X,-3PF7.2,5X,-3PF7.2,6X,-3PF7.2,7X,-3PF7.2,6X,-3P
      1F7.2)
      60  CONTINUE
      70  CONTINUE
C
C COMPUTATION PHASE
C
      D = 0.0
      I = 1
      DEN = (ASTR22 * DSTR11) + (HSTR12 ** 2)
      C1 = (2.0 * HSTR12) / (DEN * K)
      C2 = 1.0 / (DEN * (K ** 2))
      ALPHA2 = - (C1 / 4.0) + (0.5 * (C2 ** (1.0 / 2.0)))
      BETA2 = ALPHA2 + (C1 / 2.0)
      ALPHA = ALPHA2 ** (1.0 / 2.0)
      BETA = BETA2 ** (1.0 / 2.0)
      C3 = - (ASTR22 * RHO * (K ** 2))
      75  C4 = - (ALPHA * D)
      C5 = ((ALPHA * DPTH) - 1.0) / BETA
      C6 = BETA * D
      W(1) = C3 * (DPTH - D - (EXP(C4) * ((DPTH * COS(C6)) + (C5 * SIN(C
      16))))))
C
C W(1) IS THE RADIAL DEFLECTION AT A DISTANCE D FROM THE BASE OF THE
C TANK

```

```

C7 = (ALPHA2 - BETA2) - (ALPHA * (ALPHA2 + BETA2)*DPTH)
C8 = - (2.0 * ALPHA * BETA) + (BETA * (ALPHA2 + BETA2) * DPTH)
D2W(I) = ((C3 * EXP(C4)) / BETA) * ((C7 * SIN(C6)) + (C8 * COS(C6)
1))

```

C D2W(I) IS THE CURVATURE CHANGE IN THE X DIRECTION AT A DISTANCE D FROM
C THE BASE OF THE TANK

C

```
WRITE (6,111) D,W(I),D2W(I)
```

```
111 FORMAT (1H0//6X,29HDISTANCE FROM BASE OF TANK = ,F6.2,5X,6HINCHES/
170X,17HRAIDIAL DEFLECTION,10X,1H=,F11.6,1X,6HINCHES//6X,19HCHANGE U
1F CURVATURE,8X,5H= ,E13.6/9X,13H(X-DIRECTION)//2X,5HLAYER,25X,15H
1LAYER STRAINS,20X,24HPRINCIPAL LAYER STRESSES,4X,7HFAILURE/3X,3HND
1.,28X,9H(PERCENT),25X,17H(10+3 LB./SQ.IN.),7X,8HCRITERIA//4X,1HK,5
1X,4HEPSX,5X,4HEPSY,5X,5HGAMXY,4X,4HEPS1,5X,4HEPS2,5X,5HGAM12,6X,2H
1S1,9X,2HS2,7X,3HS12//)
```

C

```

DO 150 K = 1,N
RTHETA = (.1415927 * THETA(K)) / 160.0
RM = COS(RTHETA)
KN = SIN(RTHETA)
TM(1,1) = RM * RM
TM(1,2) = RN * KN
TM(1,3) = RM * RN
TM(2,1) = TM(1,2)
TM(2,2) = TM(1,1)
TM(2,3) = - TM(1,3)
TM(3,1) = - (2.0 * TM(1,3))
TM(3,2) = - TM(3,1)
TM(3,3) = TM(1,1) - TM(1,2)
DO 140 J = 1,2
IF (J .EQ. 1) GO TO 80
KP = K + 1
GO TO 90

```

```
80 KP = K
```

```

90 EX = - ((ASTR12 / (ASTR22 * K)) * W(I)) - ((BSTR11 + ((ASTR12 * HS
1TR12) / ASTR22) + Z(KP)) * D2W(I))
EY = - (W(I) / R)
EXY = - ((ASTR26 / (ASTR22 * K)) * W(I)) - ((BSTR61 + ((ASTR26 * H
1STR12) / ASTR22)) * D2W(I))

```

C EX,EY AND EXY ARE THE LAYER STRAIN COMPONENTS IN THE STRUCTURE CO-
C ORDINATE SYSTEM

```

E1 = (TM(1,1) * EX) + (TM(1,2) * EY) + (TM(1,3) * EXY)
E2 = (TM(2,1) * EX) + (TM(2,2) * EY) + (TM(2,3) * EXY)
E12 = (TM(3,1) * EX) + (TM(3,2) * EY) + (TM(3,3) * EXY)
S1 = (C(1,1,K) * E1) + (C(1,2,K) * E2)
S2 = (C(1,2,K) * E1) + (C(2,2,K) * E2)
S12 = C(3,3,K) * E12

```

C E1,E2 AND E12 ARE THE LAYER STRAIN COMPONENTS TRANSFORMED TO THE
C PRINCIPAL CO-ORDINATE SYSTEM OF THE MATERIAL IN THE KTH LAYER

C

C S1,S2 AND S12 ARE THE CORRESPONDING STRESSES,

```

IF (S1 .GE. 0.0) GO TO 100
S1AL = XP(K)

```

```

GO TO 110
100 S1AL = XA(K)
110 IF (S2 .GT. 0.0) GO TO 120
    S2AL = YP(K)
    GO TO 130
120 S2AL = YA(K)
130 S12AL = S(K)
    FC = ((S1 / S1AL) ** 2) - ((S2AL / S1AL) * (S1 / S1AL) * (S2 / S2AL)) + ((S2 / S2AL) ** 2) + ((S12 / S12AL) ** 2)
C FC IS THE DISTORTIONAL ENERGY FAILURE CRITERION VALUE
C IF FC IS LESS THAN 1, THE LAYER IS CAPABLE OF WITHSTANDING THE LOAD
C IF FC IS GREATER THAN OR EQUAL TO 1, THE LAYER HAS FAILED
C
    WRITE (6,112) K,EX,EY,EXY,E1,E2,E12,S1,S2,S12,FC
112 FORMAT (3X,I2,1X,2PF9.3,2PF9.3,2PF9.3,2PF9.3,2PF9.3,2PF9.3,-3PF10.
12,-3PF10.2,-3PF10.2,0PF9.3)
140 CONTINUE
150 CONTINUE
    IF (D .GT. 2.75) GO TO 152
    IF (D .GT. 0.19) GO TO 151
    D = D + 0.0625
    GO TO 160
151 D = D + 0.25
    GO TO 160
152 D = D + 5.0
160 IF (D .GT. DPTH) GO TO 161
    I = I + 1
    GO TO 75
161 CONTINUE
    STOP
    END

```

REFERENCES

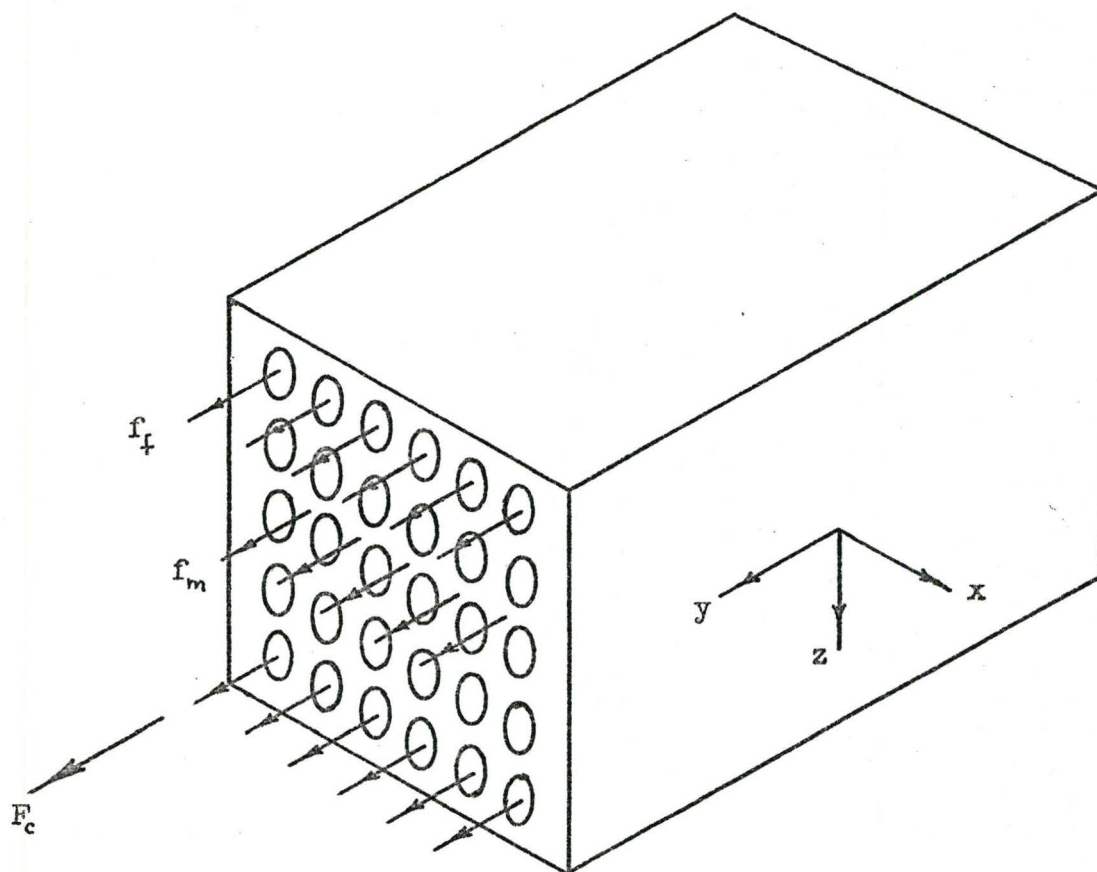
1. O'Connell, K.J., Structural Analysis of Gun-Launched Vehicles for H.A.R.P., Internal Report, Space Research Institute of McGill University, Montreal (1966).
2. Krock, R.H. and L.J.Broutman, "Principles of Composites and Composite Reinforcement", Chapter 1 in Modern Composite Materials, L.J. Broutman and R.H. Krock, editors, Addison-Wesley Publishing Company, Reading, Massachusetts, 7 (1967).
3. Maine, F.W., B.E. Riseborough and J.E. Theberge, "Some Theoretical Aspects of Fibre Reinforced Thermoplastics", Polymer Structures and Properties, Regional Technical Conference, Society of Plastics Engineers, Inc., Toronto, March 18, 1970.
4. Modern Plastics Encyclopaedia 1969-70, S. Gross, editor-in-chief, Vol. 46: 10-A, McGraw-Hill, Inc., New York (1969)
5. Broutman, L.J., "Fiber-Reinforced Plastics", Chapter 13 in Modern Composite Materials, L.J.Broutman and R.H. Krock, editors, Addison-Wesley Publishing Company, Reading, Massachusetts, 346 (1967).
6. Broutman, L.J., "Mechanical Behaviour of Fiber-Reinforced Plastics", Chapter 6 in Composite Engineering Laminates, A.G.H. Dietz, editor, The M.I.T. Press, Cambridge, Massachusetts, 127 (1969).
7. Kelly, A. and G.J. Davies, "The Principles of the Fiber Reinforcement of Metals", Metallurgical Reviews, 10, 37 (1965). (see reference (1) p.18)
8. McDanel, D.L., R.W. Jack and J.W. Weeton, "Stress-Strain Behaviour of Tungsten-Fiber-Reinforced Composites", National Aeronautics and Space Administration, NASA TN D-1881, October, 1963 (see Sutton, W.H., "Fiber-Reinforced Metals" Chapter 14 in Modern Composite Materials, L.J. Broutman and R.H. Krock, editors, Addison-Wesley Publishing Company, Reading, Massachusetts, 424 (1967).

9. Kelly, A., and N.R. Tyson, J. Mech. Phys. Solids, 13, 329, 1965 (See reference (3) p. 3).
10. Barton, R.S., R.B. Baldwin and J. Henshaw, "Avco 3-D Composites - A Tailored Materials Concept", Proc. 24th Annual Conf. SPI Reinforced Plastics/Composites Division, Section 18-B (1969).
11. Tsai, S.W. and D.F. Adams, "A Mechanics Analysis of Fiber-Reinforced Composites", Proc. 21st Conf. SPI Reinforced Plastics Division, Section 5-A (1966).
12. Fibreglass Limited, Reinforcements Division, Valley Road, Birkenhead, England, "FRP Design Data" (1968).
13. Fiberglas Canada Ltd., 48 St. Clair Ave. W., Toronto, "Fiberglas Reinforced Plastics", Book 2 (1970).
14. Owens-Corning Fiberglas Corp., Industrial Materials Division, Toledo, Ohio, "Fiberglas-Reinforced Plastics" (1969).
15. Seely, F.B. and J.O. Smith, Advanced Mechanics of Materials, Second Edition, John Wiley & Sons, Inc., New York, 10 (1959).
16. Popov, E.P., Mechanics of Materials, Prentice-Hall, Inc., Englewood Cliffs, N.J., 113-117 (1958).
17. Forrest, M.G. et al, Gibbs & Cox, Inc., Marine Design Manual for Fiberglass Reinforced Plastics, McGraw-Hill Book Company, Inc., 6-56 (1960).
18. Rosato, D.V., "History of Composites", Chapter 1 in Handbook of Fiberglass and Advanced Plastic Composites. G. Lubin, editor, Van Nostrand Reinhold Company, New York, 16 (1969).
19. Shibley, A.M., "Filament Winding", Chapter 18 in Handbook of Fiberglass and Advanced Plastics Composites, G. Lubin, editor, Van Nostrand Reinhold Company, New York, 462 (1961).
20. Rosato, D.V. and C.S. Grove, Jr., Filament Winding, Interscience Publishers, New York, 195 (1964).
21. Fischer, L., "Design of Glass-Reinforced Plastic Structures", Proc. 15th Ann. Meeting SPI Reinforced Plastics Division, Section 3-D (1960).

22. Faupel, J.H., Engineering Design, John Wiley & Sons, Inc., 278-285 (1964).
23. Plastics for Flight Vehicles, Part 1, Reinforced Plastics, MIL-HDBK-17, U.S. Government Printing Office, Washington, D.C. (1959).
24. Erickson, E.C.O., and C.B. Norris, "Tensile Properties of Glass-Fabric Laminates with Laminations Oriented in Any Way", Proc. 11th Ann. Meeting SPI Reinforced Plastics Division, Section 9-A (1956)
25. Rosen, B.W., "A Note on the Failure Modes of Filament Reinforced Materials", Proc. 19th Ann. Meeting SPI Reinforced Plastics Division, Section 6-A (1964).
26. Shaffer, B.W., "The Influence of Filament Orientation on the Material Properties of Reinforced Plastics", Proc. 19th Ann. Meeting SPI Reinforced Plastics Division, Section 6-E (1964).
27. Hearmon, R.F.S., An Introduction to Applied Anisotropic Elasticity, Oxford University Press, 3-16 (1961).
28. Lessells, J.M., and G.S. Cherniak, "Strength of Materials", Section 8 in Kent's Mechanical Engineer's Handbook, C. Carmichael, editor, Twelfth Edition, John Wiley & Sons, Inc., New York, 8-03 (1956).
29. Boresi, A.P., Elasticity in Engineering Mechanics, Prentice-Hall, Inc., Englewood Cliffs, New Jersey, 43 (1965).
30. Hill, R., "A Theory of the Yielding and Plastic Flow of Anisotropic Metals", Proceedings of the Royal Society, Series A, Vol. 193, 281-297 (1948) (see reference (31) p. 5).
31. Tsai, S.W., "Strength Characteristics of Composite Materials", National Aeronautics and Space Administration, Washington, D.C., NASA CR-224 (1965).
32. Grinius, V.G. and J.V. Noyes, "Design of Composite Materials", Chapter 23 in Handbook of Fiberglass and Advanced Plastic Composites, G. Lubin, Editor, Van Nostrand Reinhold Company, New York, 623 (1969).
33. Norris, C.B., "Strength of Orthotropic Materials Subjected to Combined Stress", Forest Products Report 1816 (1962) (see reference (31) p. 6).

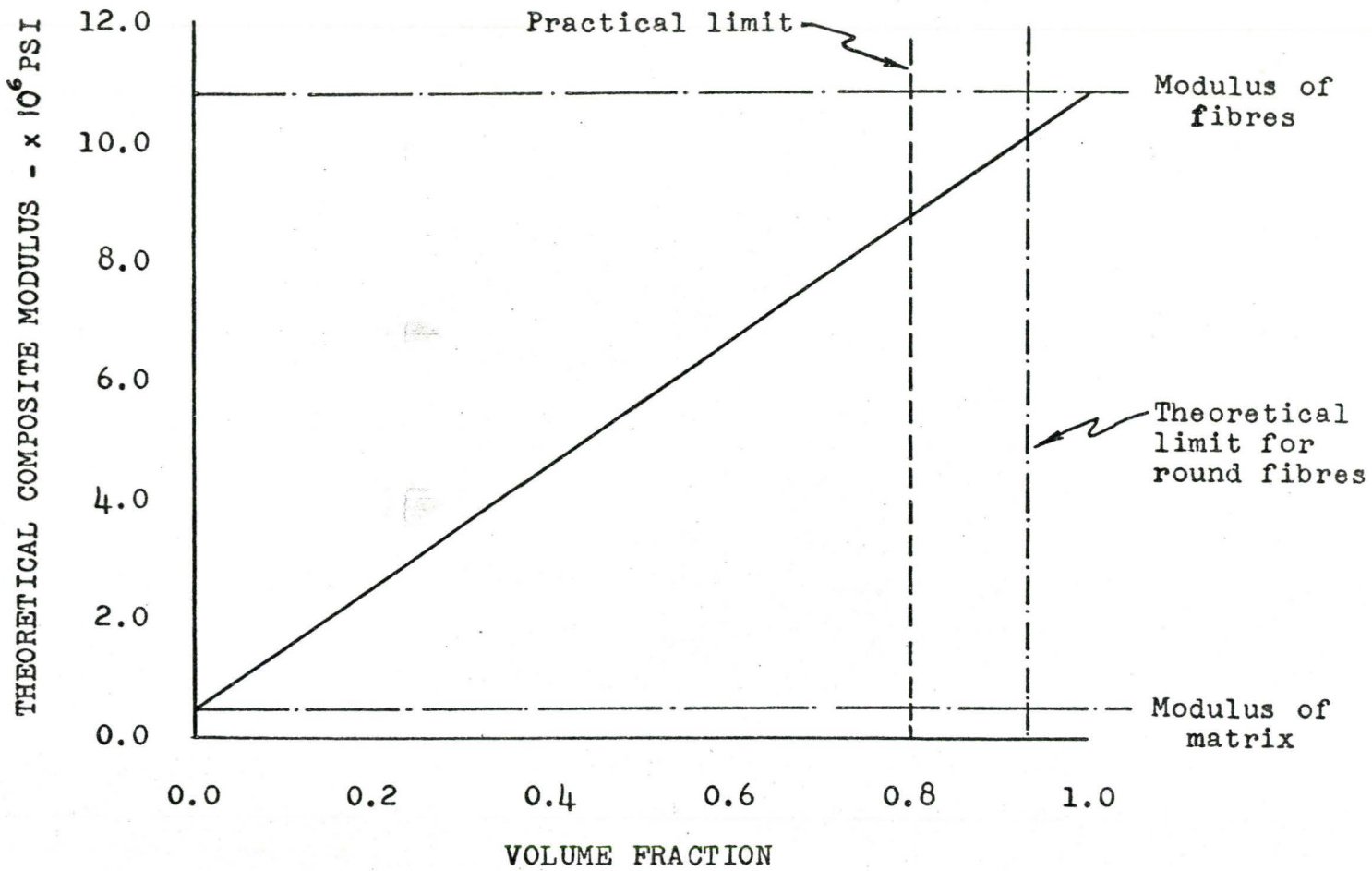
34. Stowell, E.Z. and T.S. Liu, "On the Mechanical Behaviour of Fiber Reinforced Crystalline Material", J. Mech. Phys. Solids 9, 242-260 (1961) (see reference (32) p. 621).
35. Ashton, J.E., J.C. Halpin and P.H. Petit, Primer on Composite Materials: Analysis, Technomic Publishing Co., Inc., Stamford, Connecticut, 26-29 (1969).
36. Chamis, C.C. and G.P. Sendeckyj, "Critique on Theories Predicting Thermoelastic Properties of Fibrous Composites", J. Of Comp. Mat., 2, 3, 332-358 (1968).
37. Tsai, S.W., D.F. Adams and D.R. Doner, "Analyses of Composite Structures", National Aeronautics and Space Administration, NASA CR-620 (1966).
38. Chen, C.H. and S. Cheng, "Mechanical Properties of Fiber Reinforced Composites", J. of Comp. Mat., 1, 1, 30-41 (1967).
39. Foye, R.L., Lecture Notes for the Composite Materials Workshop, University of Toronto, November 3-7, 1969.
40. Composite Materials: Testing and Design, Proc. of ASTM Symp., New Orleans, Feb. 11-13, 1969, STP-460, American Society for Testing and Materials, Philadelphia (1969).
41. Grimes, G.C. and M.E. Bronstand, "Test Methods for Composites", Chapter 26 in Handbook of Fiberglass and Advanced Plastic Composites, G.Lubin, editor, Van Nostrand Reinhold Company, New York (1969).
42. Waddoups, M.E., "Characterization and Design of Composite Materials" from Composite Materials Workshop, S.W. Tsai, J.C. Halpin and N.J. Pagano, editors, Technomic Publishing Co., Inc., Stamford, Conn. (1968).
43. Chin, K.D., "Ultimate Strengths of Laminated Composites", J. of Comp. Mat., 3, 3, 578-582 (1969).
44. Timoshenko, S. and S. Woinowsky-Krieger, Theory of Plates and Shells, Second Edition, McGraw-Hill Book Company, Inc., New York, 466-532 (1969).
45. Spiegel, M.R., Applied Differential Equations, Prentice-Hall, Inc., Englewood Cliffs, N.J., 153-156 (1958).

46. Noyes, J.V. and B.H. Jones, "Analytical Design Procedures for the Strength and Elastic Properties of Multilayer Fibrous Composites", AIAA/ASME 9th Structures, Structural Dynamics and Materials Conference, Paper No. 68-336 (1968) (see reference (43) p. 579).



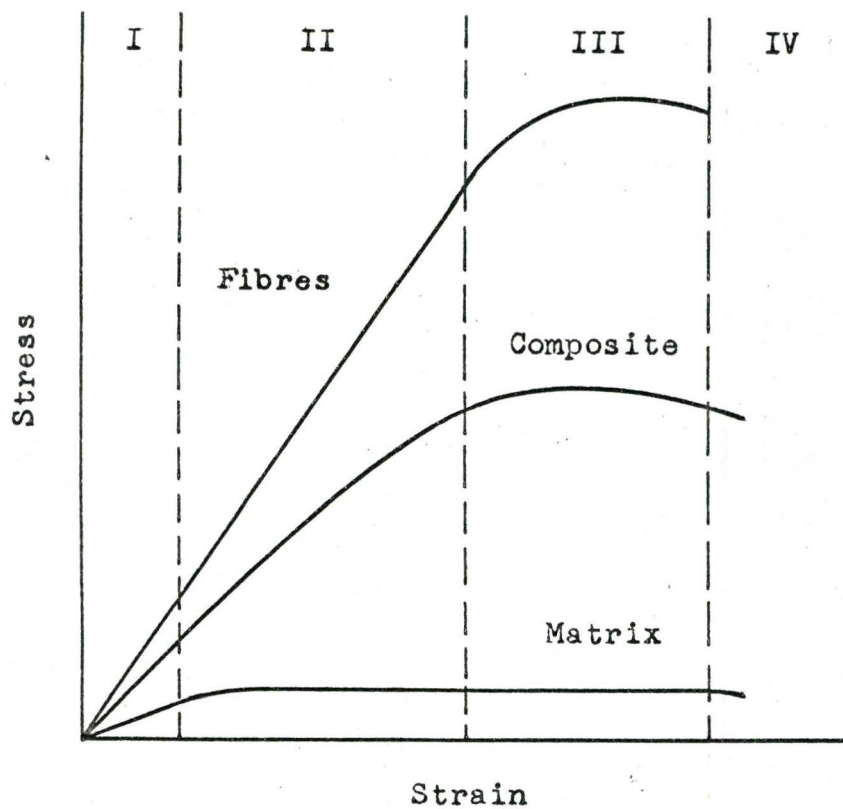
MODEL OF CONTINUOUS FIBER COMPOSITE

FIGURE 1.1



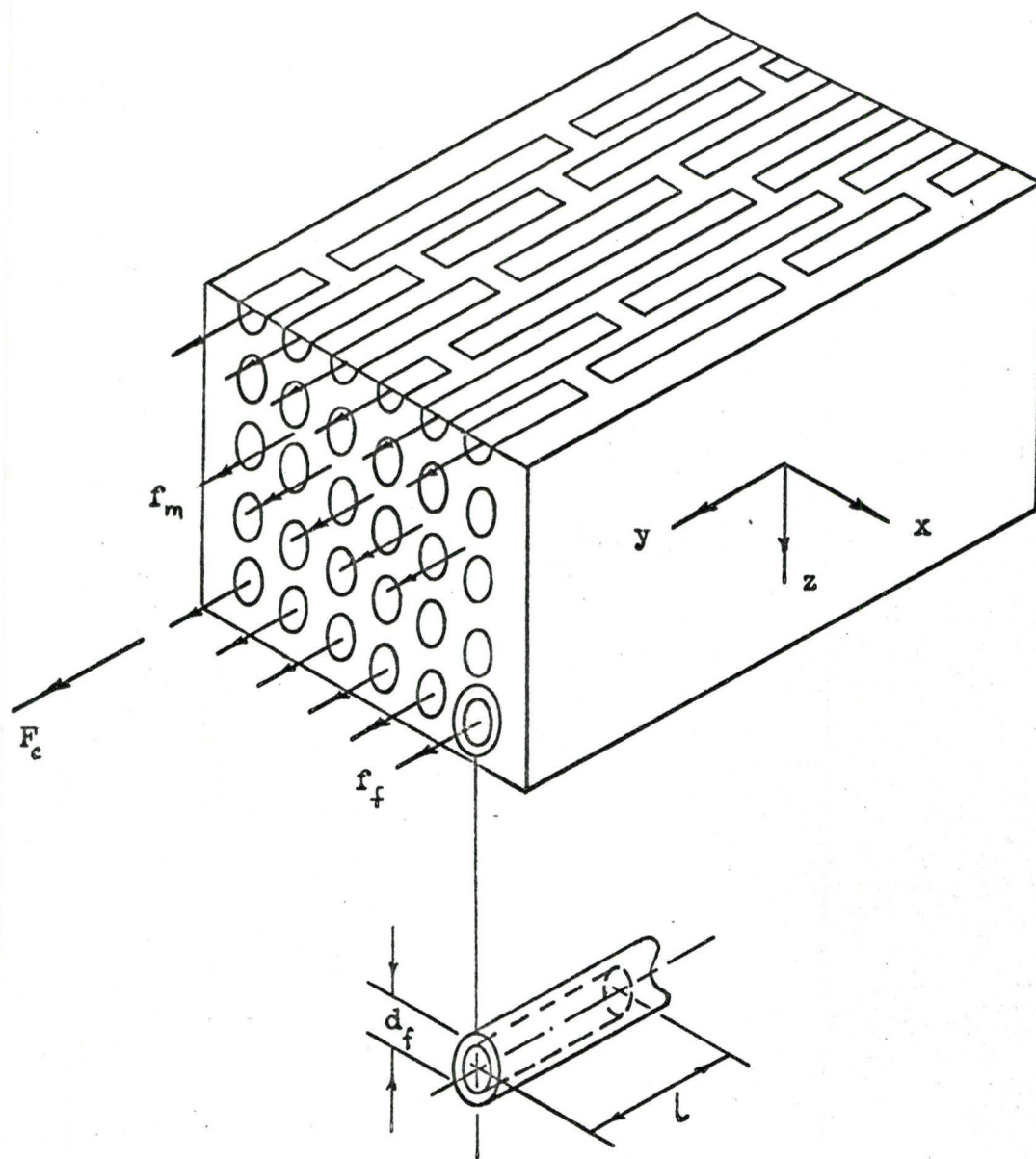
THEORETICAL VARIATION OF COMPOSITE MODULUS
WITH VOLUME FRACTION OF FIBRES

FIGURE 1.2



TYPICAL COMPOSITE STRESS - STRAIN BEHAVIOUR

FIGURE 1.3



MODEL OF DISCONTINUOUS FIBRE COMPOSITE

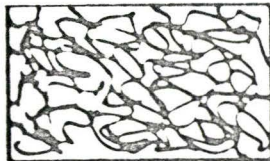
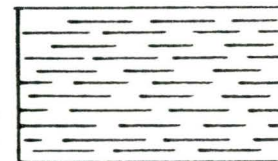
FIGURE 1.4

CONTINUOUS

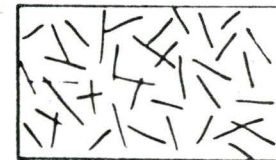
DISCONTINUOUS



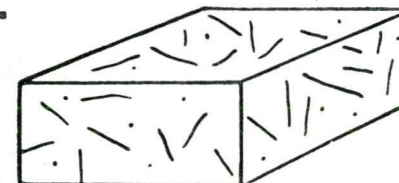
ONE DIMENSIONAL



TWO DIMENSIONAL



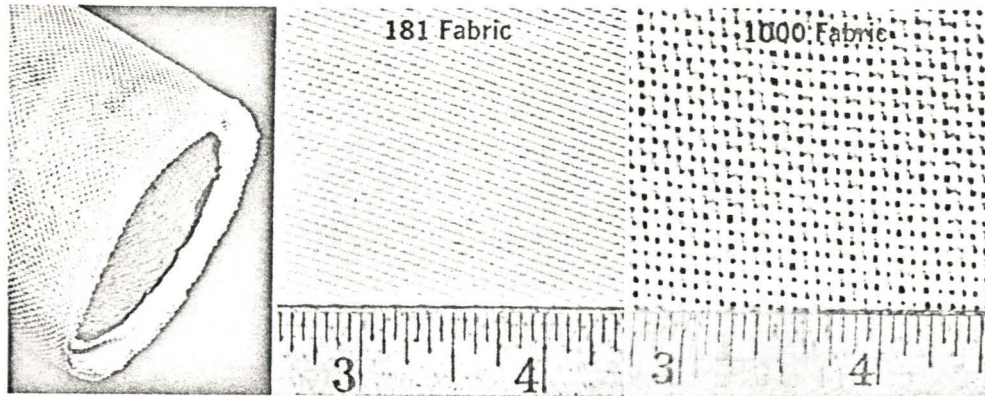
THREE DIMENSIONAL



FIBRE ORIENTATION (3)

FIGURE 1.5

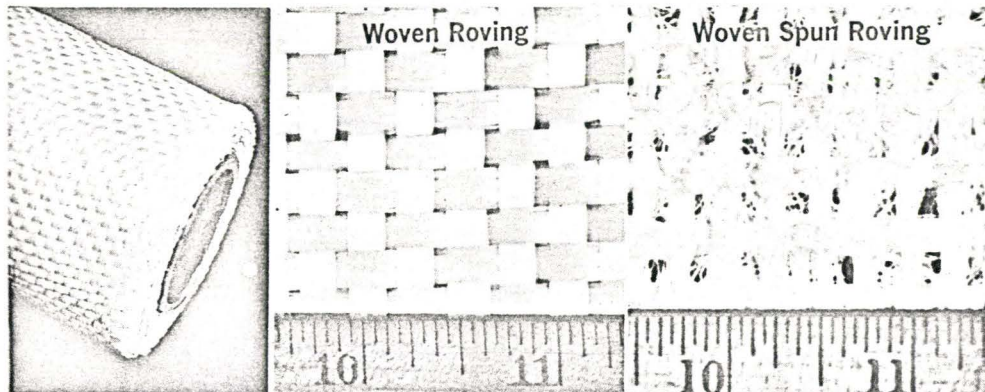
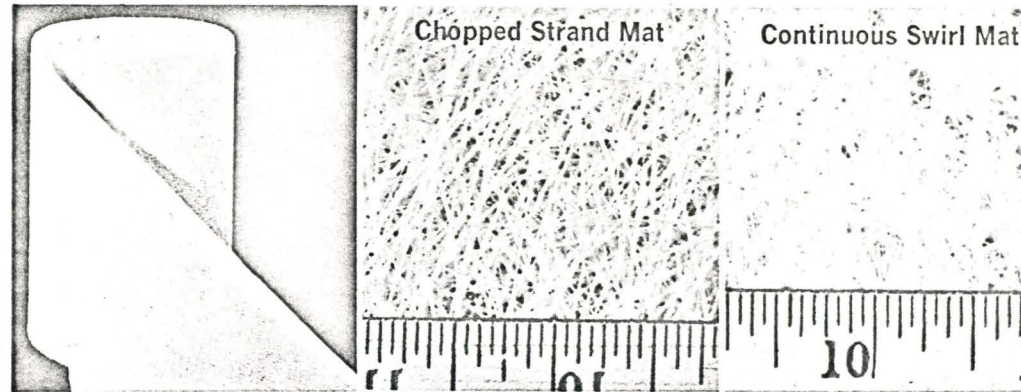
Fabric



Fabrics are woven from yarns of various twist and ply construction into a wide range of types, weights and widths. Fabrics are selected by a number of factors, but primarily thickness and weight. Weights vary from 2½ to 40 ounces a square yard. Thickness of fabrics varies from .003 inches to .045 inches. These same yarns are also fabricated into non-woven fabrics similar to cloth. Both materials come close to duplicating strength properties achieved in the use of continuous parallel strands. Maximum glass content is from 65 to 75 per cent.

Reinforcing Mats

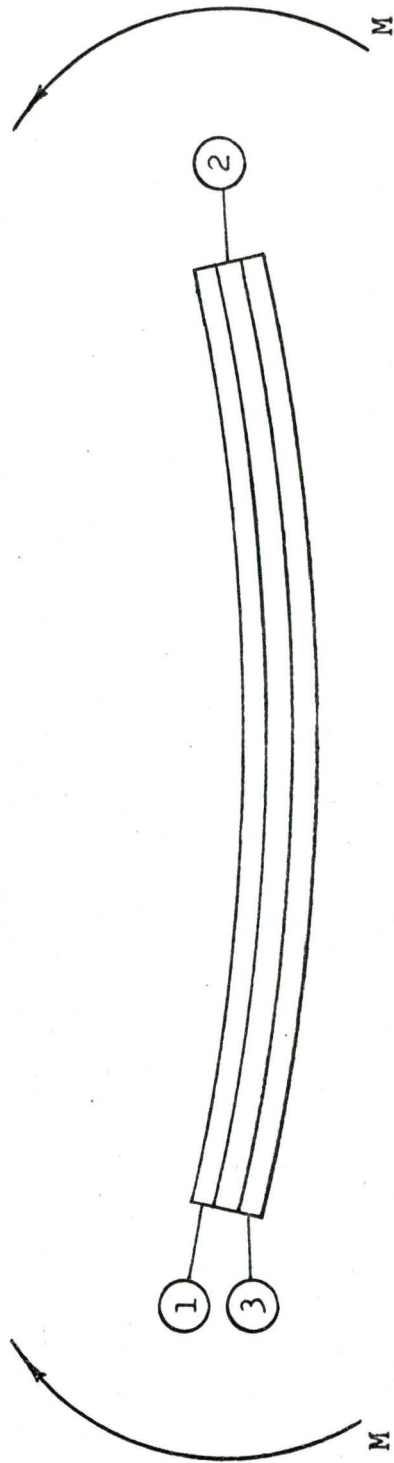
Reinforcing mats are made of either chopped strands or continuous swirl strands laid down in a random pattern. Strands are held together by adhesive resinous binders. While lower in cost than woven materials, mats are slightly more expensive than bulk chopped strands or roving. Chopped and continuous swirl strand mat weight varies from ¼ to 3 ounces per square foot. Reinforcing mats are used for medium strength parts with uniform cross section.



Woven Rovings

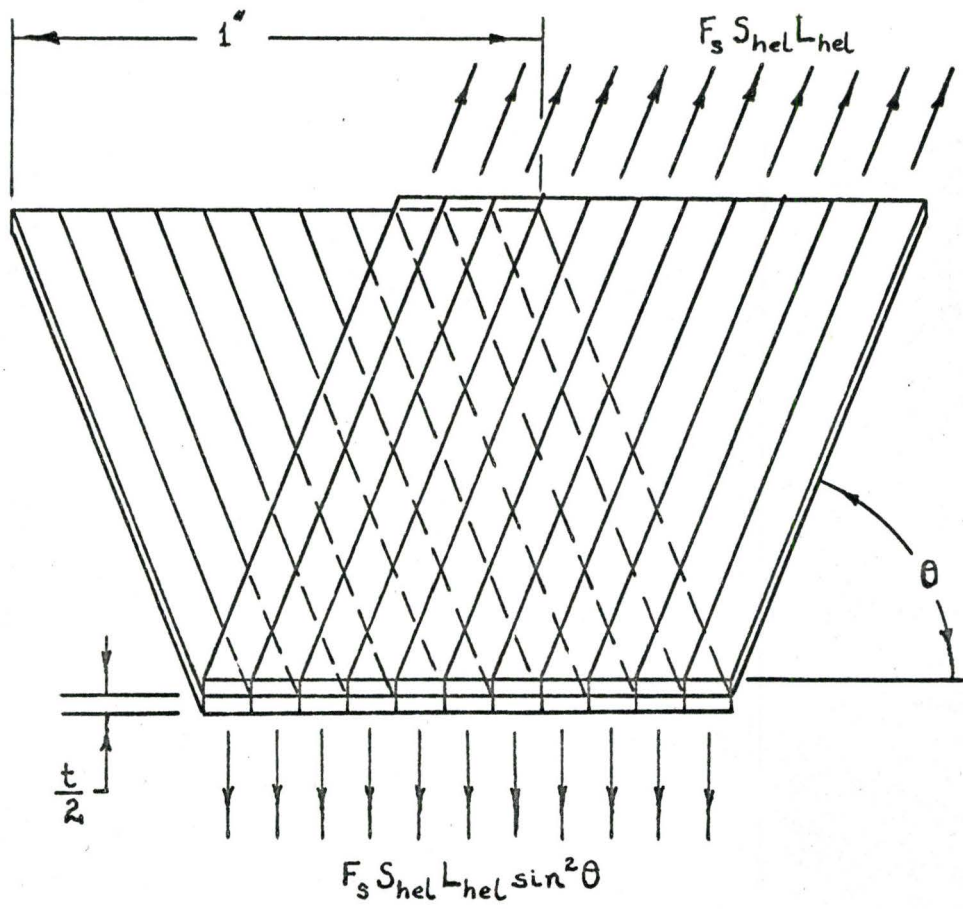
Continuous or spun rovings are woven into coarse, heavy drapeable fabrics called "woven roving". They give high strengths to a part and are lower in cost than conventional fabrics. Weight of woven roving varies from 15 to 27 ounces a square yard. Thickness varies from 0.035 to 0.048 inches. Woven roving is used mainly in the manufacture of large structural objects such as boats and swimming pools. It is also employed to make heavy-duty plastic tooling for the metal-stamping industry. A newer form of woven roving, called "woven spun roving", produces laminates with superior inter-laminar shear strength. In addition, woven spun roving improves adhesion to other materials, and the drapeability of the reinforcement.

FIGURE 1.6



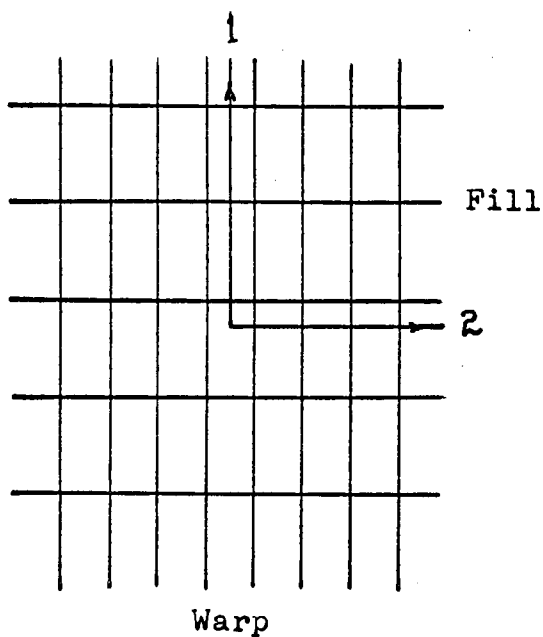
TYPICAL LAMINATE IN BENDING

FIGURE 2.1

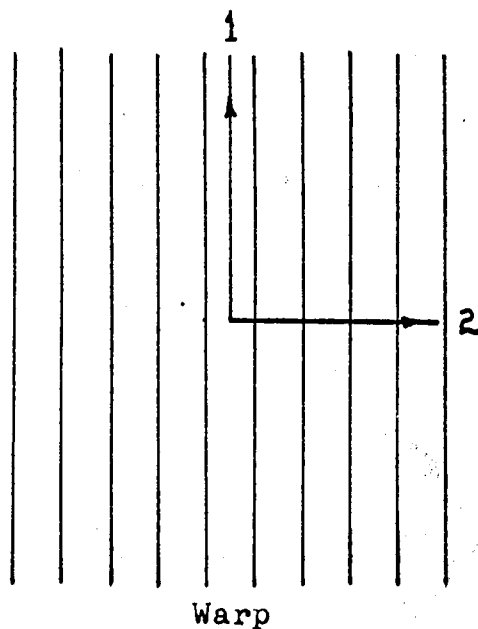


NETTING ANALYSIS LOAD DIAGRAM (20)

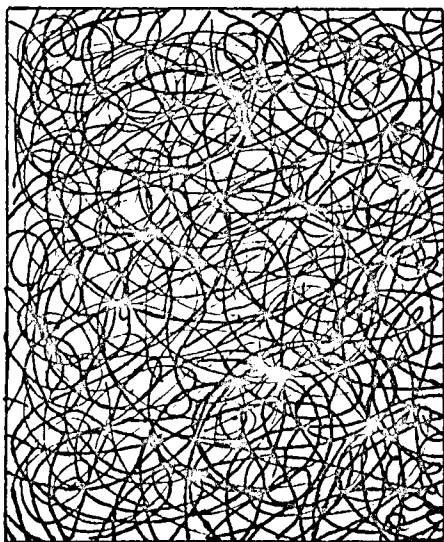
FIGURE 2.2



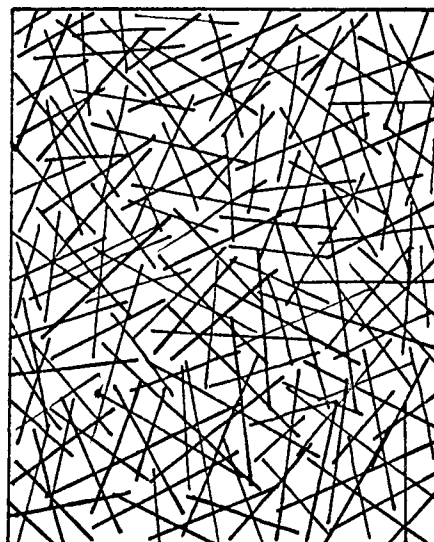
(a) Cross-plyed or woven materials



(b) Unidirectional reinforcement



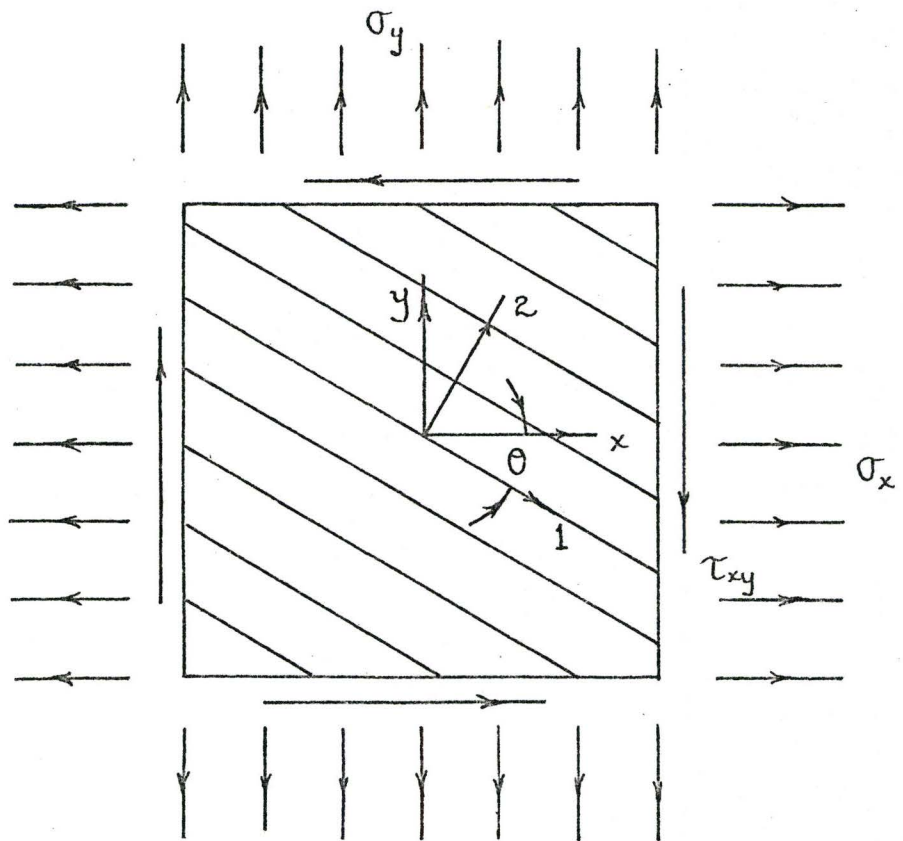
(c) Continuous strand mat



(d) Chopped strand mat

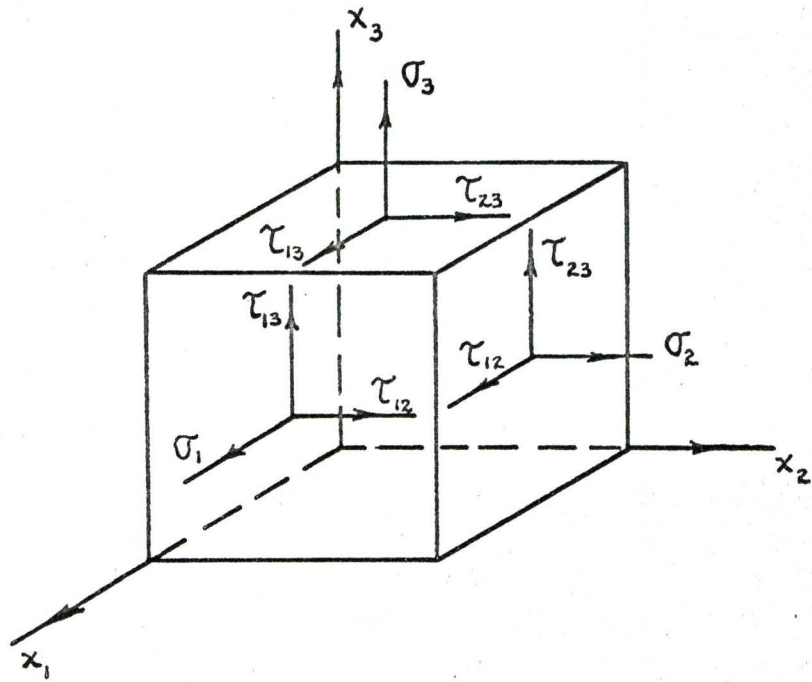
COMMON FORMS OF REINFORCEMENT

FIGURE 2.3



OFF-AXIS LOADING
OF AN ORTHOTROPIC LAYER

FIGURE 2.4



STRESSES ACTING ON A CUBIC ELEMENT

FIGURE 3.1

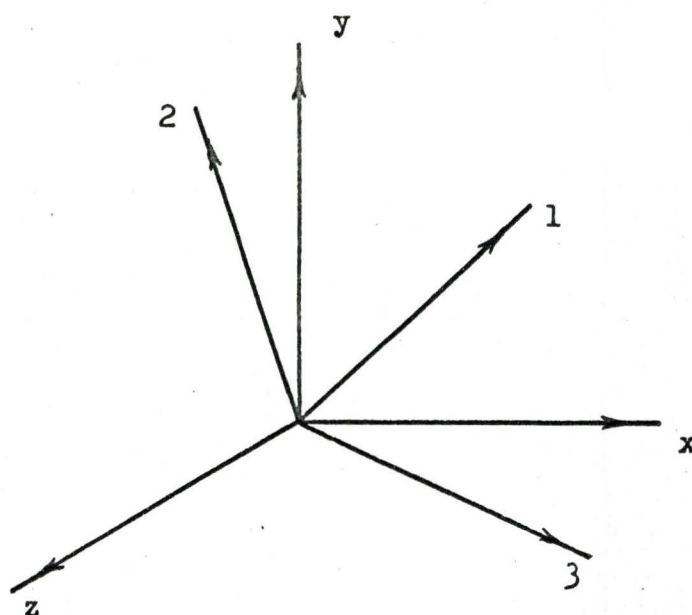


Table of Direction Cosines

	1	2	3
x	l_1	m_1	n_1
y	l_2	m_2	n_2
z	l_3	m_3	n_3

TRANSFORMATION OF STRESS COMPONENTS (29)

FIGURE 3.2

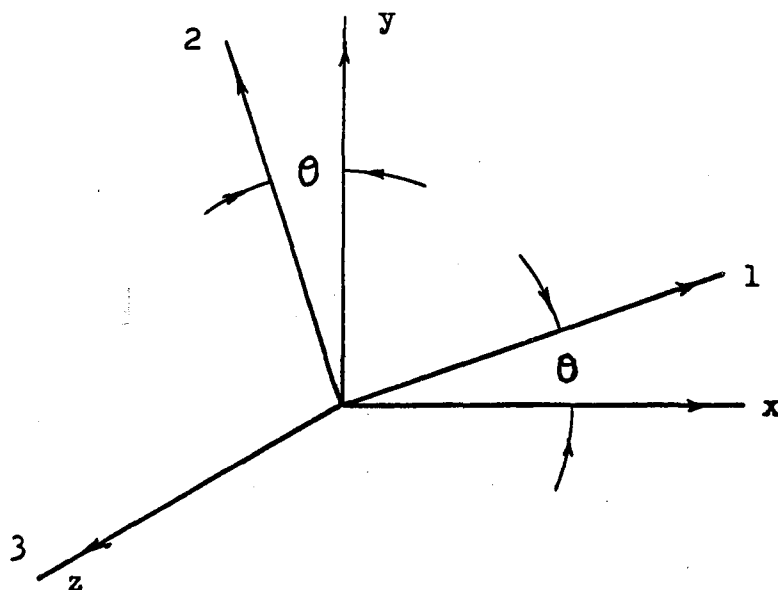
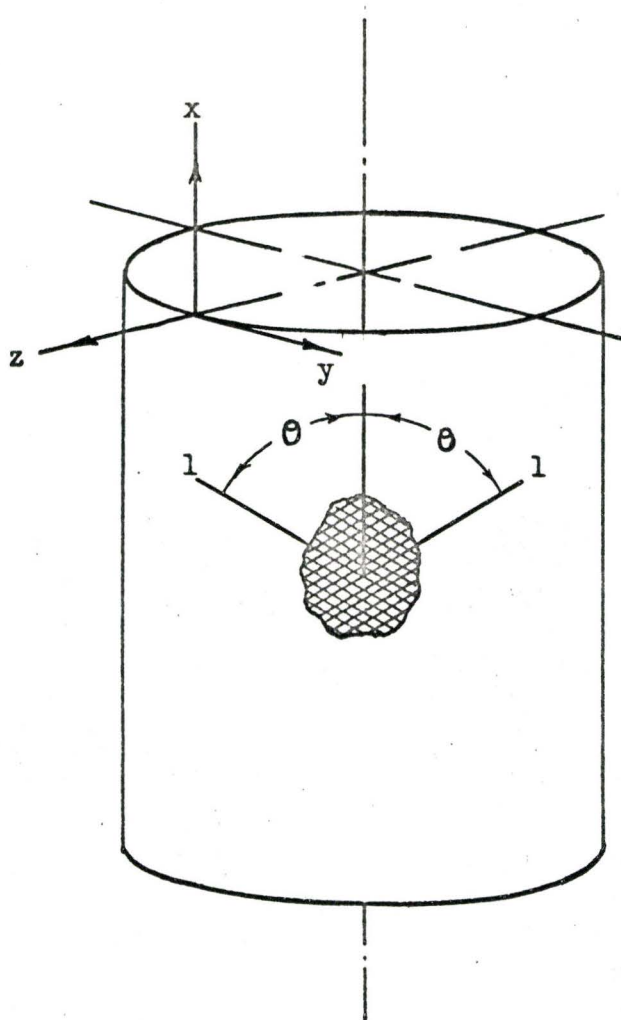


Table of Direction Cosines

	1	2	3
x	$\cos\theta$	$\sin\theta$	0
y	$-\sin\theta$	$\cos\theta$	0
z	0	0	1

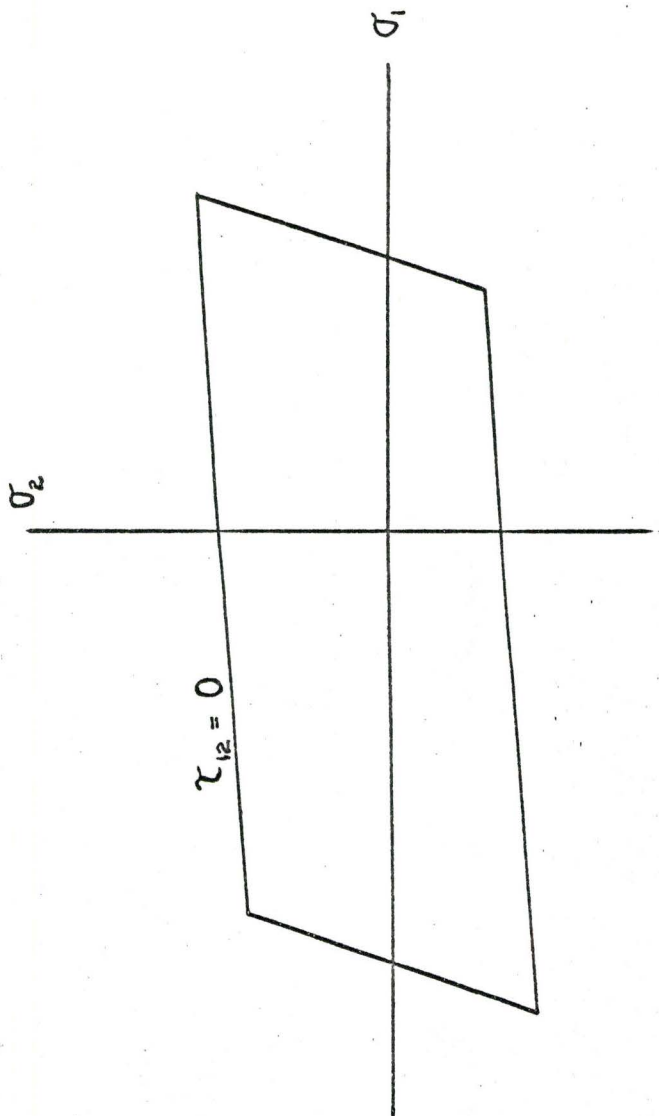
TRANSFORMATION OF STRESSES
IN THE CASE OF PLANE STRESS

FIGURE 3.3



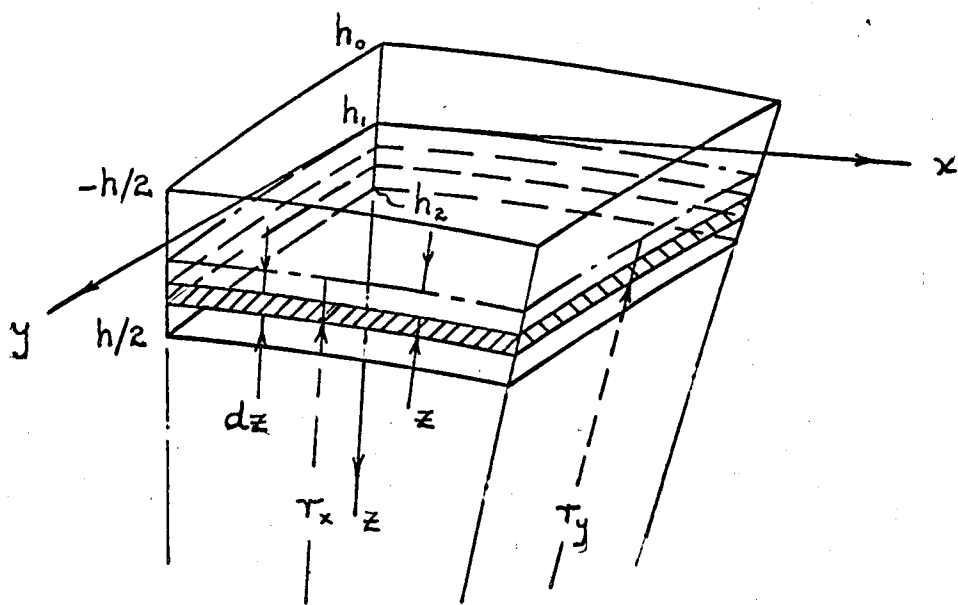
FILAMENT WOUND CYLINDER

FIGURE 3.4



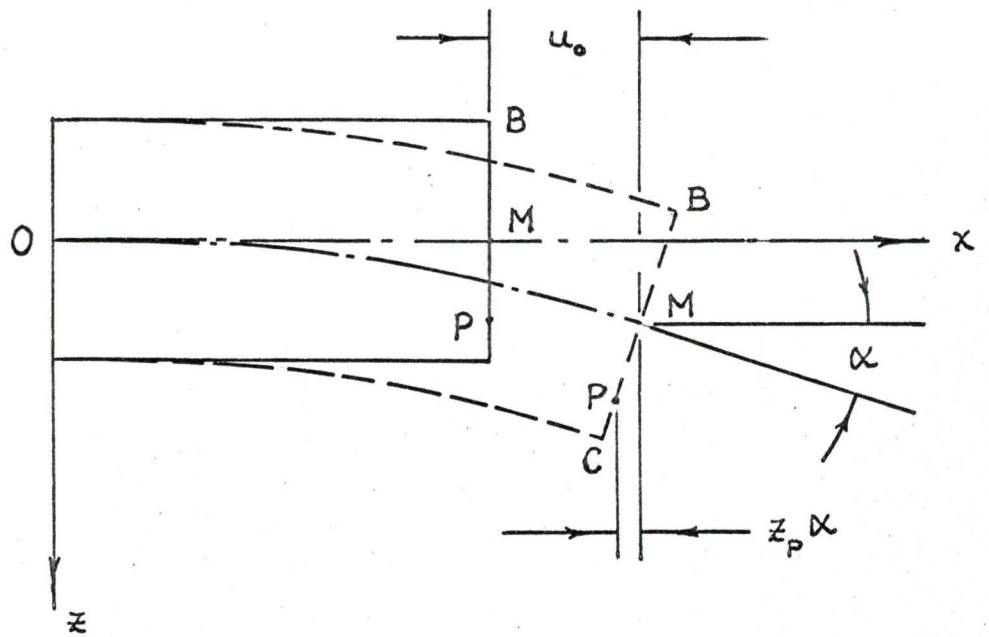
FAILURE SURFACE (35)

FIGURE 3.5



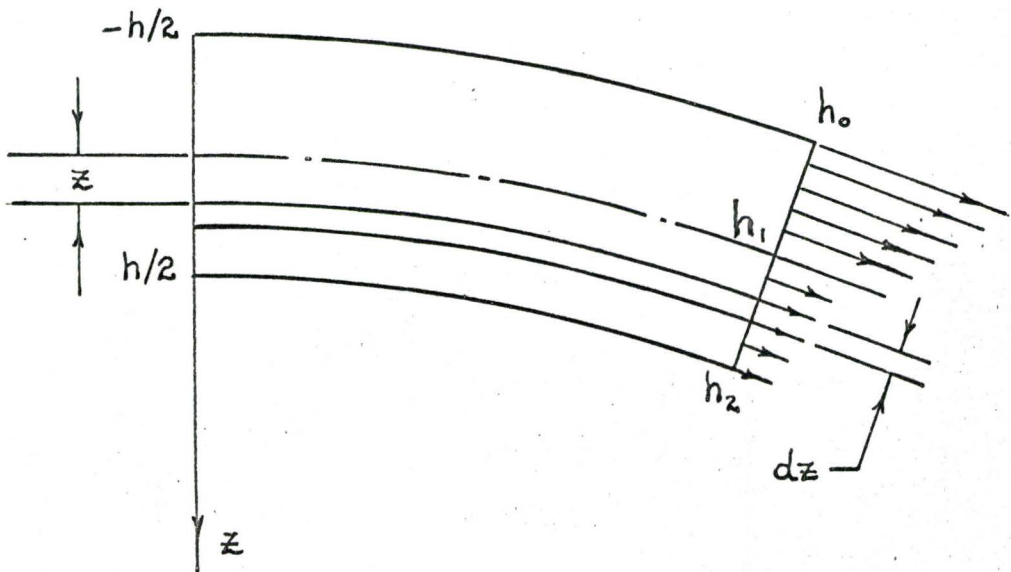
ELEMENT OF A DEFORMED
TWO LAYER LAMINATE

FIGURE 4.1



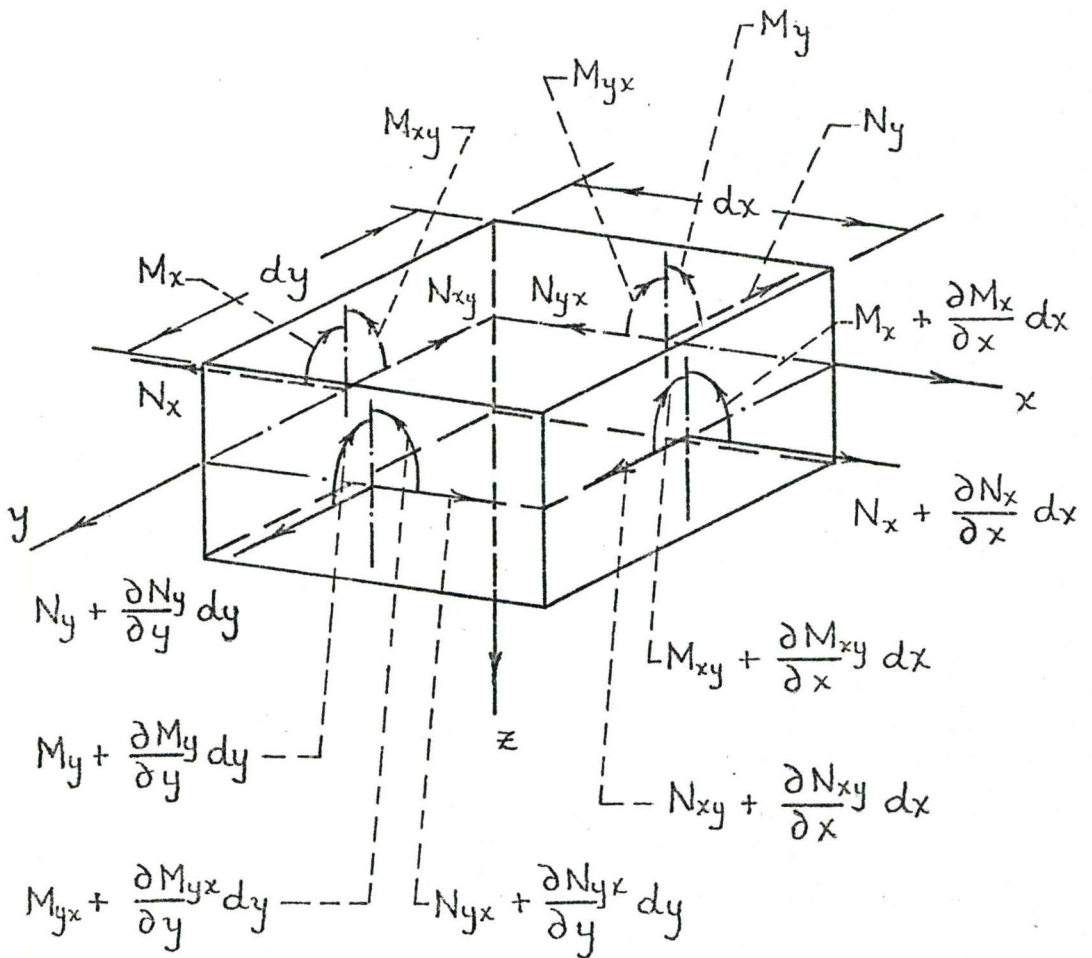
DEFORMATION IN THE X-Z PLANE

FIGURE 4.2



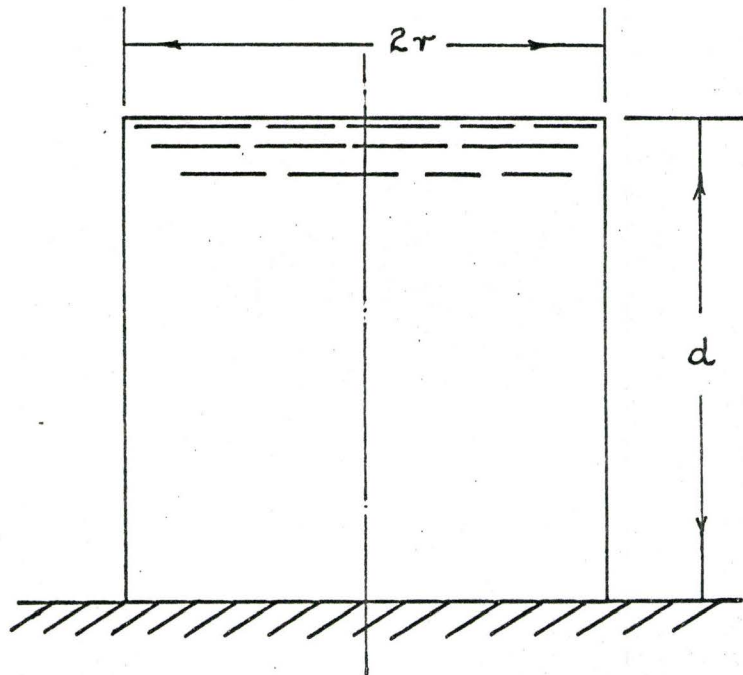
STRESS DISTRIBUTION
IN A DEFORMED LAMINATE

FIGURE 4.3



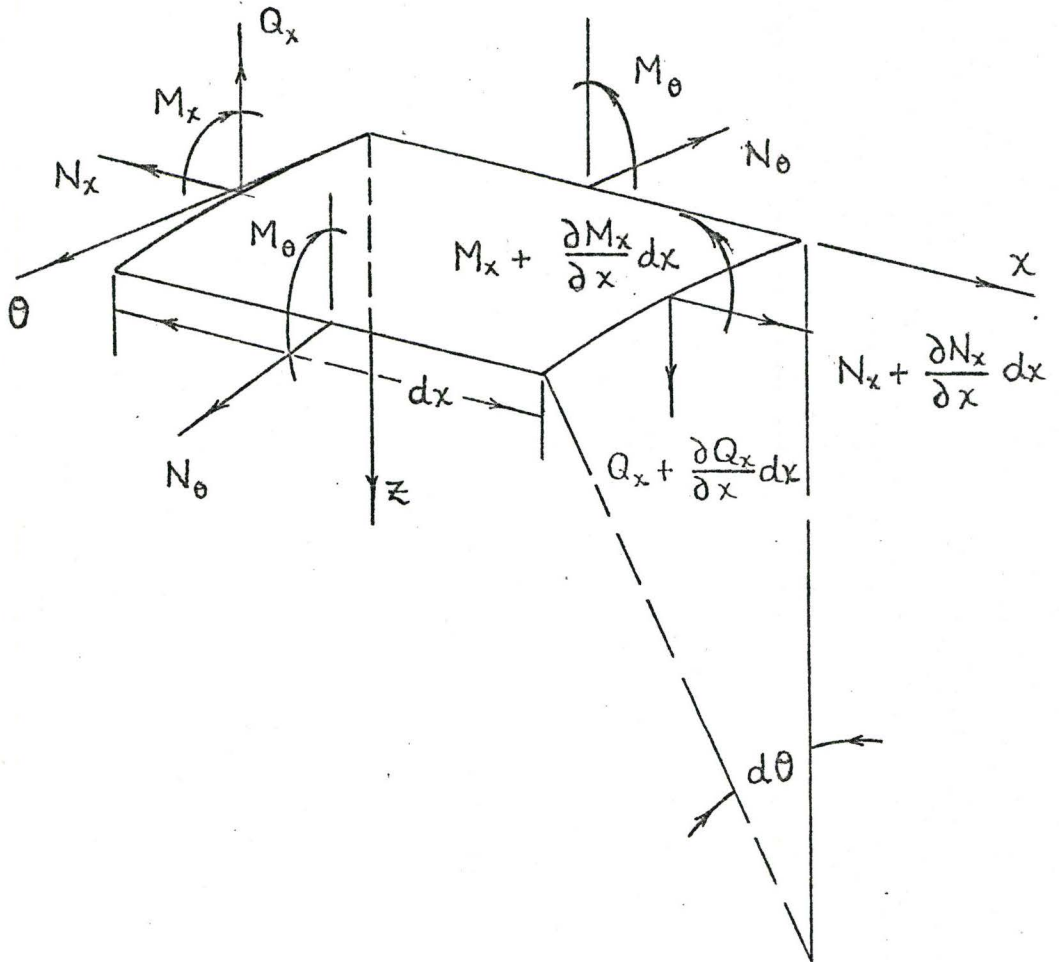
FORCE AND MOMENT RESULTANTS
ACTING AT THE GEOMETRIC MIDPLANE

FIGURE 4.4



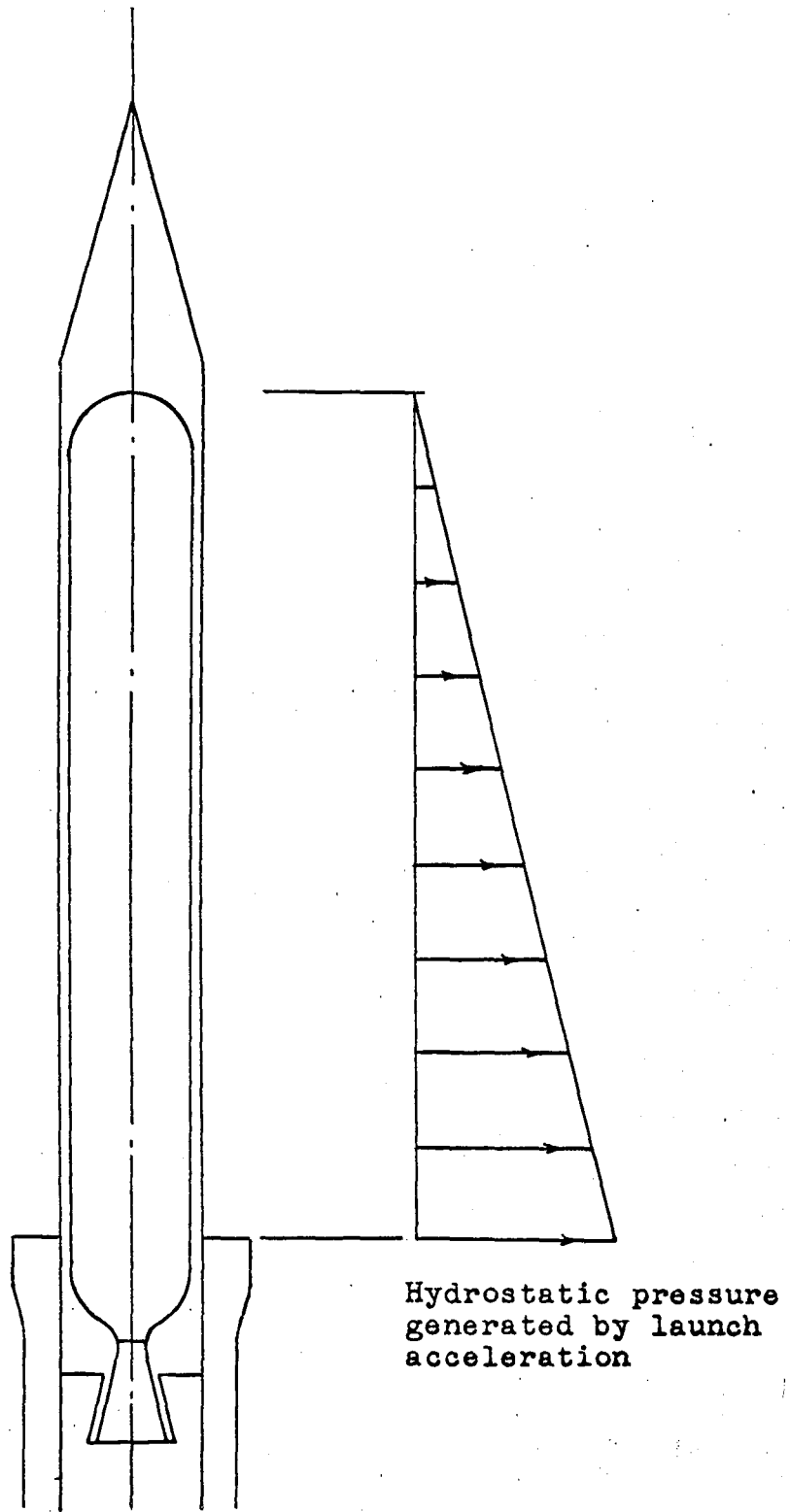
CYLINDRICAL STORAGE TANK

FIGURE 5.1



LOADS ACTING ON AN ELEMENT OF A SHELL

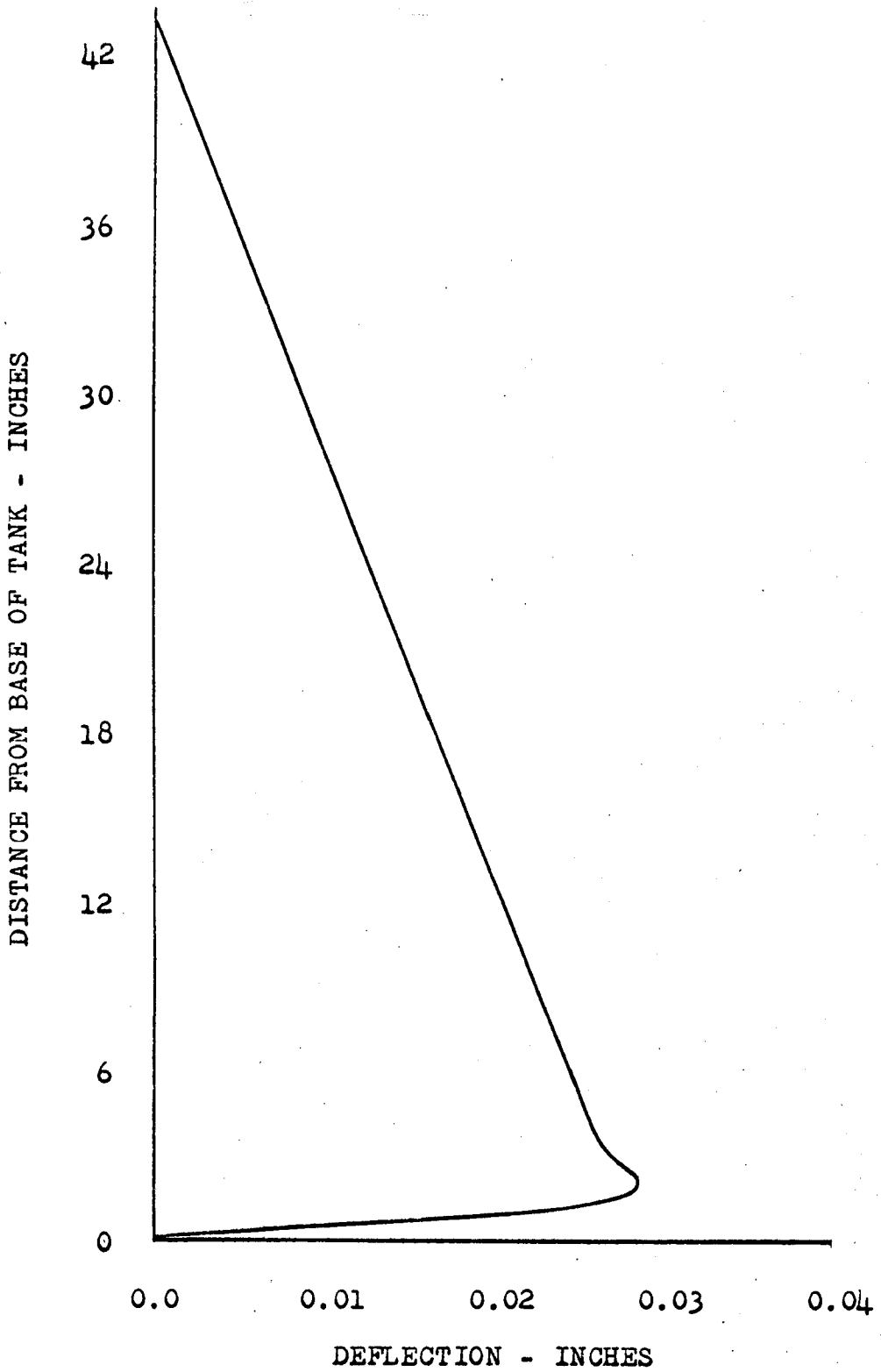
FIGURE 5.2

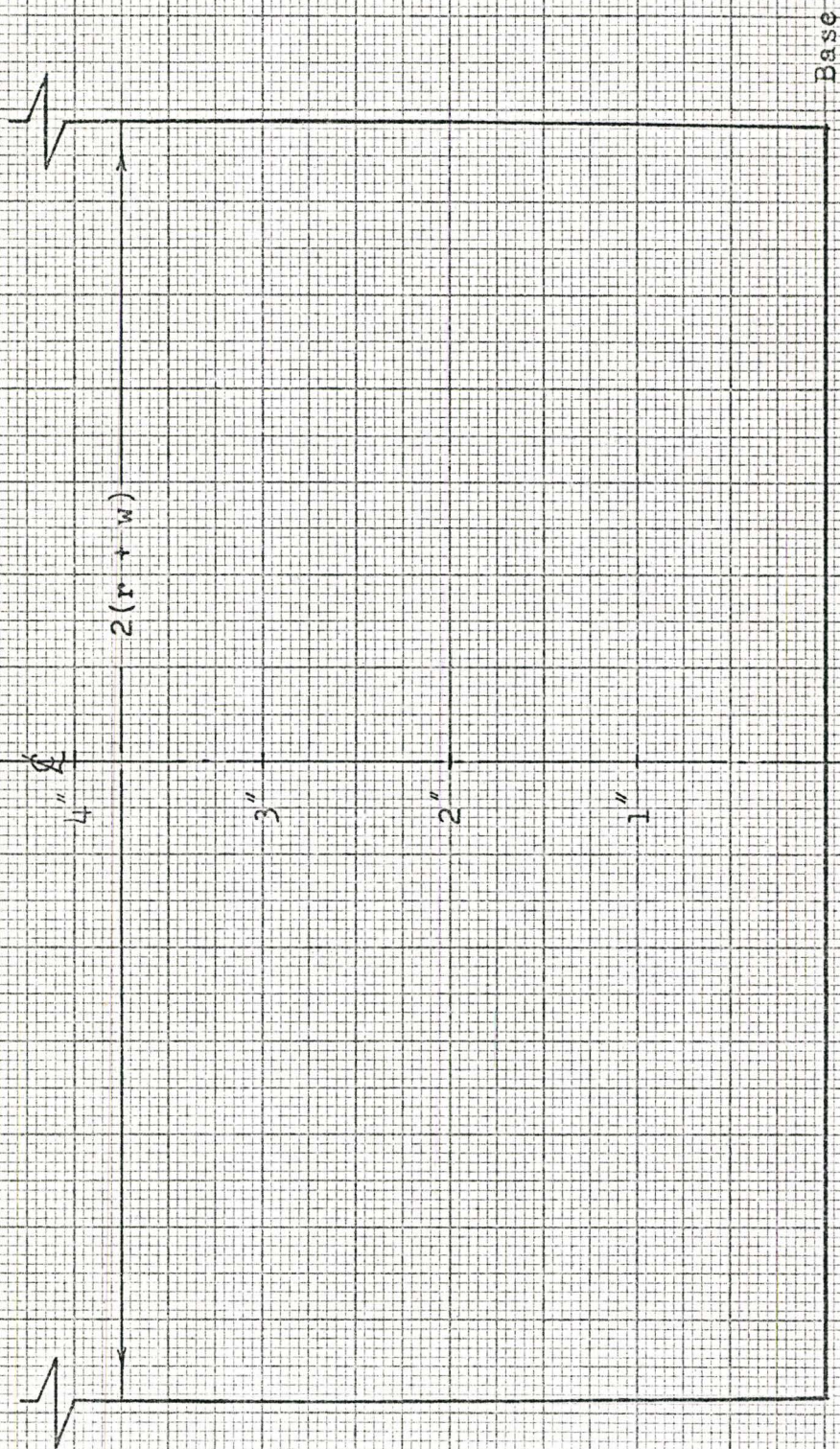


ROCKET AT GUN MUZZLE

FIGURE 5.3

FIGURE 5.4
TANK DEFLECTION CURVE





TANK DEFORMATION IN
THE VICINITY OF THE BASE

FIGURE 5.5

FIGURE 5.6

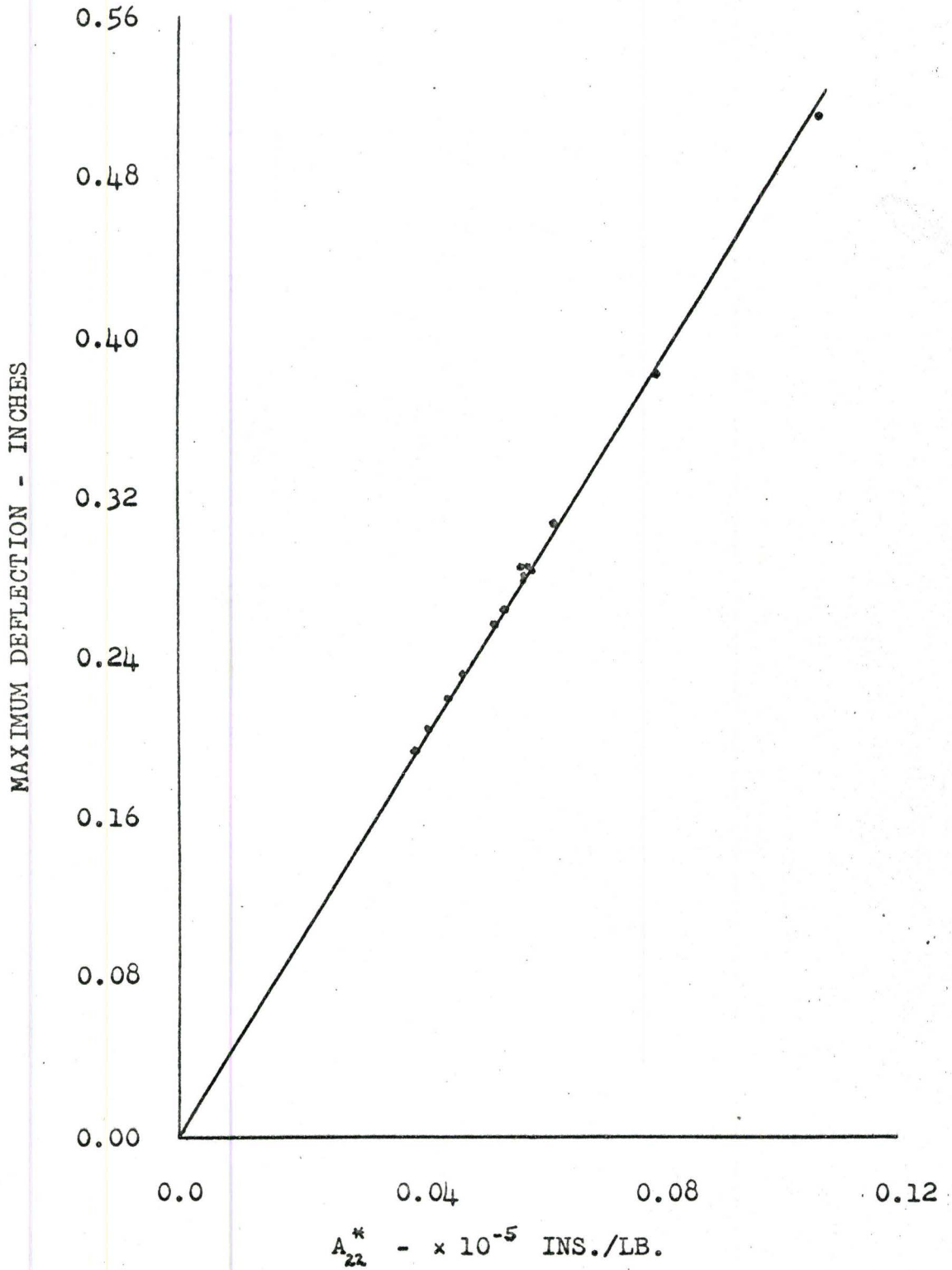
MAXIMUM DEFLECTION versus A_{22}^* 

FIGURE 5.7

AXIAL CURVATURE AT BASE versus $(A_{zz}^*/D_{II}^*)^{1/2}$

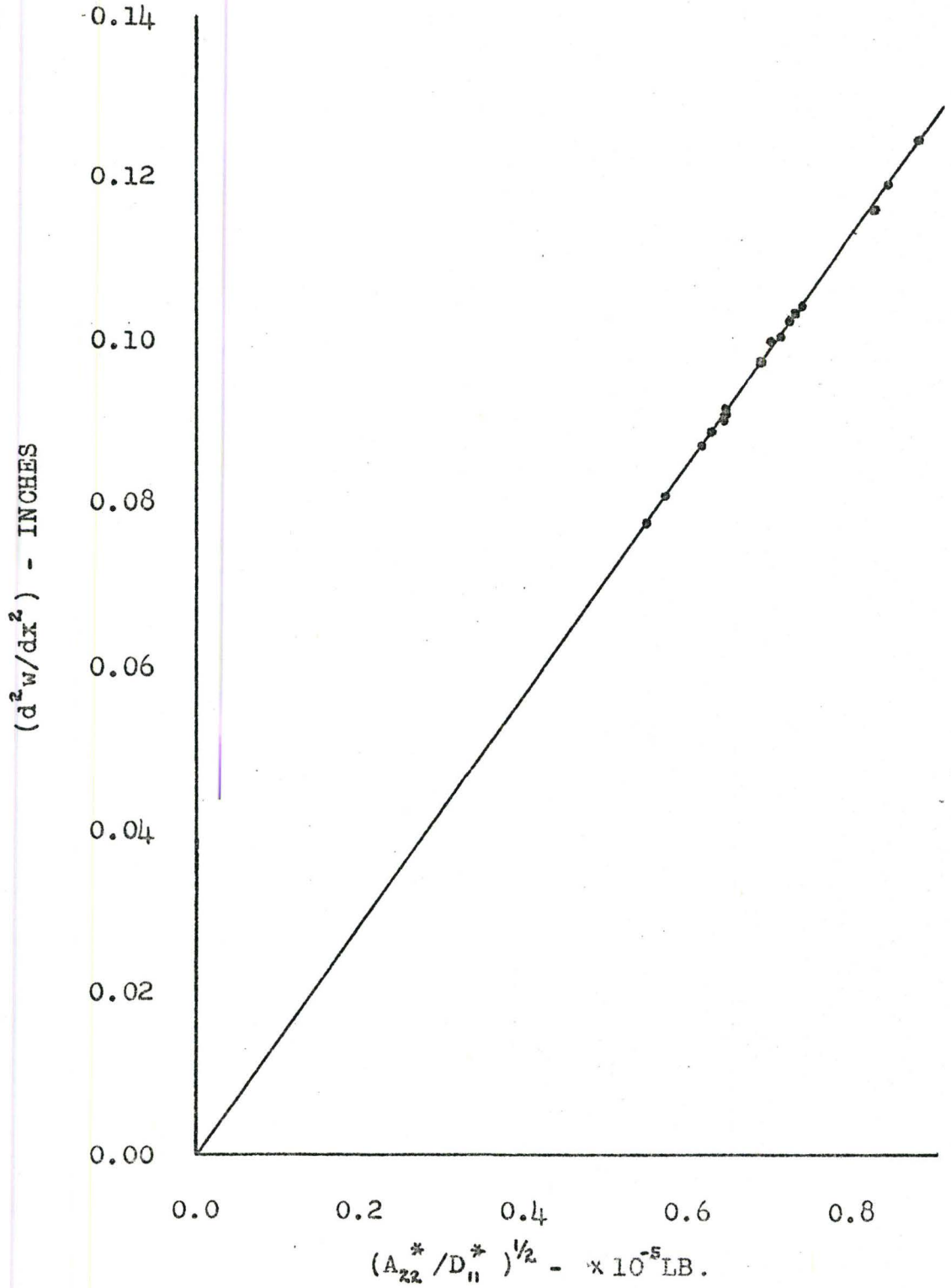


FIGURE 5.8
THE EFFECT OF HOOP WOUND LAYER THICKNESS ON
LAMINATE ELASTIC PROPERTIES

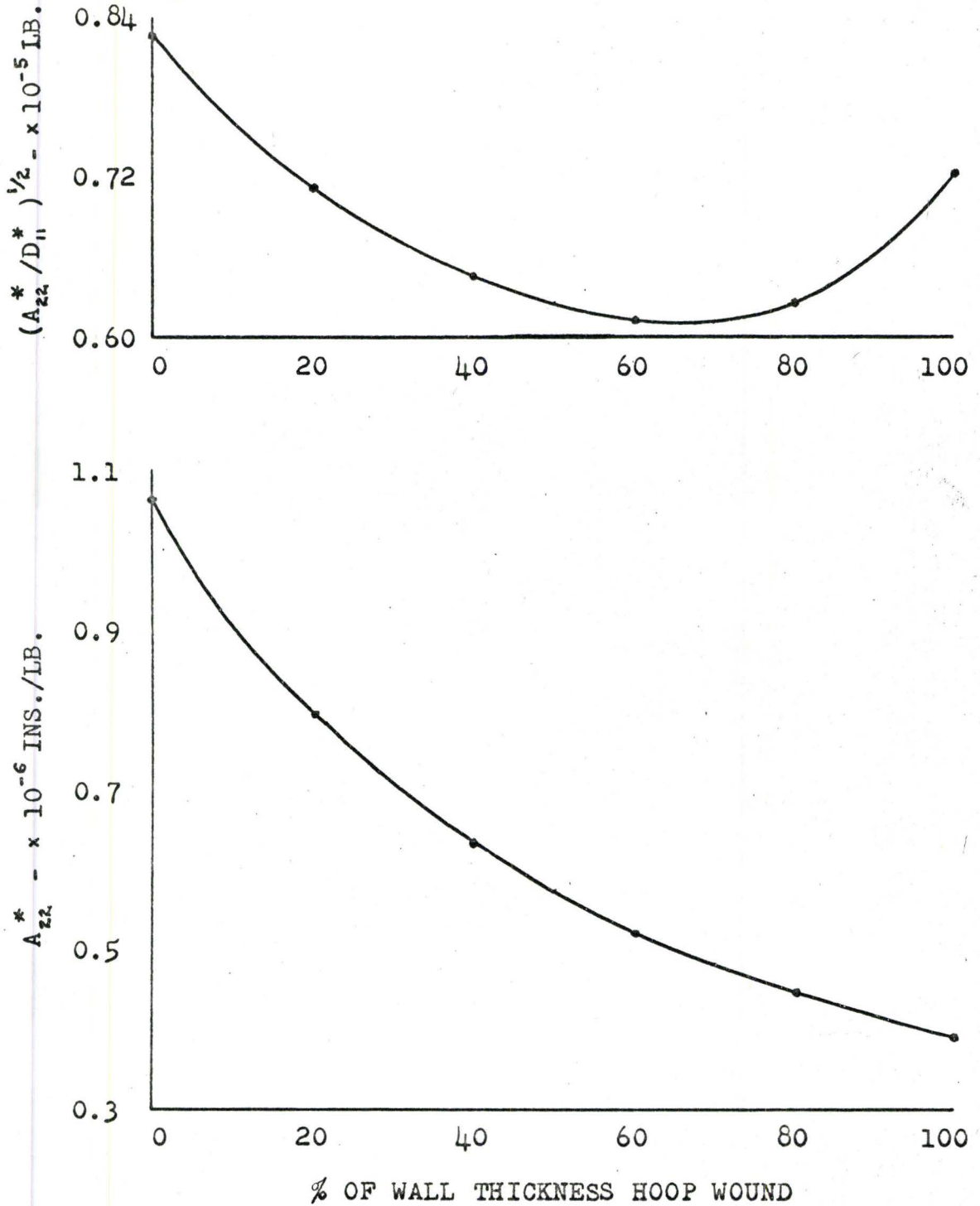


FIGURE 5.9
THE EFFECT OF HOOP WOUND LAYER THICKNESS ON
LAMINATE STRUCTURAL PERFORMANCE

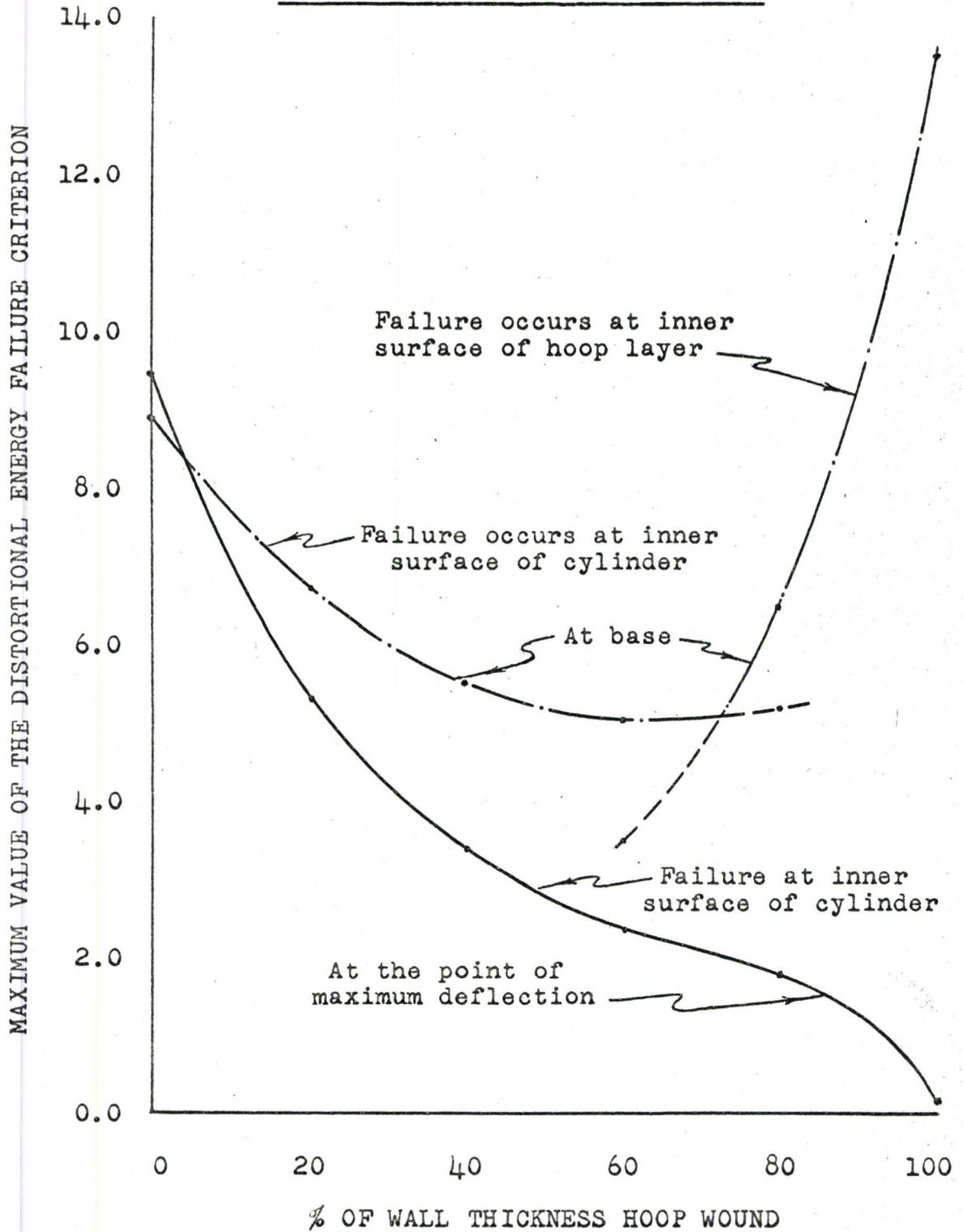


FIGURE 5.10
THE EFFECT OF THE HELICAL WIND ANGLE ON
LAMINATE ELASTIC PROPERTIES

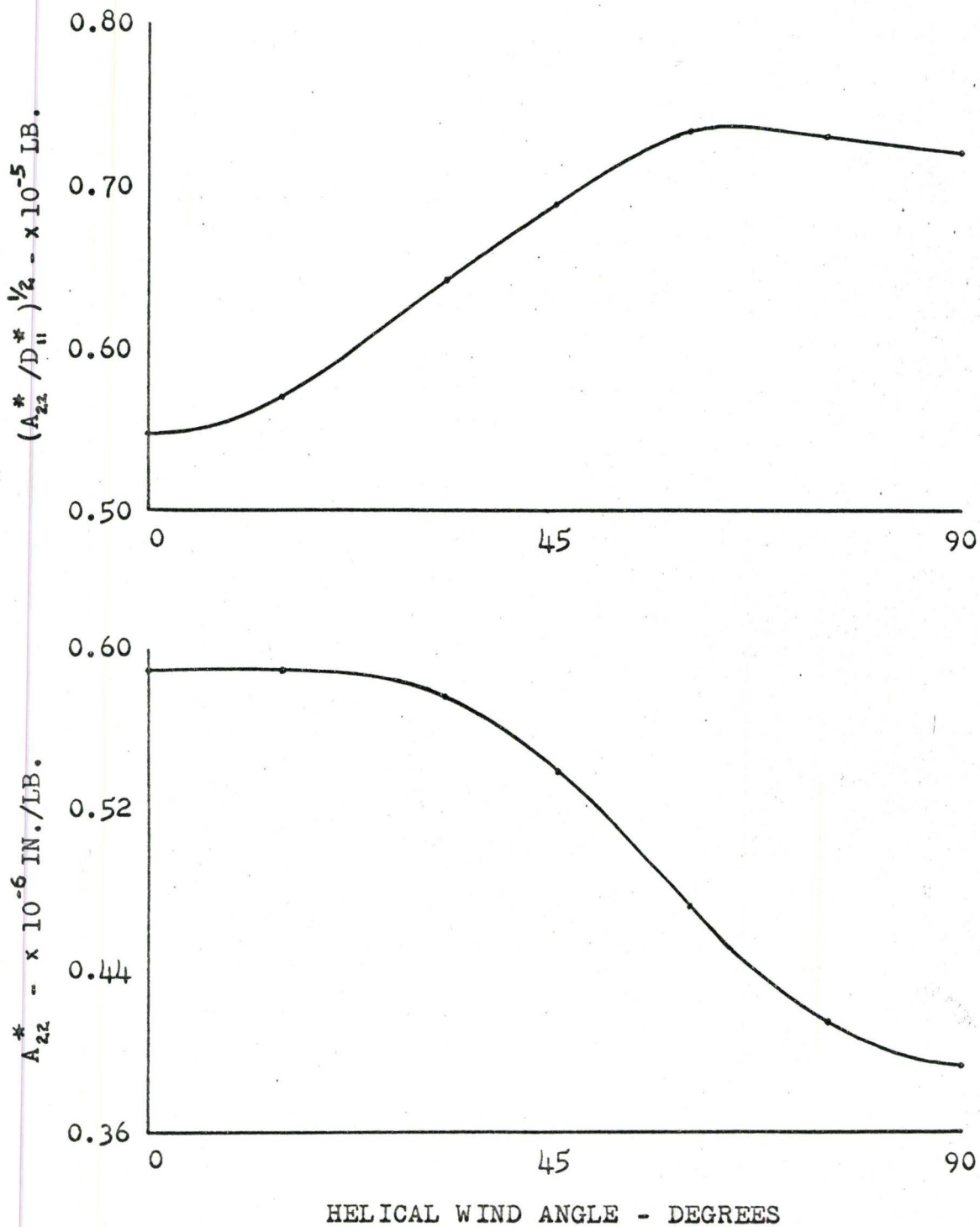


FIGURE 5.11-a

THE EFFECT OF THE HELICAL WIND ANGLE ON
LAMINATE STRUCTURAL PERFORMANCE AT THE BASE

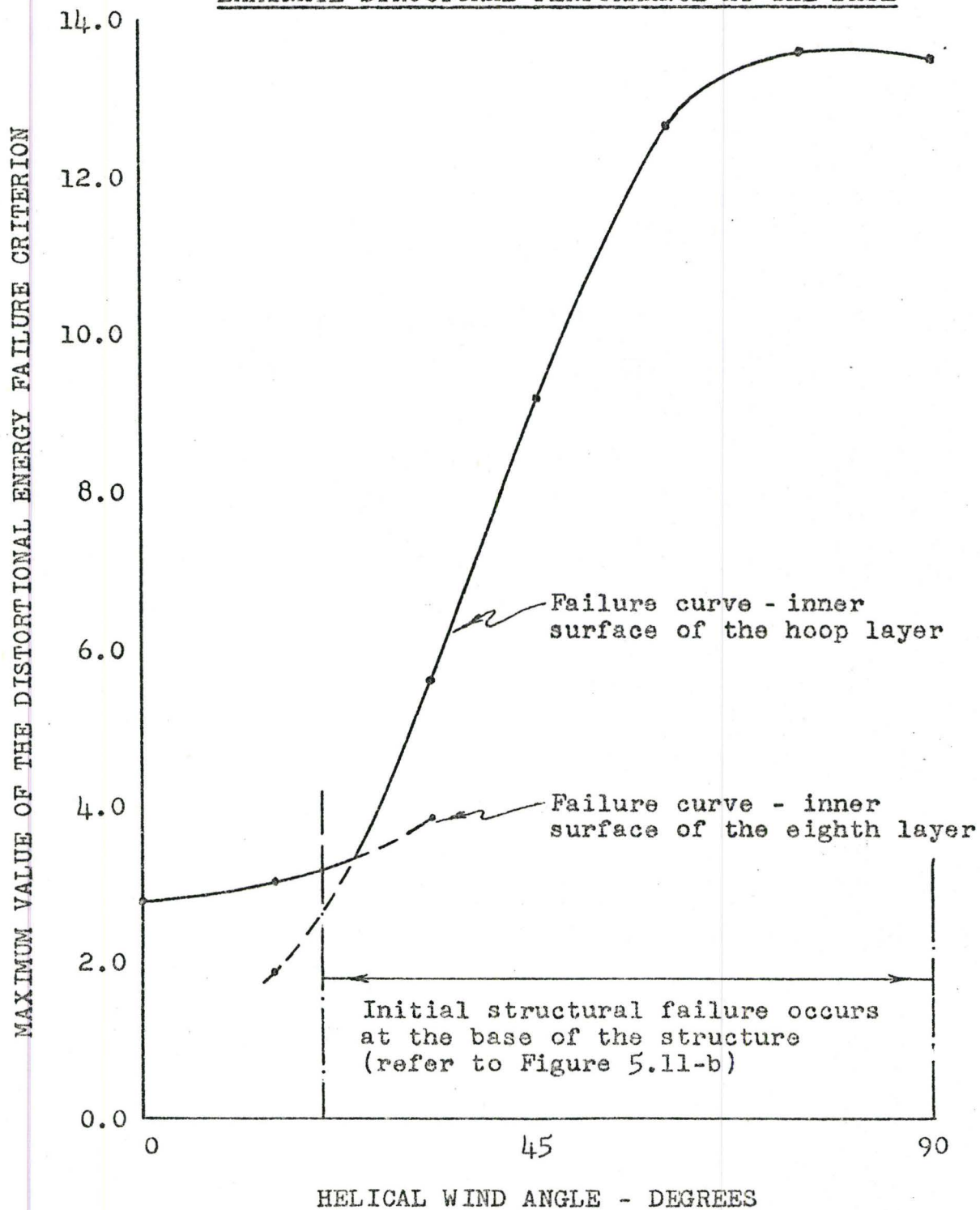


FIGURE 5.11-b
THE EFFECT OF THE HELICAL WIND ANGLE ON
LAMINATE STRUCTURAL PERFORMANCE
AT THE POINT OF MAXIMUM DEFLECTION

